Molecular profiling of presynaptic docking sites

Dissertation
for the award of the degree
"Doctor rerum naturalium" (Dr. rer. nat.)
Division of Mathematics and Natural Sciences
of the Georg-August-Universität Göttingen

submitted by
Anne Janina Boyken

from
Oldenburg, Germany

Göttingen, 2011

Members of the Thesis Committee:

Prof. Dr. Reinhard Jahn (1^{st} **Reviewer)**
Department of Neurobiology, Max Planck Institute for Biophysical Chemistry

Prof. Dr. Ralf Ficner (2^{nd} **Reviewer)**
Department of Molecular Structural Biology, GZMB, University of Göttingen

Prof. Dr. Michael Thumm
Department of Biochemistry II, University of Göttingen

Date of the oral examination:

Declaration of Authorship

Declaration of Authorship

Hereby, I confirm that I have created this work "*Molecular profiling of presynaptic docking sites*" entirely on my own and that I have only used the sources and materials cited.

Göttingen, 30th of May 2011

Anne Janina Boyken

Dedicated to 298 white wistar rats, who gave their brains for this thesis.

Abstract

In presynaptic nerve endings, exocytosis of synaptic vesicles is restricted to specialized areas of the plasma membrane, called active zones, that are distinguished by electron-dense material. Here synaptic vesicles attach to the release sites (docking) and are then activated (priming) before undergoing calcium-dependent exocytosis, releasing their neurotransmitter content into the synaptic cleft. Many of the key players of the presynaptic exocytotic machinery are known, and also the major scaffold proteins of the active zone have been identified. However, the precise molecular composition of the sites at which vesicles dock remains to be elucidated. Proteomic approaches to identify protein components of these sites are challenging because of difficulties in purifying these sites. Most importantly it has been very difficult to separate presynaptic membranes from postsynaptic membranes and the postsynaptic protein scaffold. Here we report about a new procedure allowing for an almost quantitative separation of pre- and postsynaptic membrane fractions. The procedure involves mild proteolysis resulting in the cleavage of the adhesion molecules connecting pre- and postsynaptic membranes, followed by gradient centrifugation, lysis of the presynaptic compartment, separation of free and docked vesicles, and immunoisolation using antibodies specific for synaptic vesicle proteins as the final purification step. Using quantitative proteomics we then compared the protein composition of free and docked vesicles. In the latter fraction we detected all major active zone proteins. In addition we identified many ion channels and transporters, cell adhesion molecules and plasma membrane-specific signaling proteins that have been reported to be involved in synaptic transmission. Only very few postsynaptic proteins or proteins derived from other organelles (except of mitochondria) were detected. The docked vesicle fraction contained more than 30 previously uncharacterized proteins, many of which are predicted to contain single or multiple transmembrane domains. Preliminary characterization of one of the new membrane proteins using a newly generated antibody revealed specific localization to presynaptic nerve terminals, raising the possibility that the protein is involved in presynaptic function. Additionally, this new procedure was used to quantify changes in the presynaptic proteome as a result of effector treatment. The Rab effector GDI efficiently removed Rab proteins from the docked vesicle

fraction, but no other significant changes were observed among the remaining 500 identified proteins in the docked vesicle fraction.

Contents

List of Figures

List of Tables

List of Abbreviations

AZ	Active zone
BLAST	Basic Local Alignment Search Tool
BSA	bovine serum albumin
CASK	calcium/calmodulin-dependent serine protein kinase
ERC2	ELKS/Rab6-interacting/CAST family member 2
GABA	γ-aminobutyric acid
GAP43	Growth-Associated Protein 43
GDI	GDP dissociation inhibitor
GluR1	glutamate receptor, ionotropic, AMPA1
HRP	Horse raddish peroxidase
IEF	isoelectric focusing point
iTRAQ	isobaric tag for relative and absolute quantitation
NCAM	neuronal adhesion molecule 1
NCBI	National Center for Biotechnology Information
NCX	$\mathrm{Na}^{+}/\mathrm{Ca}^{2+}$
NHE1	sodium/hydrogen exchanger 1
NR1	glutamate receptor, ionotropic, N-methyl D-aspartate 1
NSF	*N*-Ethylmaleimide sensitive factor
PBS	phosphate buffered saline
PMCA	plasma membrane $\mathrm{Ca}^{2+} - \mathrm{ATPase}$
PSD95	postsynaptic density protein 95
SCX	Strong cation-exchange chromatography
SDHA	Succinate dehydrogenase complex, subunit A, flavoprotein
SDS-PAGE	Sodium dodecyl sulfate polyacrylamide gel electrophoresis
SMART	Simple Modular Architecture Research Tool
SNARE	soluble NSF attachment protein
SPM	Synaptic plasma membrane

SV ..... Synaptic vesicle
TEMED ..... N, N, NŠ, NŠ Tetramethylethylenen-diamine
VGlut1 ..... vesicular glutamate transporter 1

1 Introduction

1.1 Key Events of Synaptic Vesicle Exocytosis

Synapses are the fundamental units of neuronal networks, representing the sites of information transfer between neurons. Structurally, synapses are characterized by their asymmetric organization consisting of a presynaptic nerve terminal containing synaptic vesicles (SV), a synaptic cleft, and a postsynaptic signaling complex called the postsynaptic density (PSD). At the synapse, an arriving electrical signal is converted into a chemical signal. Precisely, action potential depolarization of the presynaptic plasma membrane induces calcium channel opening and calcium influx into the nerve terminal that triggers exocytosis of neurotransmitter-filled synaptic vesicles. Neurotransmitter molecules then diffuse across the synaptic cleft and bind to postsynaptic receptors triggering signal transduction cascades at the postsynaptic site. This neurotransmitter release is restricted to specialized presynaptic membrane compartments called active zones, where synaptic vesicles undergo a temporally and spatial coordinated 3-step mechanism consisting of docking, priming and fusion (Fig. 1.1).

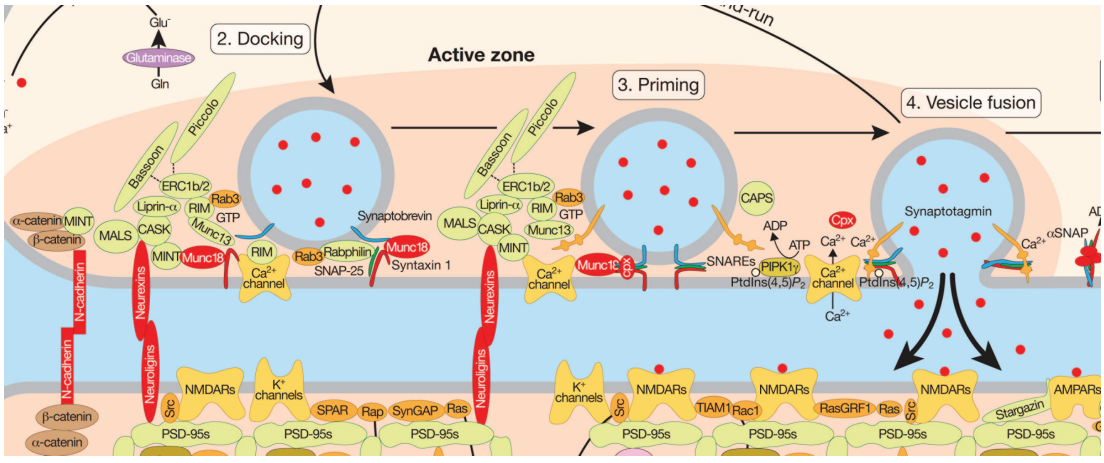

Figure 1.1: Image modified from [1]. The key stages during synaptic transmission at the active zone are the translocation and docking of SVs to the plasma membrane, priming, vesicle fusion and synaptic vesicle recycling.

1.1.1 Docking

The initial step of neuronal exocytosis requires the recruitment and localization of synaptic vesicles to the presynaptic active zone, a process termed docking. Docking is traditionally defined as the morphological attachment of synaptic vesicles to the plasma membrane. In electron micrographs, these vesicles appear without a measurable distance to presynaptic membrane (Fig. 1.2) [2, 3]. Generally, docking is thought to be the preceding step before vesicles gain fusion competence. As there is currently no defined relationship between this docking structure and function, the molecular background of docking can only be inferred from morphological phenotypes. The prime candidate believed to function as a docking factor is Munc18. A severe phenotype of a reduced vesicle docking was observed in Munc18-deficient chromaffin cells [4, 5], in neurons [6] and at neuromuscular junctions of *C. elegans* [7]. It is believed, that Munc18s role in docking is highly dependent on the interaction with the "closed" conformation of syntaxin 1 [8, 9] that occludes the binding site for the cognate SNARE partners and therefore inhibits SNARE complex assembly.

On the vesicular side, Synaptotagmin has been suggested to anchor vesicles in chromaffin cells by binding to the syntaxin-1/SNAP25 complex, an acceptor for subsequent synaptobrevin binding [10, 11]. This docking role for synaptotagmin was also reported for invertebrate synapses [12, 13, 14]. Rab proteins have also been suggested to influence docking. A docking phenotype in secretory cells was observed for Rab3 [15, 16] and Rab27 [17, 18] proteins. However, a similar phenotype for Rab3 in synapses could not be proven [19, 20]. The redundancy of Rab proteins might account for the missing phenotype in synapses, especially since Rab3 and Rab27 share overlapping functions and possibly compensate each other [21].

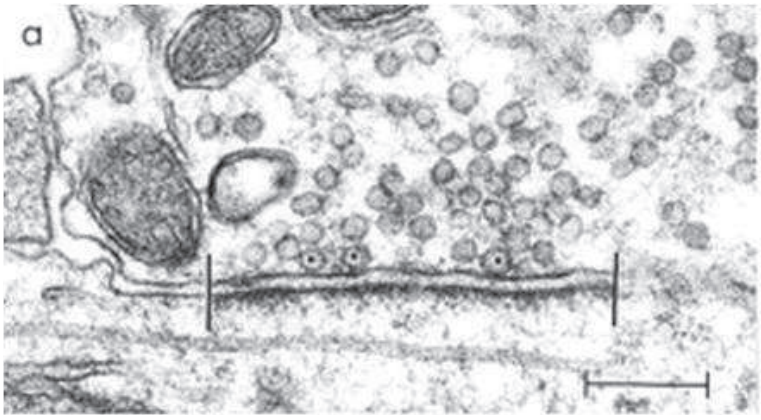

Figure 1.2: Image modified from [22]. Docking of synaptic vesicles at the active zone. Active zones are marked by vertical bars, and docked synaptic vesicles (within 10 nm of the presynaptic membrane), with black dots.

1.1.2 Priming

Priming is defined as the process that makes a (docked) vesicle fusion competent such that it can undergo exocytosis upon calcium influx. In contrast to docking, priming is primarily based on electrophysiological observations. Primed vesicles constitute the readily releasable pool of vesicles (RRP) that are released fast during a stimulus and that can be assayed by applying an emptying stimulus [23, 24, 25]. This functionally defined readily releasable pool essentially coincides with the morphologically defined docked vesicle pool, making it difficult to resolve their relationship and raising the question if priming really is an independently regulated process. However, based on observations where the number of docked vesicles differs from the number of primed vesicles, docking and priming are believed to be separate steps [26, 27]. Nevertheless, perturbations of proteins involved in priming and fusion often also impair vesicle docking, suggesting that these processes are sequentially interlinked [8, 2].

Unlike the less resolved process of docking, the molecular mechanism that underlies vesicle priming is better understood and requires the formation of the trimeric SNARE complex of syntaxin/SNAP25/synaptobrevin [28, 29, 30] and its interaction with Munc18 [31, 32]. SNARE-assembly starts by formation of a four-helix bundle of the SNARE-domains residing on two opposing membranes. This helical bundle zippers up from the N- to C-terminus, forming a *trans*-SNARE complex. The partial if not complete assembly of this *trans*-SNARE complex between the synaptic vesicle and the plasma membrane then bridges the fusing membranes, bringing them in close proximity [33, 34]. In addition to forcing the synaptic vesicle into a fusiogenic state, premature fusion has to be prevented, so that exocytosis only takes place when calcium enters the cell. In this respect, complexin has been suggested to regulate fusion by binding to the zippered SNARE complex, "clamping" it in an activated but frozen state [35, 36, 37]. How binding of complexin to the SNARE complex regulates the probability of SV fusion is controversial and to date not fully understood [38].

Aside from the components of the fusion machinery, additional proteins that regulate priming have been identified. Munc13 is the best characterized priming factor (see section 1.2.1), influencing the size of the RRP in chromaffin cells [39] and in neurons [40].

1.1.3 Fusion

After membrane docking and priming, fusion is initiated by the influx of calcium through voltage-gated calcium channels at the plasma membrane. As a consequence, calcium binding to the synaptic vesicle protein synaptotagmin triggers the molecular mechanism of membrane fusion [41, 42, 43]. Synaptotagmin contains two cytoplasmic C2 domains (C2A and C2B) that bind calcium ions enabling them to interact with phospholipids in the plasma membrane

[44, 45]. Synaptotagmin simultaneous interacts with the target membrane SNARE proteins upon binding calcium ions [46, 47], therefore synaptotagmin influences both lipid bilayers and SNARE proteins. These calcium-dependent interactions are thought to control transitions in the fusion machine. Synaptotagmin is thought to displace complexin followed by a complete zippering of the SNARE complex and fusion of the membrane [37, 48, 49]. According to the established mechanistic model, membrane fusion is driven by the free energy that is released upon formation of the fully zippered SNARE complex [50]. As the membrane fuses, SNAREs are transformed to a *cis*-complex, where the proteins reside in the same membrane. SNARE complexes are then dissociated by NSF and the soluble NSF attachment proteins (SNAPs) [51].

1.2 Molecular Organization of the Active Zone

In principle, active zones provide a molecular platform for the arriving vesicle, localizing them in close proximity to the plasma membrane (docking) and preparing them for exocytosis (priming). Already in the early 60ies actives zones were visualized as electron dense particles in electron micrographs that are precisely aligned opposite to the postsynaptic density [52, 53]. Since then, the knowledge about AZ morphology has advanced tremendously to the point of detailed 3D tomographs [54, 55, 56]. These structures revealed, that at the morphological level the active zone is identified by the presence of synaptic vesicles linked to each other and to the plasma membrane by a filamentous network (see Fig. 1.3). Unlike AZ structure, the knowledge

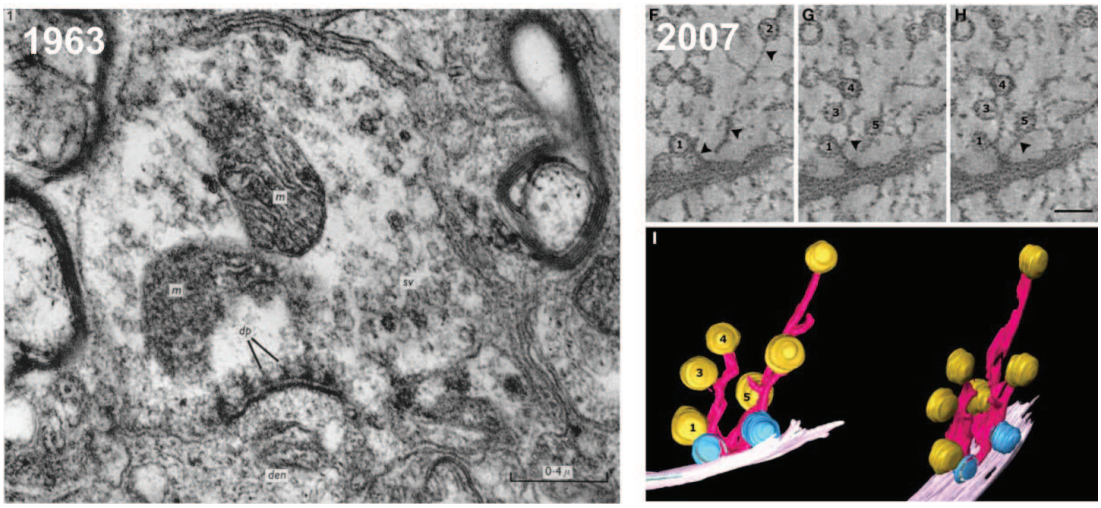

Figure 1.3: 1963: Image modidfied from [52]. Synapse of spinal cord showing regularly arranged dense projections in presynaptic processes. m: mitochondrium, dp: presynaptic dense projections, den: dendrite. **2007**: Image modified from [55]. F-H: Example of a filament contacting several SVs. I: 3D reconstruction of the filaments (pink) and the adjacent SVs.

about the molecular basis that mediates and regulates presynaptic events has advanced much slower and remains to be fully elucidated. Since its discovery in the 1960s, only a few protein families have been identified to be specifically associated with the active zone.

1.2.1 Core Active Zone Proteins

Munc13

Proteins of the Munc13 family were the first identified components of the presynaptic active zone. These proteins have originally been identified in a genetic screen for uncoordinated movements in *C.elegans* (UNC13) [57]. The mammalian homologue of unc13, Munc13, has 3 isoforms that are expressed in the nervous system [58] and that share a common multi-domain structure consisting of a C1, C2 (2x), C2B, C2C and a central MUN domain [59]. Several studies have suggested that Munc13 proteins are involved in synaptic vesicle priming [60, 61]. At the physiological level, a deletion of Munc13-1 in primary hippocampal neurons [40] as well as in neuromuscular junctions of *C.elegans* [62] and *Drosophila* [63] impairs neurotransmitter release as a result of defects in the size of the readily releasable vesicle pool. At the molecular level, Munc13 proteins interact with multiple proteins including DOC2 [64], calmodulin [65], spectrins [66], Rim [67, 68], syntaxin [69, 70, 71] and Munc18 [72]. Munc13 additionally forms inactive homodimers that can be relieved by binding to Rim [68, 73]. It has emerged recently that the interaction with syntaxin and Munc18 is the main mechanism for Munc13 in priming. It has been suggested that a weak interaction of the MUN domain with the SNARE motif of the closed syntaxin-Munc18 complex accelerates opening of syntaxin1 and thus SNARE complex assembly [72]. Munc13 function is additionally calcium regulated via its C2B domain [74, 71].

Rim

In the mammalian system, there are 7 Rim isoforms encoded by 4 genes [75, 76, 77]. Initially identified as Rab3-interacting proteins [78], these proteins have emerged to be the central organizers of the active zone. Rim has been shown to have multiple roles in neurotransmitter release including docking [79, 80, 81], priming [82, 83], calcium channel localization [84, 80] and plasticity [77, 85]. Containing various domains (Zn-finger, PDZ, C2A, C2B and a proline-rich PxxP motif) [75], Rims can interact with other active zone components e.g. Piccolo [86], ERCs [87, 88, 89], Liprins [85] and Munc13 [67]. Additionally, Rims also bind to the synaptic vesicle proteins Rab3 [78] and synaptotagmin [77], to Rim-BPs [75] and to calcium channels [77]. A global understanding of how a single protein can translate such a diverse range of interaction partners into physiological function has not been accomplished. However, some of

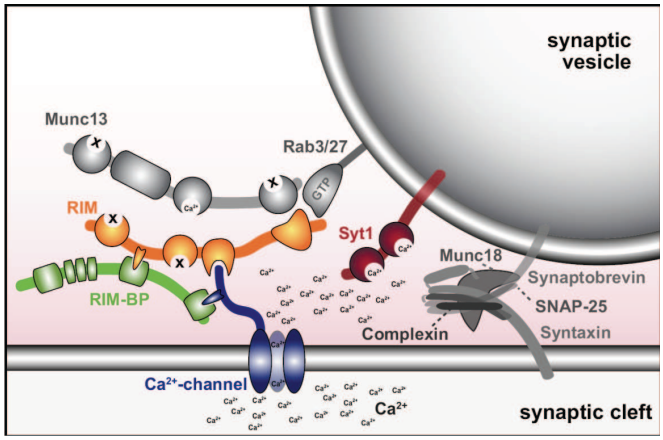

Figure 1.4: Image modidfied from [84]. Model illustrates the N-terminal priming complex of Rim with Rab3 and Munc13 and localization of calcium channels at the active zone via a direct interaction with the PDZ domain.

these molecular interactions have been unraveled and could be assigned to a specific synaptic function. For example, the N-terminal Zn-finger domain binds to Rab3 and this interaction is suggested to be involved in recruitment/docking of vesicles to the membrane [79]. This interaction presumably leads to an additional or sequential binding of Rim to Munc13, that activates priming by relieving the autoinhibitory homodimerization of Munc13 [90]. Furthermore, the Rim PDZ domain has been shown to directly interact with calcium channels, tethering them in close proximity to the release sites [84]. Thus, Rim modulates sequential steps in synaptic vesicle exocytosis through serial protein-protein interactions (see Fig. 1.4).

ERCs

ERCs [88], also known as ELKS [91] (ERC1) or CAST [87] (ERC2) are active zone components that were independently found at the same time as interaction partners for Rim in a yeast-two-hybrid screen [88] and complexed with Rim and Munc13 in PSD preparations [87]. ERCs are composed of 4 coiled-coil domains that can bind to piccolo, bassoon and liprins [92, 93] and a C-terminal-consensus binding motif that interacts with the PDZ-domain of Rim [88, 87, 89]. Hence ERCs can bind, similar to Rim, to many active zone components providing a platform for the release machinery [92]. ERCs appear to function downstream of synaptic vesicle docking [94, 95, 96], yet their precise function in neurotransmitter release is controversial. Two opposing theories, one suggesting an essential role in exocytosis affecting the Rim-Munc13 pathway [92, 94] and one establishing ERC as a negative regulator, restricting release at inhibitory synapses [96] are currently considered.

Piccolo and Bassoon

Piccolo and bassoon represent the largest active zone-specific proteins and are structurally related molecules. They are 530 and 420 kDa in size and contain multiple domains including two N-terminal zinc finger motifs, three coiled-coiled regions and, in the case of Piccolo, a PDZ and two C2 domains [97, 98, 99]. Just like Rims, Munc13s and ERCs these proteins closely interconnect with other members of the AZ (e.g., ELKs [92], Rims [86] and Liprin [100]), but piccolo additionally binds to proteins involved in the regulation of actin and SV dynamics (GIT1 [101], Abp1 [102], profilin [99], and PRA-1 [98]). Having a size of more than 400 kDa, addressing protein function of these molecules with conventional knock down strategies is elusive [103]. Additionally, the high structural similarity and overlap of binding partners possibly causes functional redundancy. Nevertheless piccolo and bassoon are suggested to be involved in the formation of active zones from precursor vesicles early in synaptogenesis [104, 105]. Bassoon additionally exhibits a unique structural role in the attachment of ribbon synapses [106, 107], while piccolo's role has not been completely resolved yet. On the one hand it is believed that piccolo functions as a negative regulator of exocytosis by -either direct or indirect- modulating synapsin dynamics that affects the recruitment of synaptic vesicles from the reserve pool to the readily releasable pool [108]. On the other hand it is thought that piccolo does not directly participate in vesicle exocytosis, but has a significant role in maintaining vesicle clusters [109].

α-liprins

α-liprins are the least characterized active zone components. Although their presence is not restricted to active zones, α-liprins are considered an integral part of presynaptic release site [110]. These proteins were originally identified as LAR interaction partners and exist in 4 structurally homologous isoforms, consisting of several N-terminal coiled-coil domains and a C-terminal liprin homology (LH) domain [100]. As the other active zone proteins, liprins can directly interact with Rim [85], ERC1 [93, 111]and CASK [112]. Liprins are thought to play a crucial role in active zone organization [113, 111]. Precisely, α-liprins are thought to be upstream effectors of Rim, possibly by localizing Rim to active zones [85]. Evidence that liprins and Rim act in the same pathway can be provided by the similarity of the morphological and physiological phenotypes [81, 114]. It has also been suggested that binding to ERC in turn influences the presynaptic localization of liprins [93, 111].

CASK, Mint, MALS

CASK, MALS (Veli) and Mint form a ternary complex [115, 116] that possibly occurs on both sides of synaptic junctions [117, 112, 118, 119]. Presynaptically, proteins of this complex

interact with neurexin (CASK)[117] and Munc18 (Mint) [120] while the assembled complex associates with α-liprins [112]. The function of this complex in synaptic transmission remains elusive, but there are indications that it is involved in replenishing the readily releasable pool from the reserve pool of synaptic vesicles at the active zone and that liprin might participate in this function [112].

Protein	Interaction partner	Reference
ERC2	bassoon and piccolo	[92]
	RIM and Munc13	[87]
	α-liprins	[93]
Rim	Rab3	[78]
	Munc13	[67]
	N- and P/Q-type $\mathrm{Ca}^{2+} - \mathrm{channels}$	[84]
	α-liprins	[85]
CASK	liprin-α2	[112]
	Mint1 and MALS	[115]

Table 1.1: Compendium of known interactions between active zone components.

1.2.2 Proteins involved in Synaptic Exocytosis

Adhesion Molecules

Although not classified as true active zone components, cell adhesion molecules participate in the function and plasticity of synapses aside from their structural role [121]. As an example, the presynaptic adhesion molecules α-neurexins have been suggested to regulate calcium channel function, because a loss of these molecules resulted in a decrease of whole cell calcium currents [122]. In addition, neurexin can bind to the active zone protein CASK [117]. There is also evidence for a role of NCAMs and cadherins in synaptic plasticity, but these adhesion molecules reside on both sites of the synapse, which makes it difficult to unravel only their presynaptic function. Cadherins are thought to contribute to synaptic plasticity by interacting with catenins. These complexes are known to regulate postsynaptic AMPAR trafficking and are involved in dendritic spine formation. On the presynaptic site, N-cadherins are localized close to the active zone and have been demonstrated to influence synaptic vesicle release at glutamatergic synapses [123].

Cytoskeletal Elements

Cytoskeletal components, especially actin, are highly enriched at synapses. Actin does not only

define synapse morphology, it is additionally thought to be involved in the regulation of synaptic transmission. However, the mechanisms of actin dynamics regulating synapse function is not completely understood. The actin cytoskeleton is suggested to function as a physical barrier in the nerve terminal that is necessary to maintain the required distance between different vesicle pools or opposing membranes. Thus, actin is thought to function as a negative regulator, restricting vesicle recruitment and fusion. However, actin also facilitates the delivery of synaptic vesicles from the reserve pool to the RRP through molecular motors and therefore positively influences the synaptic vesicle exocytosis (for review see [124]). Interestingly, presynaptic proteins such as the SV protein synapsin [125] or the active zone protein piccolo [C. Waites, data not published] can directly associate with the actin cytoskeleton, but the precise function of these interactions are not fully understood.

1.3 Excitatory and Inhibitory Synapses

The brain is composed of many different types of neurons that form very specific synapses. Already the earliest morphological studies proved that synapses are not equivalent, but exist in different types (Gray's type I and type II) [126]. With the current knowledge, it is well-known that in the central nervous system (CNS) synapses are either excitatory and inhibitory. These synapses differ in the identity of neurotransmitters, in receptor types at the postsynaptic site, and the ability to depolarize or hyperpolarize neurons. The majority of the synapses in the CNS are in fact excitatory synapses that mediate synaptic transmission by the neurotransmitter glutamate. Glutamate binds postsynaptically to the ionotropic N-methyl-D-aspartic acid (NMDA) receptor and the α-amino-3-hydroxy-5-methyl-4-isoxazolepropionic acid (AMPA) receptor. Only a small portion of the synapses (10-20%) are inhibitory synapses. Synaptic transmission at these synapses is dependent on gamma aminobutyric acid (GABA), which activates a family of GABA receptors on the postsynapt site.

Although the machinery of synaptic exocytosis is present in both types of synapses, surprisingly few proteins are common to all synapses, but are expressed in different isoforms. Recent evidence is suggesting that GABAergic and glutamatergic neurons express different isoforms of molecular components that regulate pre-and postsynaptic functions. On the postsynaptic site, neuroligins and gephyrins for example have been shown to be differentially expressed among synapse types [127, 128]. On the presynaptic site, Munc13s and synapsins have been suggested to play different roles in excitatory and inhibitory synapses [61, 129]. Interestingly, immunoisolated SVs specific for the different neurotransmitter do not differ significantly in their protein composition apart from the vesicular neurotransmitter transporter [130], indicating that SVs do not make the key difference in these synapses.

1.4 Synapse Proteomics

1.4.1 Proteomic Analysis of Synaptic Subdomains and Complexes

Although the knowledge of the molecular components in the presynaptic nerve terminal remains limited, proteomic studies have produced a wealth of qualitative data so far. Such studies have contributed to the understanding of synaptosomes, synaptic sub-compartments such as the postsynaptic density or synaptic vesicles.

Almost a decade ago, the first large-scale proteomic analysis of the NMDA receptor complex was carried out, identifying more then 70 proteins in a single multi-protein signaling complex [131]. The identification of a physical and functional unit comprised of receptos, adaptors, signaling and cytoskeletal components was a novelty. It complemented and exceeded previous studies that were based on yeast-two-hybrid screens and additionally provided new insights into NMDA receptor function. Around the same time, major efforts started to identify postsynaptic proteins from the purified PSD fraction by large-scale proteomic analyses [132]. To date, several hundred proteins are identified reflecting the diversity and complexity of the postsynaptic density, among them are ion channels, scaffolding molecules, signaling and cytoskeletal elements, proteins involved in sorting and trafficking as well as protein synthesis [133, 134, 135]. Novel proteins identified by these proteomic studies were then followed up and integrated into the existing model of the postsynaptic density.

Another example that has been extensively analyzed by proteomic studies, is the synaptic vesicle [136, 137, 138] (see Fig. 1.5). In 2006, two independent studies comprehensively characterized the SV proteome and could identify 185 [137] and 410 [138] proteins, depending on sample preparation and subsequent mass spectrometric analysis. The large number of proteins detected on a organelle with an average diameter of 40 nm was surprising and gave rise to the necessity of additional quantitation methods to distinguish bona fide organellar proteins from those who are contaminating. Therefore, Takamori and co-workers performed a comprehensive Western blotting profiling of subcellular fractions to discriminate between proteins co-purified with synaptic vesicles, proteins distributed throughout all subcellular fractions and proteins that are depleted from the SV fraction. The principle of such a procedure is known as protein correlation profiling and was introduced to study the human centrosome [139]. Nowadays, due to the high sensitivity of mass spectrometers, protein correlation profiling has become almost indispensable to generate reliable subcellular proteomes.

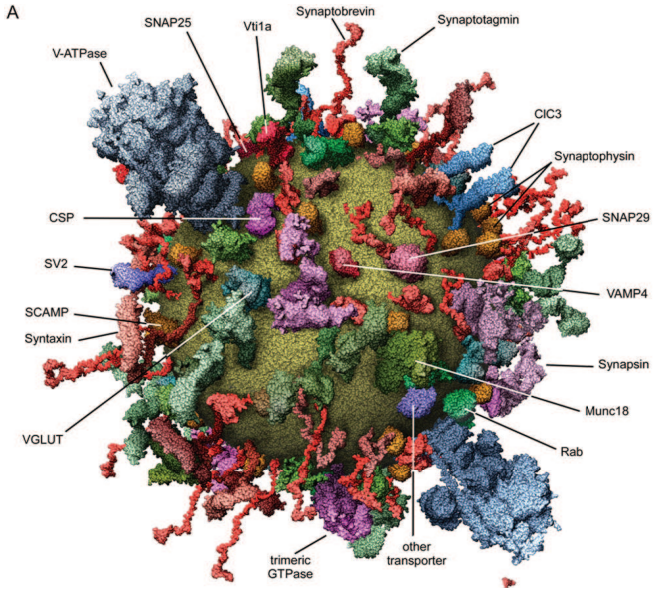

Figure 1.5: Image modidfied from [138] shows a 3D-model of an average synaptic vesicle. The quantitative description of a SV was generated by molecular, biophysical, electron microscopy, and modeling techniques.

1.4.2 Comparative and Quantitative Mass Spectrometry

Due to the increasing sensitivity of mass spectrometers, the necessity for quantification in addition to identification has emerged. The isolation procedure of subdomains or organelles merely enriches proteins, so that preparations may contain a considerable amount of contaminants. Instead of doing time consuming Western blotting profiling, quantitative mass spectrometry has moved into focus. Early approaches used a label-free quantitation based on peptide ion intensities that are correlated to the concentration of the peptides [139]. However, this method strongly depends on the stability of LC separation and MS analysis and is complicated when analyzing complex samples. Apart from protein correlation profiling, quantitative information of protein and protein complexes have a great prospect. Takamori and co-workers provided the first quantitative description of a organelle by quantifying all major SV proteins by time- and work-consuming Western blotting, taking purified proteins as a reference [138]. Nowadays, tools have been developed that enable quantitative measurements and comparisons of complex protein samples by using stable isotope labeling on either protein or peptide level.

- **ICAT**
  Isotope-coded affinity tagging (ICAT) chemically labels reduced cysteinyl residues of the proteins [140]. It allows a relative quantification based on the enrichment of labeled

peptides in the MS analysis. However, proteins containing no cysteine can not be quantified.

- **iTRAQ**
  Isobaric tags for relative and absolute quantitation (iTRAQ) labels trypsin digested peptides at N-termini and lysine-residues [141]. A collision-induced dissociation of the labeled peptide generates signature ions, whose intensities are used to calculate the relative quantity of a protein. Labeling efficiency is an issue with this method and needs to be checked.

- **AQUA**
  Absolute QUAntification (AQUA) is the only absolute quantification method. It is based on internal heavy isotope labeled peptide standards that are chemically synthesized and spiked into the sample [142]. The absolute quantity of native peptides can be calculated using mass spectrometric peak ratios. A major drawbacks of this method are high costs and the impracticalness of synthesizing large numbers of peptides to cover the desired proteome.

- **SILAC**
  Stable isotope labeling with amino acids in cell culture (SILAC) is an in vivo approach that metabolically labels proteins during cell growth [143]. SILAC relies on the incorporation of stable isotopic nuclei that generate a light (12C, 14N) or heavy (13C, 15N) form of the amino acid into the proteins. The labeling efficiency with this method is nearly 100%, but labeling of non-mitotic cells or tissue can not be achieved.

One of these methods, ICAT was first used to distinguish postsynaptic density specific proteins from co-purifying contaminants [134]. By correlation-profiling of synaptic membranes containing the PSD and isolated PSD fractions, a number of proteins were depleted, indicating that they were contaminants of the PSD preparation.

With AQUA, it is even possible to measure molar concentrations and relative stoichiometries of proteins within a sample. By using this method, absolute amounts of several key PSD proteins, e.g. glutamate receptor subunits, were measured for the first time [135].

An approach that involves the stable isotope reagent iTRAQ has a major advantage as it allows to analyze up to 8 samples simultaneously. Using this approach, a quantitative comparison of glutamatergic and GABAergic synaptic vesicles was done showing that the vesicular transporters are the only components essential for defining the neurotransmitter phenotype of a SV [130].

The study of synaptic regulation and function often involves post-translational modifications such as phosphorylation. In this respect, although not always quantitative, large-scale phosphoproteome analyses involving an affinity isolation step to enrich phosphopeptides have been carried out on synaptosome and PSD preparation [144, 145]. Impressively, nearly 1000 phosphorylated peptides from 287 proteins were identified from PSD preparation [145]. There are many more examples of quantitative proteomics that have been successfully applied to analyze proteomic changes, for example during brain development or in knockout mice models. All these analyses have contributed to the fundamental question of how a complex protein network drives synaptic function.

1.4.3 Presynaptic proteomics

The main advantage of synaptosomes, PSDs and SVs is that they can be isolated in high amounts and with a sufficient purity. Synaptosomes are generated during homogenization of brain material. The applied mechanical forces tear the nerve terminal apart from the axon, which then reseals to form a membrane enclosed giant organelle that includes the presynaptic release machinery, a large number of synaptic vesicles, mitochondria and cytosolic components. On the outside of the synaptosomal membrane, main parts of the postsynaptic density are attached through the transsynaptic scaffold (see Fig. 1.6). These artificial organelles can be isolated by density gradient centrifugation [146]. The postsynaptic density can be obtained from synaptosomes by extraction with Triton-X-100. The PSD remains as a detergent resistent, unsoluble fraction that can be collected by another round of gradient centrifugation. Synaptic vesicles are also isolated from synaptosomes, they are released by hypoosmotic shock and further fractionated by gradient centrifugation, controlled pore-glass bead chromatography or immunoisolation [147].

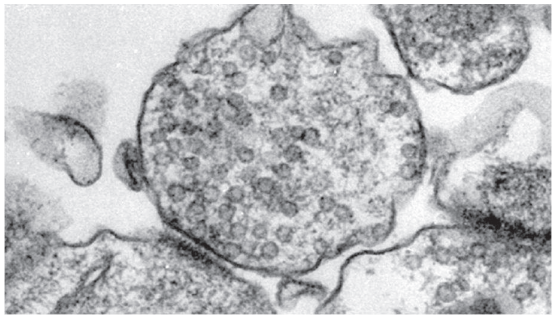

Figure 1.6: Image modidfied from [148]. An electron micrograph of a synaptosome prepared by shearing of brain tissue, showing pre- and postsynaptic compartments with retention of the adhesive contacts between the membranes at the synapse.

Unlike these well established isolation protocols, it is technically difficult to obtain a presynaptic membrane preparation [149, 150]. Since proteomic analyses are strictly dependent on the availability of a purification protocol, studies on the presynaptic side have lagged behind. Although a first detergent based protocol to isolate a presynaptic fraction was reported in 2001 [151], the comprehensive proteomic analysis of this fraction 4 years later was not very clearcut with respect to both quantity and quality [152]. None of the active zone components were detected among the 110 identified proteins in this presynaptic fraction. Interestingly some of them were present in the analyzed PSD fraction. This was the only comprehensive proteomic study on the presynapse available by the time this project started. Only recently, another attempt to purify a presynaptic fraction by immunoisolation of docked vesicles revealed a larger number of proteins [153], but remained limited in comparison to the wealth of information that was obtained for the postsynaptic side.

1.5 Aims of this Work

Considering the observed electron density at the synapse and the fact that active zones determine not only the site and but also the timing for synaptic transmission, the number of known active zone proteins is surprisingly low. In comparison to the PSD, it is believed that the composition of presynaptic nerve terminal is only party uncovered yet. In order to fully understand the mechanisms that regulate the formation, maintenance and function of neurotransmitter release, it is necessary to reveal the exact protein composition of the active zone and analyze the interactions.

Due to the fact that proteomic studies mainly failed, because presynaptic preparations were scarce and insufficient, the main goal of this thesis was to develop an isolation protocol for a presynaptic fraction that allows for comprehensive proteomic studies. This protocol required an efficient removal of the postsynaptic density from synaptosomes, a challenging task that engaged a significant part of this work. Based on this protocol I wanted to validate presynaptic candidates and identify novel molecular players that are required for the docking of synaptic vesicles to the plasma membrane. By performing state-of-the-art quantitative proteomics, I hope to discriminate true presynaptic proteins from other contaminations. With this method I additionally wanted to describe changes in the presynaptic proteome in response to biological perturbations since this has not been done for the presynaptic site. Such an applicational example will hopefully provide a basis for further similar studies that will help to understand the mechanisms of synaptic transmission.

2 Material & Methods

2.1 Materials

2.1.1 Chemicals

Standard chemicals used in this study were obtained from either Sigma-Aldrich (Steinheim, Germany), Roth (Karlsruhe, Germany), Merck (Darmstadt, Germany), Boehringer (Ingelheim, Germany), Fluka (Buchs, Germany), Serva (Heidelberg, Germany), Roche (Basel, Switzerland) or Waters (Eschborn, Germany). All chemicals were of at least analytical purity. Other chemicals are listed below (2.1).

Chemical	Source
Pefabloc	Roche
Pepstatin	Peptide institute
Phenylmethylsulfonylfluorid (PMSF)	Roth
Eupergit C1Z beads	Roehm Pharma
GTPγS	Roche
GDP	Sigma Aldrich
Ni-NTA Agarose	Qiagen
5 ml MonoQ column	Amersham
RapiGest	Waters
Triethylammonium bicarbonate (TEAB)	Sigma Aldrich
Trifluoracetic acid	Sigma Aldrich
Formic acid	Fluka
Triton-X-100	Sigma-Aldrich
Triton-X-114	Sigma-Adrich
Dulbecco's Modified Eagle's Medium (DMEM)	Lonza
Penicillin/Streptomycin	Lonza

Table 2.1: Chemicals used in this study.

2.1.2 Enzymes

The enzymes that were used in this study are listed in 2.2 and were obtained from Fermentas (St. Leon-Rot, Germany), New England Biolabs (NEB; Ipswich, MA, USA), Promega (Madison, WI, USA) or Roche (Basel, Switzerland). All restriction enzymes, ligases and polymerases were used according to manufacturer's instructions (including the supplied buffers).

Enzyme	Application	Source
Proteinase K	Synaptosome digest	Roche
Trypsin	Synaptosome digest	Roche
Trypsin (sequence grade modified)	In-solution digest for MS	Promega
Restriction enzymes	DNA digest	NEB or Fermentas
Ligase	DNA ligation	NEB
Pfu polymerase	Polymerase chain reaction	Promega

Table 2.2: Enzymes used in this study.

2.1.3 Kits

The commercially purchased kits used in this study are listed in 2.3 and were used for the stated application according to manufacturer's instructions (including the supplied buffers).

Kit	Application	Source
Western Lightening ™*Plus*-ECL	Chemoluminescence detection	Perkin Elmer
Pierce ®BCA Protein assay	protein quantification	ThermoFisher
Lipofectamine ™2000	transient cell transfection	Invitrogen
NucleoBond ®Xtra	Plasmid purification (preparative scale)	Macherey-Nagel
NucleoSpin ®Plasmid	Plasmid purification (analytical scale)	Macherey-Nagel
NucleoSpin ®Extract	DNA clean-up	Macherey-Nagel
iTRAQ ™reagent multiplex Kit	quantitative peptide labeling	Applied Biosystems

Table 2.3: Kits used in this study.

2.1.4 Antibodies

Antibodies used in this study are listed in Table 2.4. Antibodies were either generated in this laboratory or purchased at Abcam (Cambridge, UK), BD Bioscience (Erembodegem, Belgium), BioRad (Hercules,CA, USA), Jackson Immunoresearch Europe (Newmarket, UK), NeuroMab (Davis, USA), Synaptic Systems (Göttingen, Germany).

Antibody	Species	Epitope	Application	Source
Synaptophysin 7.2	mouse monoclonal, affinity purified	cytoplasmic tail	WB (1:1000), IP	[154]
Synaptophysin G96	rabbit polyclonal, serum	cytoplasmic tail	IF (1:200)	[154]
Synaptobrevin 69.1	mouse monoclonal, ascites	SATAATVPPAAPAGEG	WB (1:2000)	[155]
Munc18	rabbit polyclonal, serum	full length	WB (1:1000)	
Munc13	mouse, monoclonal, affinity purified	aa 3-317	WB (1:1000)	Synaptic Systems
Piccolo	rabbit polyclonal, affinity purified	aa 439 - 4776	WB (1:500), IF (1:100)	Synaptic Systems
Bassoon	rabbit polyclonal, serum	C-terminus	WB (1:500)	Synaptic Systems
Synaptotagmin 41.1	mouse monoclonal, ascites	cytoplasmic domain	WB (1:1000), IF (1:100)	[156]
PSD95	mouse monoclonal, affinity purified	aa 77-299	WB (1:2000), IF (1:200)	NeuroMab
Homer	rabbit polyclonal, affinity purified	aa 1-186	WB (1:1000)	Synaptic Systems
Syntaxin1A 78.2	mouse monoclonal, ascites	N-terminus	WB (1:1000), IF (1:100)	[46]
NMDA receptor	mouse monoclonal, ascites	aa 660-811	WB (1:1000)	[157]
AMPA receptor	rabbit polyclonal, affinity purified	C-terminus aa 826-906	WB (1:1000)	Synaptic Systems
Na^+/K^+ ATPase alpha 1	mouse monoclonal, ascites	not known	WB (1:2000)	Abcam
SDHA	mouse monoclonal, affinity purified	not known	WB (1:2000), IF (1:200)	Abcam
Neuroligin	rabbit polyclonal, affinity purified	extracellular aa 46-165	WB (1:1000)	Synaptic Systems
RIM	mouse monoclonal, affinity purified	aa 602-723	WB (1:500)	BD Biosciences
VGlut1	rabbit polyclonal, serum	C-terminus aa 456-560	WB (1:1000)	[158]
Mint1	rabbit polyclonal, affinity purified	aa 2-265	WB (1:1000)	Synaptic Systems
CASK	mouse monoclonal, affinity purified	aa 318-415	WB (1:1000)	NeuroMab
ERC 1b/2	rabbit polyclonal, affinity purified	CDQDEEEGIWA	WB (1:1000)	Synaptic Systems
GFP	rabbit polyclonal, serum	full length	WB (1:10000)	Synaptic Systems
SynCAM	rabbit polyclonal, affinity purified	aa 167-181	WB (1:1000)	Synaptic Systems
mouse IgG (Cy2 or Cy3 labeled)	goat polyclonal, affinity purified	IgG (H+L)	IF (1:400)	Jackson Immunoreserach
rabbit IgG (Cy2 or Cy3 labeled)	goat polyclonal, affinity purified	IgG (H+L)	IF (1:400)	Jackson Immunoresearch
mouse IgG (HRP labeled)	goat polyclonal	IgG (H+L)	WB (1:2000)	BioRad
rabbit IgG (HRP labeled)	goat polyclonal	IgG (H+L)	WB (1:2000)	BioRad

Table 2.4: Antibodies used in this study: IF (Immunfluorescence), WB (Western Blot), IP (Immunoprecipitation). Dilutions are marked in brackets.

2.1.5 Buffers and media

Buffer/media	Composition
PBS	2.7 mM KCl, 1.5 mM KH_2PO_4, 137 mM NaCl, 8 mM Na_2HPO_4, pH7.3
TBST	15 mM Tris-HCl, pH 7.4, 150 mM NaCl, 0.5 % (v/v) Tween 20
SDS running buffer	25 mM Tris-HCl, 192 mM Glycine, 0.1 % SDS
Transfer buffer	200 mM Glycine, 25 mM Tris, 0.04 % SDS, 20 % Methanol
Homogenization buffer	320 mM sucrose, 5 mM Hepes, pH 7.4
Sodium buffer	10 mM Glucose, 5 mM KCl, 140 mM NaCl, 5mM $NaHCO_3$, 1 mM $MgCl_2$, 1.2 mM Na_2HPO_4, 20 mM HEPES pH 7.4
1x IP buffer	1x PBS, 5 mM Hepes pH 8.0, 3 mg/ml BSA
2x IP buffer	2x PBS, 5 mM Hepes pH 8.0, 6 mg/ml BSA
Cell culture media	DMEM, 10 % FCS, 4 mM glutamine, 100 U/ml penicillin and streptomycin
Luria-Bertani medium (LB)	10 g tryptone, 5 g yeast extract and 10 g NaCl per 1L

Table 2.5: Buffers and composition that were regularly used in this study.

2.1.6 Mammalian cell lines and bacterial strains

The Human Embryonic Kidney 293 cell line (HEK293) were used for over-expression studies. *E.coli* DH5α strains were used for molecular cloning and *E.coli* BL21 (DE3) for protein expression.

2.1.7 DNA constructs

The plasmid encoding JB1 was synthesized and purchased from GENEART (Regensburg, Germany) according to the sequence obtained from NM_001108129. Codon usage was optimized for mammalian expression systems. The plasmid encoding GDP-dissociation inhibitor GDI (R. norvegicus) was a kind gift from Dr. Nathan Pavlos (University of Western Australia, Perth, Australia).

2.2 Methods

2.2.1 Molecular Biology Methods

2.2.1.1 Molecular Cloning

The cDNA of JB1 was subcloned into the EGFP-N1 vector (Clontech) using XhoI and BamHI restriction sites for expression in HEK293 cells. GDI was subcloned into pET-28. Molecular cloning was performed with standard procedures for DNA restriction and purification, ligation of DNA constructs and transformation into competent DH5α-cells [159]. Plasmid purification was done according to the manufacturer's instructions (Macherey-Nagel). DNA primers were purchased from Sigma-Aldrich and DNA sequencing was done by MWG-Biotech AG.

2.2.1.2 Protein Expression

Recombinant His-tagged GDI was expressed and purified according to [160]. Briefly, GDI-His was expressed in *E. coli*-BL21(DE3) cells in 5x 500 ml LB-medium at $37\,^{\circ}\mathrm{C}$. Protein expression was induced at OD_{600} = 0.6 with 0.1 mM IPTG. The bacteria were incubated for 14 h at $29\,^{\circ}\mathrm{C}$ and harvested by centrifugation at 4000 rpm for 15 min. Cell pellets were washed once with ice-cold PBS, frozen in liquid nitrogen and stored at $-80\,^{\circ}\mathrm{C}$. For purification, pellets were resuspended in 100 ml cold lysis buffer (50 mM Tris, 1 mM EDTA, 10 mM β-mercaptoethanol, pH 8 at $4\,^{\circ}\mathrm{C}$), supplemented with 0.5 mg/ml lysozyme and incubated for 30 min at $4\,^{\circ}\mathrm{C}$ followed by two freeze/thaw cycles (liquid N_2, $32\,^{\circ}\mathrm{C}$). NaCl was added to a final concentration of 300 mM, $\mathrm{MgCl_2}$ to 10 mM, sodium deoxycholate to 0.5 mg/ml and DNAse I to 0.05 mg/ml. Samples were incubated for 45 min at $4\,^{\circ}\mathrm{C}$ and centrifuged for 30 min at 13 5000 rpm. The GDI containing supernatant was combined with 5 ml Ni-NTA-agarose beads and rotated for 1 h at $4\,^{\circ}\mathrm{C}$. The beads were collected in a column and washed with 50 ml NTA-buffer (50 mM MES, 300 mM NaCl, 50 μM EGTA, 1 mM $\mathrm{MgCl_2}$, 10 mM β-mercaptoethanol and 25 mM imidazol, pH 6). GDI was eluted in 5 ml steps with NTA-elution buffer (50 mM MES, 300 mM NaCl, 50 μM EGTA, 1 mM $\mathrm{MgCl_2}$, 10 mM β-mercaptoethanol and 400 mM imidazol, pH 6). Distribution of His-GDI was determined by SDS-PAGE and the fractions containing His-GDI dialyzed over night against 2 L MonoQ buffer (25 mM Tris, 1 mM DTT, 0.5 mM EDTA, 1% sodium cholate, pH 7.4 at $4\,^{\circ}\mathrm{C}$). The dialyzed solution was filtered through a 0.22 μM membrane and loaded on a 5 ml MonoQ column (Amersham) using an Akta-purifier FPLC system (GE Healthcare). The protein was eluted with a linear gradient of 0-500 mM NaCl in MonoQ buffer. Samples containing GDI were pooled, concentrated and dialyzed against 2x 1 l 25/125 buffer (25 mM HEPES-KOH, 125 mM potassium acetate, pH 7.4). Proteins were frozen in liquid nitrogen and stored at $-80\,^{\circ}\mathrm{C}$.

2.2.1.3 Protein Determination

Protein concentrations were determined using BCA [161]. Micro BCA assays were performed in a 96-well plate using Pierce BCA Protein Assay Kits (ThermoFischer) according to the manufacturer's manual.

2.2.2 Cell Biological Methods

2.2.2.1 Cell Culture

HEK293

Cells were cultured in the following growth medium (DMEM, 10% fetal calf serum (FCS), 4 mM glutamine and 100 units/ml each of penicillin and streptomycin). Cells were grown to 80% confluence on 10 cm culture dishes, at $37\,^{\circ}\mathrm{C}$ with 10% CO_2 and 90% humidity. HEK293 cells were passaged 3 times a week by detaching them from the plates using trypsin/EDTA (Lonza GmbH, Wuppertal, Germany).

Primary Neurons

High density hippocampal primary neurons were prepared from brains of newborn rats as describend in [162]. Neurons grown 10-14 DIV were used for the experiments performed here. The cultures were kindly provided by Martina Bremer (ENI, Goettingen).

2.2.2.2 Transient Transfection

HEK293 cells were seeded in 6-well plates one day before transfection. For transient transfection, the Lipofectamine 2000 transfection reagent was used. For each well, 4 μg of purified plasmid DNA was mixed with 250 μl DMEM without supplements. 10μl of Lipofectamine 2000 reagent were separately mixed with another 250 μl DMEM (no supplements) and left for 5 min at room temperature. Afterwards, the lipofectamine-DMEM solution was mixed with the DNA-solution and left for 20- 40 min at room temperature. Subsequently, a total volume of 500 μl lipofectamine-DNA-mixture was added to the cells and incubated for 24 hours.

For expression level analysis of the transfected DNA, cells were lysed the next day. Therefore cells were washed once with ice-cold PBS and then incubated with 500 μl lysis buffer (150 mM NaCl, 1 mM EDTA, 1% Triton X-100, 50 mM HEPES-KOH, pH 7.3 supplemented with Complete protease inhibitor cocktail (Roche)) for 15 min on ice. The cell suspension was centrifuged for 10 min at 10000 rpm at $4\,^{\circ}\mathrm{C}$ and the supernatant analyzed by Western blotting.

2.2.2.3 Immunofluorescent Staining

Hippocampal neurons were grown for 10-14 days in vitro (DIV) and fixed with 3.7% paraformaldehyde (PFA) in PBS. PFA was removed and coverslips were washed 3 times with PBS for 5 min each. Afterwards, neurons were permeabilized by incubation with 0.3% Triton-X-100 in PBS for 5 min and washed again 3x 5min with PBS before they were blocked in 10% normal goat serum (NGS) in PBS for 30 min at room temperature. Primary antibodies were diluted as indicated in 10% NGS/PBS. In a dark humidified chamber, coverslips were inverted on 25 μl drops of antibody solution that were placed on parafilm. Incubation with primary antibodies was done for 1 h. Afterwards, coverslips were replaced into the 24-well plate and washed for 3x 5 min with PBS. This procedure was repeated for incubation with the secondary antibody. Stained coverslips were mounted on microscope slides by inverting them on a drop of mounting medium (Fuoro-Gel, Electron Microscopy Sciences). Excess mounting medium was removed and samples solidified overnight at $4\,^{\circ}\mathrm{C}$.

For immunofluorescent staining of synaptosomes, coverslips were pre-coated with poly-L-Lysine. 2 ml synaptosomes collected from sucrose gradients (as described in section 2.2.4.1) were diluted in 5 ml PBS and centrifuged for 30 min at 5500 *g* at $4\,^{\circ}\mathrm{C}$. The synaptosomal pellet was resuspended in 2.4 ml PBS. 200 μl of this synaptosomal solution was carefully placed on a coated coverslip placed in a 12-well plate and incubated for 45 min at room temperature. Afterwards, 1 ml PBS was added to each well and synaptosomes pelleted on the coverslip by centrifugation for 30 min at 5500 rpm. Fixation and staining of synaptosomes was done as described for hippocampal neurons.

2.2.2.4 Image acquisition and processing

Neuronal and synaptosomal images were acquired using a AOBS SP2 confocal microscope (Leica Microsystems) with a 63x oil-immersion objective, standard filter sets (Leica Microsystems) and Leica LCS Lite software. For linescan analyses and overlays, images were processed using the LAS AF Lite software (Leica).

2.2.3 Biochemical Methods

2.2.3.1 SDS-PAGE and Western Blotting

For the analysis of regular proteins (<130 kDa), samples were separated in a 10% denaturating Tris/Tricine SDS polyacrylamide gel electrophoresis system, as described by [163] and [164]. The resolving gel (10% bis-acrylamide, 0.1% SDS, 10% glycerol, 1 M Tris pH 8.45) and the stacking gel (4% bis-acrylamide, 0.1% SDS, 1 M Tris pH 8.45) were polymerized by adding ammoniumpersulfate and TEMED . Samples were incubated 10 min at $70\,^{\circ}\mathrm{C}$ before loading. Separation was performed in a discontinuous buffer system, with a 0.2 M Tris pH 8.9 anode buffer and a 0.3 M Tris pH 8.45, 0.03% SDS cathode buffer. For the analysis of large proteins (>130 kDa), precasted NuPAGE®Bis-Tris gradient gels containing 4-12% acrylamide were used. The NuPAGE®system is based upon a Bis-Tris-HCl buffered pH 6.4 polyacrylamide gel, with a separating gel that operates at pH 7.0.

Western blotting was done according to [165]. Protein transfer from the gel to a nitrocellulose membrane was achieved in transfer buffer (200 mM Glycine, 25 mM Tris, 0.04 % SDS, 20 % Methanol) by applying 50 mA for an hour using a semi-dry gel transfer apparatus. Large protein were transferred in MOPS buffer (Invitrogen) by using a tank apparatus and applying 40 mA for 1 h. After transfer, membranes were blocked for 30 min at room temperature with blocking buffer (5% nonfat milk powder in TBST) and then incubated with the primary antibody diluted in blocking buffer at $4\,^{\circ}\mathrm{C}$ overnight. Membranes were washed 3 times with TBST for 10 min and then incubated with HRP-conjugated secondary antibodies in blocking buffer for 1 hour at room temperature. After another 3 washes (10 min each), membranes were covered with Western Lightening ™*Plus*-ECL and protein bands visualized by using chemiluminescence detection on a LumiImager (Boehringer Ingelheim).

2.2.3.2 Protein Extraction with Triton-X-114

Membrane proteins were enriched from cytosolic proteins using the detergent Triton-X-114 as described in [166]. Protein samples were diluted with PBS to a final concentration of 1 mg/ml. Triton-X-114 was added to a final concentration of 1% followed by an incubation on ice for 15 min. Undissolved particles were removed by centrifugation for 5 min at 5000 rpm and $4\,^{\circ}\mathrm{C}$. To achieve phase partitioning, the supernatant was heated to $30\,^{\circ}\mathrm{C}$ for 5 min and afterwards laid on top of a warm sucrose cushion consisting of 6% sucrose in PBS and 0.06% Triton-X-114. The sample was spun for 3 min at 300g and room temperature in a swing-out rotor. The detergent phase containing hydrophobic proteins was collected as an oily droplet

at the bottom of the tube. The extraction was repeated one more time and the final detergent pellet resuspended in ice cold PBS.

2.2.3.3 Preparation of Immunobeads

Conjugation of synaptophysin antibody to Eupergit C1Z beads to was done as described in [167]. Before the coupling procedure, synaptophysin antibody (ascites) was dialyzed extensively against 150 mM NaCl for 3 days with at least 7 changes. After dialysis, the solution was centrifuged for 15 min at 10000 *g* and the supernatant used for coupling. The desired amount of beads was washed twice with H_2O by vortexing vigorously and applying ultrasonication in a waterbath for 2 min. Beads were centrifuged for 6 min at 1300 *g* and resuspended in the synaptophysin solution containing at least 1 mg/ml antibody. 1 mg antibody for 0.1 g beads was used. Beads were vortexed and rotated for 8 h at $21\,^{\circ}\mathrm{C}$. Afterwards, coupled beads were centrifuged for 6 min at 1300 *g* and the supernatant saved for protein determination in order to measure coupling efficiancy. 1 M glycine was added to the bead pellet, resuspended by vortexing and rotated for at least 8 h at room temperature to quench remaining binding sites. Beads were washed 3 times alternating with 0.1 M sodium acetate, 0.5 M NaCl pH 4.5 and 0.1 M Tris, 0.5 M NaCl pH 8.0 (6 washes total). As a final step, beads were washed once with PBS and resuspended in 4 dry volumes PBS (4 ml per 1 g beads). Beads can be stored at $-80\,^{\circ}\mathrm{C}$ without loss of activity.

2.2.3.4 Preparation of Synaptosomes

Synaptosomes were isolated from 6-weeks old wistar rats as described in [149]. Briefly, 2 rats were decapitated and cortices and cerebellum dissected. Samples were homogenized with a glass-teflon homogenizer in 30 ml ice-cold homogenization buffer (320 mM sucrose, 5 mM Hepes, pH 7.4) supplemented with PMSF/Pepstatin using 9 strokes at 9000 rpm. To remove cell debris, the homogenate was centrifuged 2 min at 5000 rpm and $4\,^{\circ}\mathrm{C}$ in a SS34 rotor. The supernatant was collected and re-centrifuged for 12 min at 11000 rpm. The supernatant containing brain cytosol was discarded and the synaptosome containing pellet resuspended in 5 ml homogenization buffer. A small brownish mitochondial fraction in the pellet was cautiously avoided. The suspension was laid on two 3-step discontinuous Ficoll gradients (one gradient per cortex) consisting of 4 ml 13% Ficoll (in homogenization buffer), 1 ml 9% Ficoll and 4 ml 6% Ficoll. Gradients were centrifuged 35 min in a SW41 swing-out rotor (Beckman) at 22500 rpm and the resulting band at interface between 13% and 9% Ficoll collected. Bands were diluted with 10 ml homogenization buffer and pelleted by centrifugation for 12 min at 11000 rpm. The final synaptosomal pellet was resupended in 5 ml fresh homogenization buffer and

the protein concentration was determined using BCA. Generally, yields range between 7-10 mg synaptosomes per 2 rat brains.

2.2.4 Protease Treatment of Synaptosomes

Five mg synaptosomes (isolated as described above) were carefully centrifuged for 3 min at 8700 *g*. The pellet was resuspended in 20 ml sucrose buffer (320 mM sucrose, 5 mM Hepes, pH 8 at room temperature) and supplemented with 500 μl of a trypsin solution (0.1 mg/ml, Roche) resulting in a protein-protease ratio of 100:1. Synaptosomes were incubated for 30 min at $30\,^{\circ}\mathrm{C}$ with occasional mixing. Afterwards, synaptosomes were pelleted again for 3 min at 8700 *g* and protease activity was stopped by resuspending the pellet in the desired amount sucrose buffer containing 400 μM Pefabloc.

2.2.4.1 Separation of Protease Treated Synaptosomes from the PSD

Protease treated synaptosomes (as described above) were resuspended in 5 ml sucrose buffer containing 400 μM Pefabloc. To separate shaved synaptosomes from the postsynaptic densities, 3 ml of the sample were loaded on a continuous sucrose gradient (25-50% (w/v) sucrose in 5 mM Hepes pH 8.0) and centrifuged for 3 h at 180000g (28000 rpm) in a SW28 swing-out rotor (Beckman). Continuous sucrose gradients were generated with an automatic gradient mixer (Gradient master, Biocomp) aacording to the manufacturer's instructions. After centrifugation, 1.5 ml fractions were collected from the gradient from bottom to top using a semi-automatic pump system (Minipuls3, Abimed Gilson).

Fractions containing digested synaptosomes, so called "shaved" synaptosomes, were either identified by measuring the refraction index or dot blotting. Shaved synaptosomes were found in the fractions with a refraction index of 1.391-1.392, which corresponds to 1.2 M sucrose. For dot blotting, 2 μl of each fraction was spotted on a dry nitrocellulose membrane and soaked in for 5 min. Afterwards, the membrane was incubated for 10 min at room temperature in blocking buffer (5% non-fat milk powder in TBST). Incubation with the primary antibody against synaptophysin was done for 15 min in blocking buffer. After washing the membrane 3 times for 3 min each with blocking buffer, the blot was incubated with secondary antibody for 15 min. After another 3 washes (3 min each) with TBST, membranes were incubated with Western Lightening $^{\text{TM}}$*Plus*-ECL and protein bands visualized by using chemiluminescence detection on a LumiImager.

2.2.4.2 Immunoisolation of Docked Vesicles from Protease treated Synaptosomes

Protease-treated synaptosomes (as described previously) were resuspended in 300 μl sucrose buffer containing 400 μM Pefabloc. Synaptosomes were lysed by adding 2.7 ml ice-cold H_2O followed by homogenization with a glass-teflon homogenizer with 3 strokes at maximum speed. Afterwards, 15 μl 1 M Hepes pH 8, 3 μl 200 mM PMSF (in ethanol) and 3 μl 2 mg/ml pepstatin (in DMSO) were added immediately to the solution. Docked and free synaptic vesicles were separated on a 15-45 % continuous sucrose gradient (w/v) prepared with a gradient mixer (Gradient master, Biocomp). Samples were loaded on the gradient and centrifuged for 1 h at 100000 *g* in a SW28 swing-out rotor (Beckman). Twenty-four 1.5 ml fractions were collected from bottom to top and analyzed by dot blotting for synaptophysin (as described before). Docked vesicles were generally localized in fractions 4-7 and free vesicles in fractions 19-21. Fractions containing docked vesicles were pooled (SPM), the same was done for fractions containing free vesicles (SV). For one immunoisolation, 5 μl Eupergit C1Z beads coupled to the antibody for synaptophysin (Eupergit-7.2) were washed with 1x IP buffer (1x PBS, 3 mg/ml BSA, 5 mM Hepes pH 8.0). For docked vesicles, 600 μl SPM fraction and 600 μl 2x IP buffer (2x PBS, 6 mg/ml BSA, 5 mM Hepes pH 8.0) were added to the bead pellet. For the isolation of free vesicles, 300 μl SV fraction and 900 μl 1x IP buffer was used. Beads were gently vortexed and rotated over night at $4\,^{\circ}\mathrm{C}$. Afterwards, beads were spun down for 3 min at 2000 rpm in a table top centrifuge. Immunoisolates were washed 3 times with PBS by vortexing, incubation on ice for 5 min and centrifugation for 3 min at 2000 rpm. After a final centrifugation step for 3 min at 10000 *g*, immunoisolates were either eluted by adding 2x LDS sample buffer and incubation for 10 min at $70\,^{\circ}\mathrm{C}$ or were processed for mass spectrometric analysis according to the iTRAQ labeling method (see section 2.2.5.1.

2.2.5 Mass Spectrometry Methods

2.2.5.1 iTRAQ labeling

Ten immunoisolations for both docked and free vesicles were done simultaneously and samples from 5 immunoisolations were pooled after the washing steps, resulting in 4 final samples (2x SPM, 2x SV). Immunoisolated docked and free SVs were then solubilized by resuspension of the bead pellets in 28 μl 1 % RapiGest SF (Waters) in 100 mM triethylammonium bicarbonate (TEAB) buffer and incubated for 10 min at $70\,^{\circ}\mathrm{C}$. Solubilized proteins were digested in the presence of the beads by trypsin according to [168]. Briefly, 4 μl 100 mM TEAB buffer and 2 μl reducing agent (supplied with the iTRAQ Kit) were added to the beads and incubated for 1 h at $37\,^{\circ}\mathrm{C}$ with shaking (750 rpm). Afterwards, the bead suspension was supplemented with 1 μl

200 mM iodoacetamide and incubated for another 20 min at $37\,^{\circ}\mathrm{C}$ with shaking (750 rpm). For digestion of the proteins, 5 μl trypsin (0.2 μg/μl in 100mM TEAB, Promega) was added and incubated overnight at $37\,^{\circ}\mathrm{C}$ with shaking. Beads were pelleted for 20 min ($4\,^{\circ}\mathrm{C}$) at maximum speed in a table top centrifuge and the supernatants transferred to clean tubes. Tryptic peptides were then tagged with iTRAQ reagent according to manufactures instructions (iTRAQ reagent kit, Applied Biosystems). iTRAQ reagents were spun down before use and ethanol added to a final volume of 170 μl per tube. Eighty-five μl of reagent was added to both of each sample (docked SVs were tagged with iTRAQ 117, and free SVs with iTRAQ 116) and incubated for 3 h at $37\,^{\circ}\mathrm{C}$ with shaking (750 rpm). Afterwards, each sample labeled with iTRAQ-116 was mixed with one labeled with iTRAQ-117. The resulting samples were supplemented with 20 μl 5% trifluoracetic acid (TFA) for pH adjustments (pH = 2) and incubated for 1 h at $37\,^{\circ}\mathrm{C}$ with shaking. After centrifugation for 30 min at maximum speed at $4\,^{\circ}\mathrm{C}$, supernatants were of all samples were combined in one tube.

2.2.5.2 SCX Fractionation

After tryptic diegestion and iTRAQ labeling the peptides were fractionated manually over an ICAT strong cation-exchange (SCX) column (Applied Biosystems) according to the manufacturer's instructions. The sample volume of about 800 μl was reduced to less than 200 μl using a vacuum centrifuge at medium heat and then diluted in 2 ml SCX loading buffer (10 mM $\mathrm{KH_2PO_4}$, 25% acetonitrile, pH 3.0). The SCX column was equilibrated by injecting 2 ml of loading buffer before the sample was slowly loaded. The column was washed by injecting 1 ml of loading buffer. Peptides were eluted stepwise by adding 500 μl of KCl-solutions of increasing concentration (5, 100, 150, 200, 300, 400, 500, 600, 800, and 1000 mM) in 10 mM $\mathrm{KH_2PO_4}$, 25% acetonitrile, pH 3.0. The samples were desalted on a hand made micro column with POROS Oligo R2 RP material as described in [169]. Briefly, all 10 SCX fractions were dried in a vacuum centrifuge at medium heat until salt precipitation has occurred and the precipiates were resuspended in 100 μl 0.3% TFA. High salt fractions (800 and 1000 mM KCl) were resuspended in 200 μl of 0.3% TFA. Samples were incubated for 30 min at room temperature with shaking. Each SCX fraction was cleaned as followed: The handmade RP column was washed by applying 100 μl of 0.1% TFA with a syringe, followed by loading of the sample on the column, a washing step with 100 μl of 0.1% TFA and an elution by applying 20 μl of 50% acetonitrile, 0.5% formic acid. At the end all remaining peptides were eluted with 20 of μl 90% acetonitrile. Samples were dried using a vacuum centrifuge and stored at $-20\,^{\circ}\mathrm{C}$.

2.2.5.3 Mass Spectrometry and Quantification

The SCX-fractions were dissolved in 12μl 5% formic acid of which 5μl were analyzed on a Thermo LTQ XL Orbitrap (Thermo Fisher Scientific) that is coupled to an Agilent 1100 series LC-system (Agilent Technologies). In the LC system, peptides were separated at a flow rate of 200-300 nl/min on a self-made reversed phase column (C18, Reprosil, Maisch) and eluted with a 118 min gradient from 7.5-40% mobile phase B (80% acetonitrile, 0.15% formic acid). Peak list analysis was done by searching against NCBI RefSeq database of r.norvegicus using Mascot v.2.2.04 as the search engine. Mass accuracy was 10 ppm for the parent ion and 30 ppm for fragment ions. For the analysis, only tryptic peptides with a maximum of 2 missed cleavages were taken into account. Fixed modifications included carbamidomethylation of cysteines, whereas oxidations of methionine residues were considered as variable modification. Quantification was done by using Mascot v 2.2.04. and was constrained to peptides with a scores >15. The protein ratio was calculated as a weighted median ratio, but only included proteins quantified with unique peptides and a minimum of 3 peptides.

2.2.5.4 Data Normalization

The analysis of the statistical distribution of the docked/free vesicles peptide and protein ratios from each biological replicate showed a minor bias towards the free vesicles in one biological replicate, indicating that the number of immunoisolated vesicles was slightly more than in the docked vesicle sample in this replicate. A normalization to equal amounts of vesicles was done on the protein level, taking the vacuolar ATPase as a reference. For this replicate, all protein ratios were multiplied by 0.67 resulting in a balanced distribution around a 1.1 ratio for all major SV proteins. In the other two biological replicates, the amount of immunoisolated vesicle proteins within the docked and free vesicle fractions were comparable without normalization.

2.2.6 Rab Extraction Assay

Rab extraction by GDI was performed as described in [170]. Docked vesicles were collected from the sucrose gradient (as described in section 2.2.4.2) and diluted 1:1 in 2x IP buffer (2x PBS, 5 mM Hepes pH 8.0, 6 mg/ml BSA). Samples were supplemented with GDP or GTPγS to a final concentration of 500 μM and Complete protease inhibitor cocktail (Roche) and kept on ice for 15 min. Afterwards purified GDI (see 2.2.1.2) was added to a concentration of 0.5 μM and samples incubated for 30 min at 37 °C.

Samples were either further processed by immunoisolation of vesicles (as described in section 2.2.4.2) or fractionated by a floatation assay. For the floatation assay, a 3-step discon-

tinuous sucrose gradient was generated by overlaying 1 ml of the sample with 500 μl 0.7 M sucrose and 500 μl 0.32 M sucrose. The gradient was centrifuged for 3 h at 255000 *g* in a TLS-55 rotor (Beckman) and fractions carefully collected from the top by pipetting 200 μl aliquots.

2.2.7 Electron Microscopy

Electron microscopy on synaptosomes was carried out by Dr. Dietmar Riedel (MPI for Biophysical Chemistry, Goettingen). Synaptosomes were fixed by aldehydes and embedded in epon for preparing ultra-thin sections. Sections were analyzed using a Philips 120 kV BioTwin microscopes equipped with a 1024x1024 pixel GATAN CCD camera.

3 Results

3.1 Establishment of a protocol for the isolation of presynaptic membrane fractions

Although many key players of the presynaptic active zone have been identified, the exact molecular architecture of the sites at which synaptic vesicles are attached to the plasma membrane is still not fully understood. To provide insights into the protein composition of synaptic vesicle docking sites, it is necessary to isolate such fractions with sufficient purity. So far it has been very challenging to separate presynaptic membranes and the postsynaptic protein scaffold. The protocol developed in this work is based on the biochemical properties of conventionally isolated synaptosomes [149]. Synaptosomes are resealed nerve terminals. As such they are membrane enclosed sacks that contain the presynaptic excitatory machinery as well as cytosolic proteins and other organelles e.g. mitochondria. Additionally, a portion of the postsynaptic density remains tightly attached on the outside of these resealed compartments and accounts for its copurification with the presynaptic compartment [171]. With this in mind, the approach employed here includes a mild proteolysis of the synaptosomes to remove the postsynaptic membranes. Such a proteolytic treatment is expected to cleave the synaptic adhesion molecules responsible for the tight attachment between pre- and postsynaptic components as well as the extracellular domains of receptors and ion channels. In contrast, components of active zones are protected from proteolytic degradation since the membrane enclosing the presynaptic compartment presents a physical barrier against protease entry. Unfortunately, most of the PSD proteins appeared to be largely resistant to proteolysis. Therefore, an additional sucrose gradient centrifugation step was necessary to effectively separate PSD components from presynaptic proteins according to their mass and density (see Fig.3.1 A). As mentioned above, the interior of synaptosomes include mitochondria, docked as well as free vesicles and cytosolic proteins. To separate these contents, the protease treated and purified synaptosome fraction was lysed by osmotic shock prior to the continuous sucrose density gradient centrifugation. In a final step, docked vesicles and free vesicles were purified from a fraction of this gradient by

immunoisolation using Eupergit C1Z beads containing immobilized antibodies specific for the synaptic vesicle protein synaptophysin (Fig. 3.1 B).

3.1.1 Removal of the postsynaptic density from synaptosomes

3.1.1.1 Optimization of the protease treatment and separation of pre- and postsynaptic compartments

Following the purification of synaptosomes according to the protocol described by [149], the synaptosomes were resuspended in a suitable buffer and several modifications to a basic digestion protocol were systematically introduced and experimentally assessed for their effectiveness in removing PSD components from intact synaptosomes.The basic digestion protocol involves the following steps:

(a) Digestion of synaptosomes with proteases
(b) Stopping protease activity
(c) Harvesting of the digested synaptosome

Modifications to this protocol are described in the remainder of this section. Of the commercially available proteases, trypsin and proteinase K were tested in this study for their efficiancy in removing the PSD. Trypsin is the preferred protease, because it is compatible with subsequent sample preparation procedures for mass spectromic analysis. Proteinase K with its versatility and consistent activity in a broad range of conditions was tested as an alternative candidate. The enzymatic activity of proteases depends on several parameters including their concentration (protein:protease ratio), incubation temperature and time, buffer composition. To obtain the optimal digestion conditions, each of these parameters were systematically tested.

The buffer system was first chosen to provide basic conditions for optimal digestion. Two different buffer systems are commonly used when working with synaptosomes. A low ionic strength sucrose buffer (320 mM sucrose, 5 mM HEPES pH 7.4) is used during the preparation of synaptosomes and a moderate salt solution "sodium buffer" (10 mM Glucose, 5 mM KCl, 140 mM NaCl, 5 mM $NaHCO_3$, 1 mM $MgCl_2$, 1.2 mM Na_2HPO_4, 20 mM HEPES pH 7.4) is often employed in stimulation-dependent glutamate release assays [149]. Both buffer systems were tested for their compability with the selected proteases. Trypsin was added to the synaptosomes at a protein/protease ratio of 1:300, followed by an incubation for 10-60

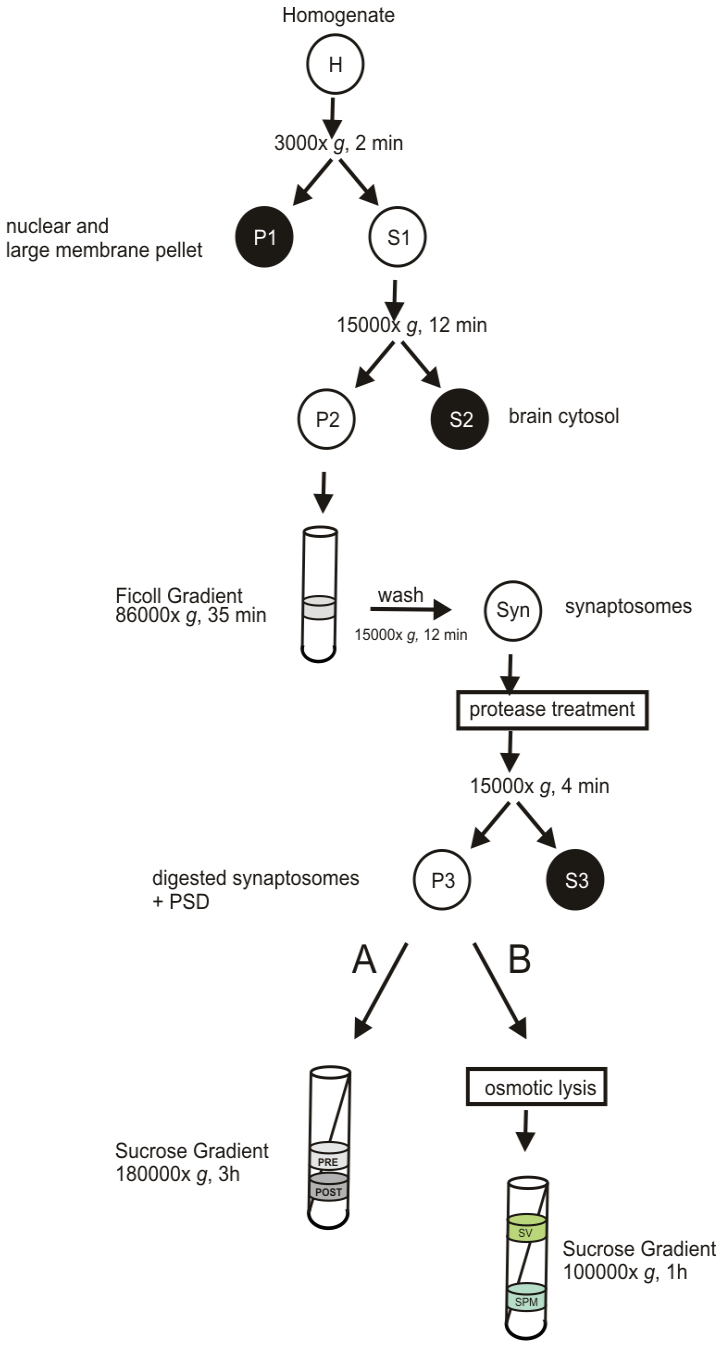

Figure 3.1: Schematic overview of the protocol for isolating presynaptic membrane fractions. Synaptosomes were prepared as described in [149] and subjected to mild protease treatment to digest the proteins in the synaptic cleft. Afterwards, shaved synaptosomes were either (A) separated from postsynaptic membranes in a continuous sucrose gradient afterwards or (B) lysed and fractionated on a continuous sucrose gradient yielding a docked vesicle fraction (SPM) and and a free vesicle fraction (SV).

minutes at $30\,^{\circ}\mathrm{C}$. Afterwards the enzyme activity was stopped by adding the irreversible serine protease inhibitor Pefabloc to the sample. Synaptosomes were then pelleted and washed once with buffer. The efficiency of digestion was assayed by monitoring the amount of postsynaptic receptor NR1 remaining after the reaction was stopped. Additionally, levels of the presynaptic protein Munc18 and the synaptic vesicle protein synaptophysin were also analyzed to determine if undesired proteolytic degradation had occured in the presynaptic compartments. Interestingly, synaptosomal digestion by trypsin in sucrose but not sodium buffer led to a gradual decrease in the amount of NR1 (Fig 3.2 A). In both buffers, proteins localized inside the synaptosome are not affected. This result indicated that the sodium buffer is unsuitable for use as a buffer in this procedure. One likely explanation for this is that synaptosomes appear to aggregate in the sodium buffer but not the sucrose buffer after the pelleting steps in the procedure.

Next, the efficiancy of trypsin versus proteinase K was assessed. As shown in Fig. 3.2 B, proteinase K is a more potent protease that also digested proteins inside the synaptosome exemplified by Munc18. In theory, this protein is protected by the synaptosomal membrane and should not be degraded. Nevertheless, these experiments indicated that proteinase K was able to enter the synaptosome. Interestingly, proteins residing in the vesicle membrane were not affected by any of the proteases. Since proteinase K digested proteins inside of the synaptosomal membrane, trypsin was used in all further experiments.

The effect of temperature and time on the effectiveness of trypsin digestion was subsequently examined. As expected, proteolytic activity increases at higher temperature (Fig.3.2 C). However, for the purification of the docked vesicle fraction it was deemed important to keep the temperature as low as possible. Elevated temperatures raise the possibility of unwanted endogenous protein degradation within the synaptosome as well as other temperature-dependent effects on biological activity (e.g. exocytosis). Consequently, although initial experiments were performed at $30\,^{\circ}\mathrm{C}$, digestions at $25\,^{\circ}\mathrm{C}$ was also tested (Fig.3.2 C). At $25\,^{\circ}\mathrm{C}$, NR1 was inefficiently cleaved, suggesting this temperature is insufficient for optimal proteolytic activity despite prolonging the extension time to 60 min. For practical issues, a further extension of the incubation time longer than 60 minutes was not considered.

Finally, the concentration of trypsin was optimized. Protease/protein ratios of 1:100, 1:200, 1:300 and 1:500 were tested and the efficiency of digestion evaluated over different time intervals. As shown in Fig. 3.2 D, cleavage of NR1 is significantly enhanced at higher protease:protein ratios. At a ratio of 1:100, NR1 became undectable after a 20 minute digestion. In contrast, complete abolishment of the signal was not achieved even after 60 minutes when a 1:500 protease/protein ratio was used. Importantly, the stability of the presynaptic proteins

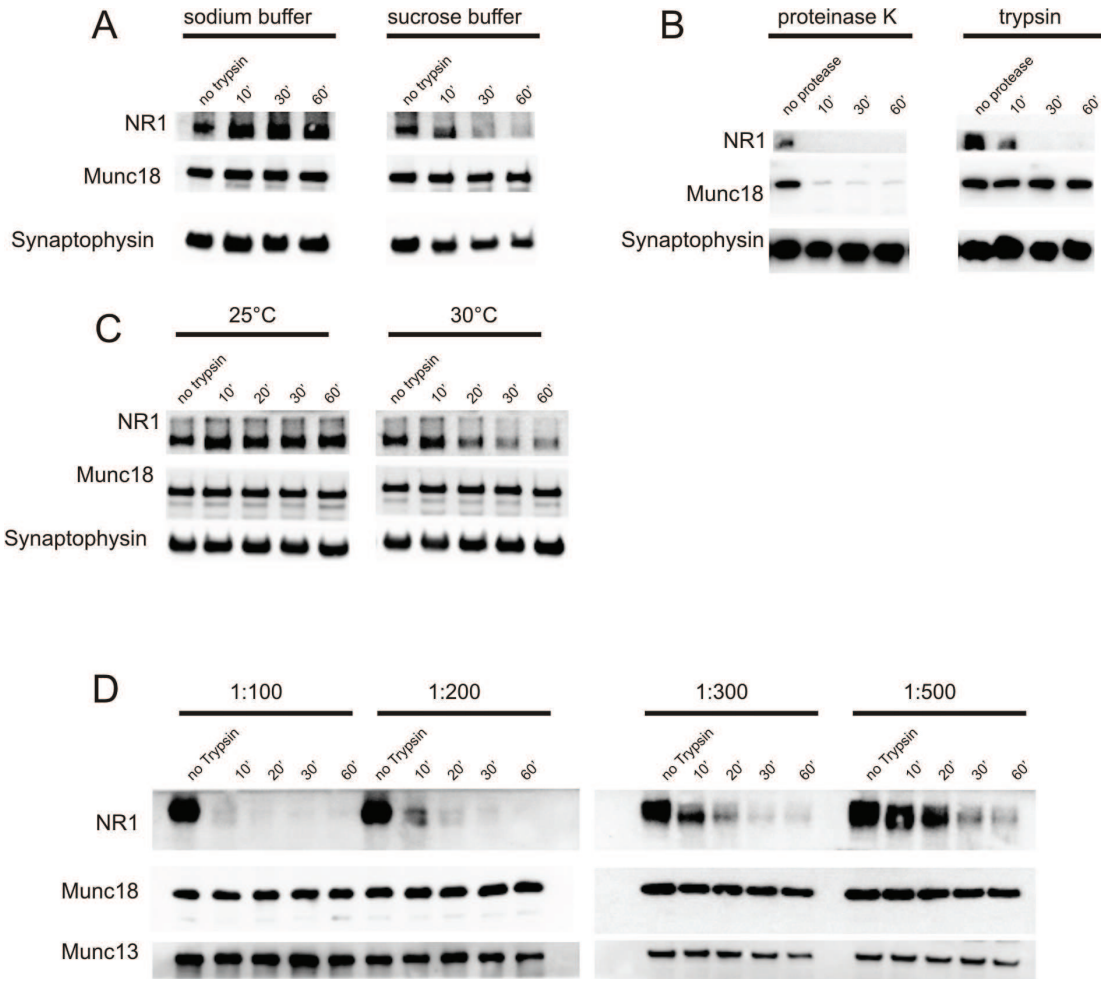

Figure 3.2: Optimization of proteolysis. (A) Proteolytic efficiency in different buffer systems. By using trypsin (protease:protein ratio of 1:300), the postsynaptic NR1 receptor was time-dependent digested in sucrose buffer but not in sodium buffer. Proteins inside the synaptosomal membrane (Munc18 and synaptophysin) are not digested. (B) Comparison of synaptosomal digestion by trypsin and proteinase K. Trypsin induced degradation only affected proteins outside the synaptosomal membrane (NR1). Proteinase K dependent digestion was additionally observed for cytosolic proteins inside of the synaptosome, e.g. Munc18. (C) Temperature dependency of proteolytic activity. NR1 digestion (protease:protein ratio of 1:300) was observed after 20 min at $30\,^{\circ}\mathrm{C}$, but was not achieved after 60 min at $25\,^{\circ}\mathrm{C}$. (D) Effect of trypsin concentration and incubation time on the cleavage of postsynaptic membranes. Digestion of NR1 was time- and concentration-dependant. For NR1 cleavage, a protease:protein ratio of 1:100 was sufficient after 10 min whereas the same degree of digestion needed 60 min at a 1:500 ratio. Presynaptic proteins (Munc13 and Munc18) remain unaffected.

Munc18 and Munc13 remains unaffected. Based on these data, the final digestion protocol was performed using a 1:100 ratio of trypsin to protein concentration in sucrose buffer (320mM Hepes, pH 8) with incubation time of 30 minutes at $30\,^{\circ}\mathrm{C}$.

To better characterize the effect of protease treatment on synaptosomes, additional synaptic proteins were analyzed for their stability by western blotting after trypsinization (see Fig. 3.3). As expected, adhesion molecules that span the synaptic cleft were efficiently degraded after the 30 min digestion. In contrast, presynaptic proteins (including large proteins like Piccolo or Munc13) and synaptic vesicle proteins remain intact. The postsynaptic receptors NR1 and GluR1 appear to be digested. In fact, the epitopes of these proteins recognized by the antibodies used are mapped to the extracellular domains facing the synaptic cleft. Surprisingly, the postsynaptic proteins PSD95 and Homer were resistant to proteolysis. Conceivably, the localization of these proteins deep within the protein network of the postsynaptic specialization renders them less accessible to proteases.

Thus, while the protease treatment succeeded in removing trans-synaptic molecules, certain integral components of the PSD persisted. This suggested that the tight attachment of the PSD to the synaptosome is abolished and led to the idea to separate pre- and postsynaptic compartment according to their biochemical nature. This idea was tested by adding a sucrose density gradient step after the digestion protocol.

3.1.1.2 Separation of pre- and postsynaptic compartments

It is well known that pre- and postsynaptic specializations differ with respect to ultrastructure and biochemical properties [126]. PSDs appear proteinaceous compared to the presynaptic boutons, which are more membraneous. Thus, buoyant densities are suggested be different. In fact, early experiments showed that purified postsynaptic densities are enriched at a 1.4/2.2 M sucrose interface of a discontinuous sucrose gradient [172] whereas synaptosomes are localized to 1.0/1.2 M interfaces in sucrose gradients [150]. Hypothesizing that there might be a shift in the density of the shaved membranous synaptosome versus the protein dense PSD after digestion, a 0.75 M-1.5 M continuous sucrose gradient was chosen to attempt separation of the postsynaptic density from the shaved synaptosome. Indeed, a shift in the migration of PSD95 was observed in protease treated synaptosomes that was not seen for untreated samples (see Fig. 3.4A). Importantly, the signals of the pre- and postsynaptic markers no longer showed significant overlap, indicating that the remaining synaptosomes were devoid of the postsynaptic density. These "shaved" synaptosomes sediment at fractions with an refraction index of 1.391, which corresponds to about 1.2 M sucrose. Additionally, electron microscopy was used to assess if the protease treatment affected the integrity of or induced ultrastructural changes to

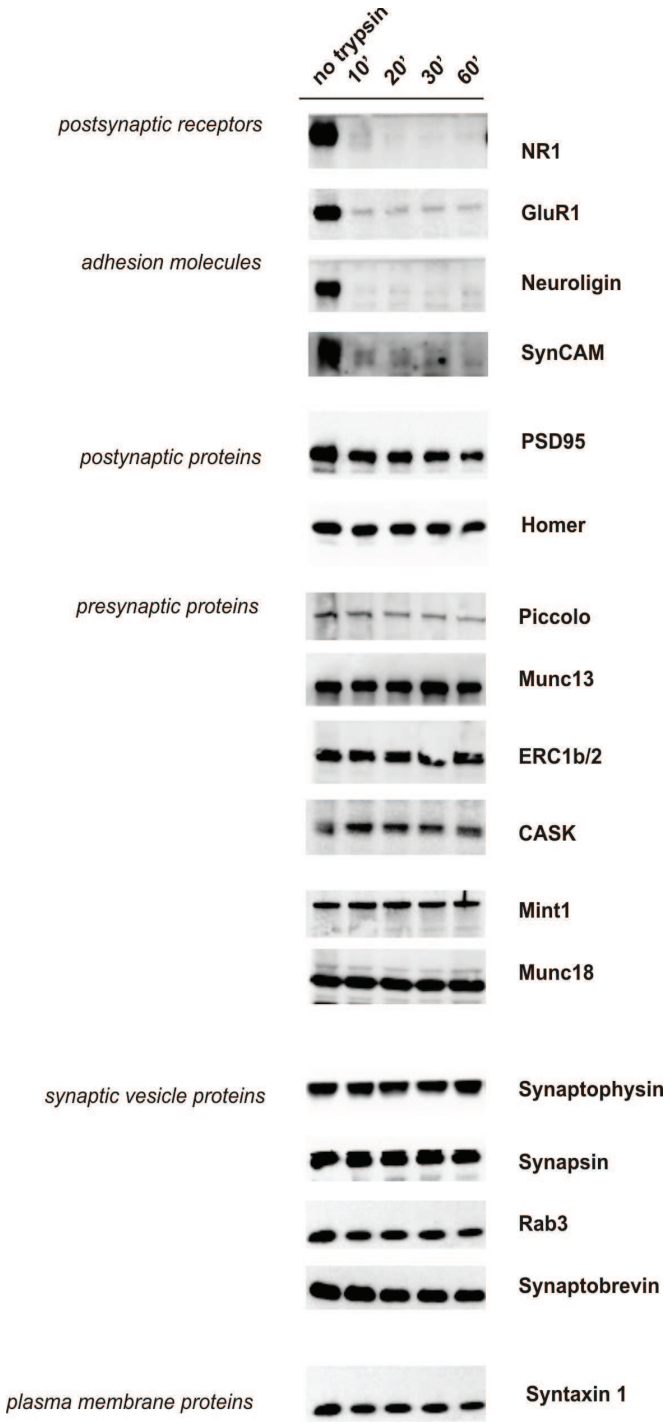

Figure 3.3: Effect of protease treatment on various protein groups. Presynaptic proteins and synaptic vesicle proteins are not affected in their stability after digestion whereas postsynaptic receptors and adhesion molecules are efficiently cleaved. Proteins localized deep inside the postsynaptic density appear resistent to proteolysis.

the synaptosomes. As shown in Fig. 3.4 B, the morphology of synaptosomes was unchanged after trypsination. Specifically, the synaptosomal plasma membrane was intact and the interior filled with synaptic vesicles. Lower magnification electron microscopy pictures also showed that the quantity of synaptosomes appear in the same range.

To validate that the second centrifugation step indeed resolves the two compartments, immunofluorescence microscopy was employed to analyze the distribution of pre- and postsynaptic marker proteins in the protease treated synaptosomes after sucrose gradient centrifugation. Therefore, synaptosomal fractions corresponding to 1.2 M sucrose were collected from the gradient by pelleting on poly-L-lysine coated coverslips and analyzed. The samples were then immunostained with antibodies directed against synaptophysin and PSD95 and their distribution examined by confocal microscopy. Trypsination of synaptosomes is expected to change the intensity of the fluorescence signal detected for postsynaptic proteins (proportional to the protein amount) and extent of co-localization between PSD95 and synaptophysin. As shown in Fig. 3.5A, untreated synaptosomes displayed a very high degree of co-localization of both proteins. In contrast, shaved synaptosomes exhibited both a decrease in PSD95 puncta as well as an abolishment of co-localization between the two proteins. No changes in the signal intensities for synaptophysin was observed. Linescans analysis of the images further verified these observations (Fig.3.5B). Thus, the data demonstrate that the established protocol efficiently removes postsynaptic densities from synaptosomes.

3.1.2 Isolation of a fraction enriched in docked vesicles

3.1.2.1 Lysis of synaptosomes

It is well established that synaptosomes undergo lysis and release synaptic vesicles and mitochondria when they are exposed to hypotonic conditions. Afterwards synaptic membranes and synaptic vesicles can be isolated from the lysate by sedimentation through a density gradient [146]. Such a procedure does not completely separate synaptic vesicles from the membrane. Indeed, lysis generates two different synaptic vesicle populations in the gradient. One vesicle pool migrates at lighter fractions and are identified as free vesicles (SV) and the other population accumulates at denser fractions. These latter synaptic vesicles co-migrate with proteins of the plasma membrane (SPM) as well as with proteins of the postsynaptic density and are therefore assumed to be docked vesicles [173].

Here, protease treated synaptosomes were lysed and the components separated on a 0.4-1.4 M continuous gradient. As previously reported, two vesicle populations were observed corresponding to free (SV) and docked vesicles (SPM) (Fig. 3.6). A more detailed western

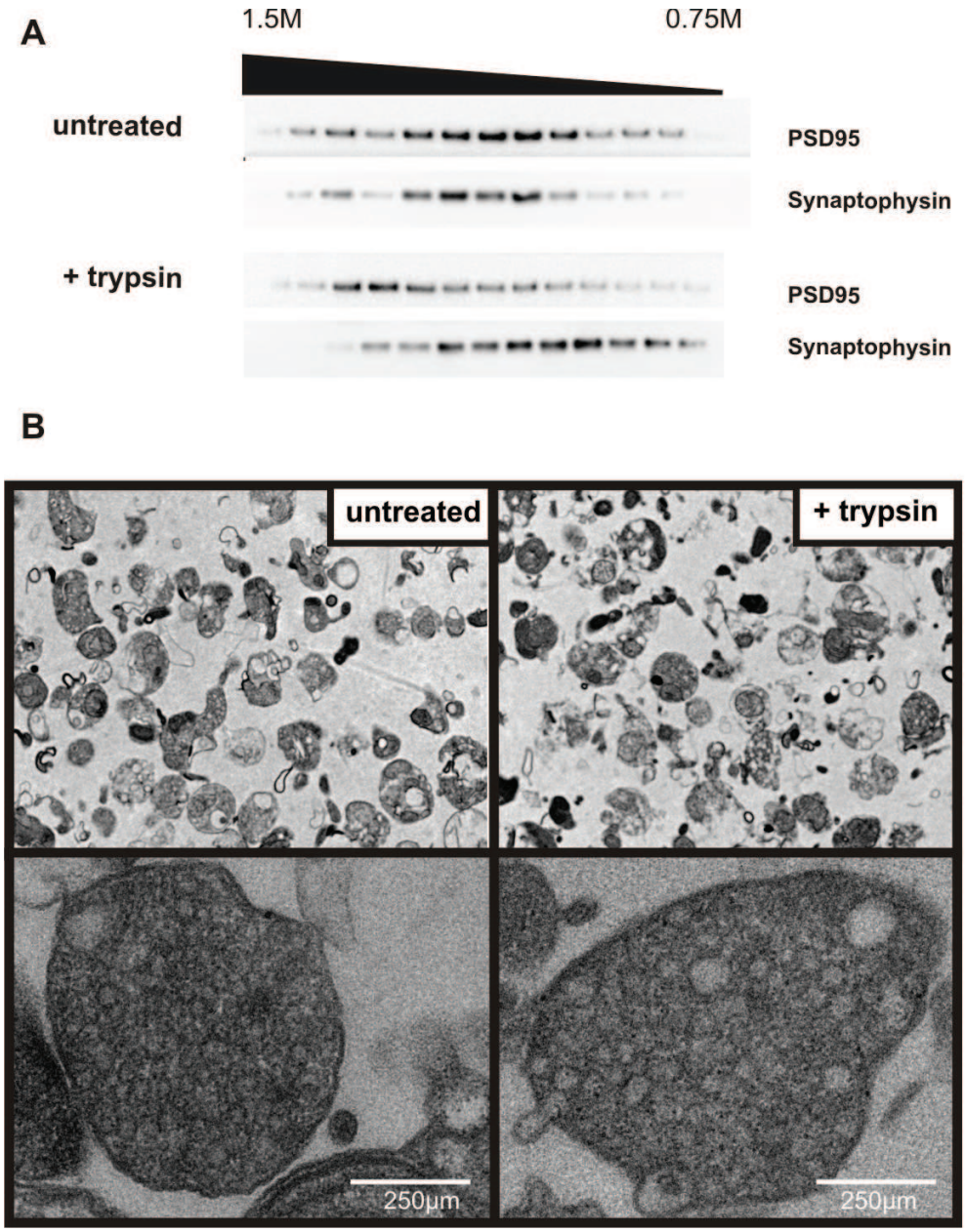

Figure 3.4: (A) Migration pattern of pre- and postsynaptic proteins in a continuous sucrose gradient. After protease treatment, synaptosomes were washed and loaded on a 0.75-1.5 M sucrose gradient. Protease treatment of synaptosomes induced a migration shift of postsynaptic proteins. (B) Electron microscopy of untreated and trypsin treated synaptosomes from a continuous sucrose gradient. Fractions at 1.2 M sucrose were diluted 1:5 in 5 mM Hepes pH 7.4 and pelleted. No obvious change in synapotosome morphology was observed.

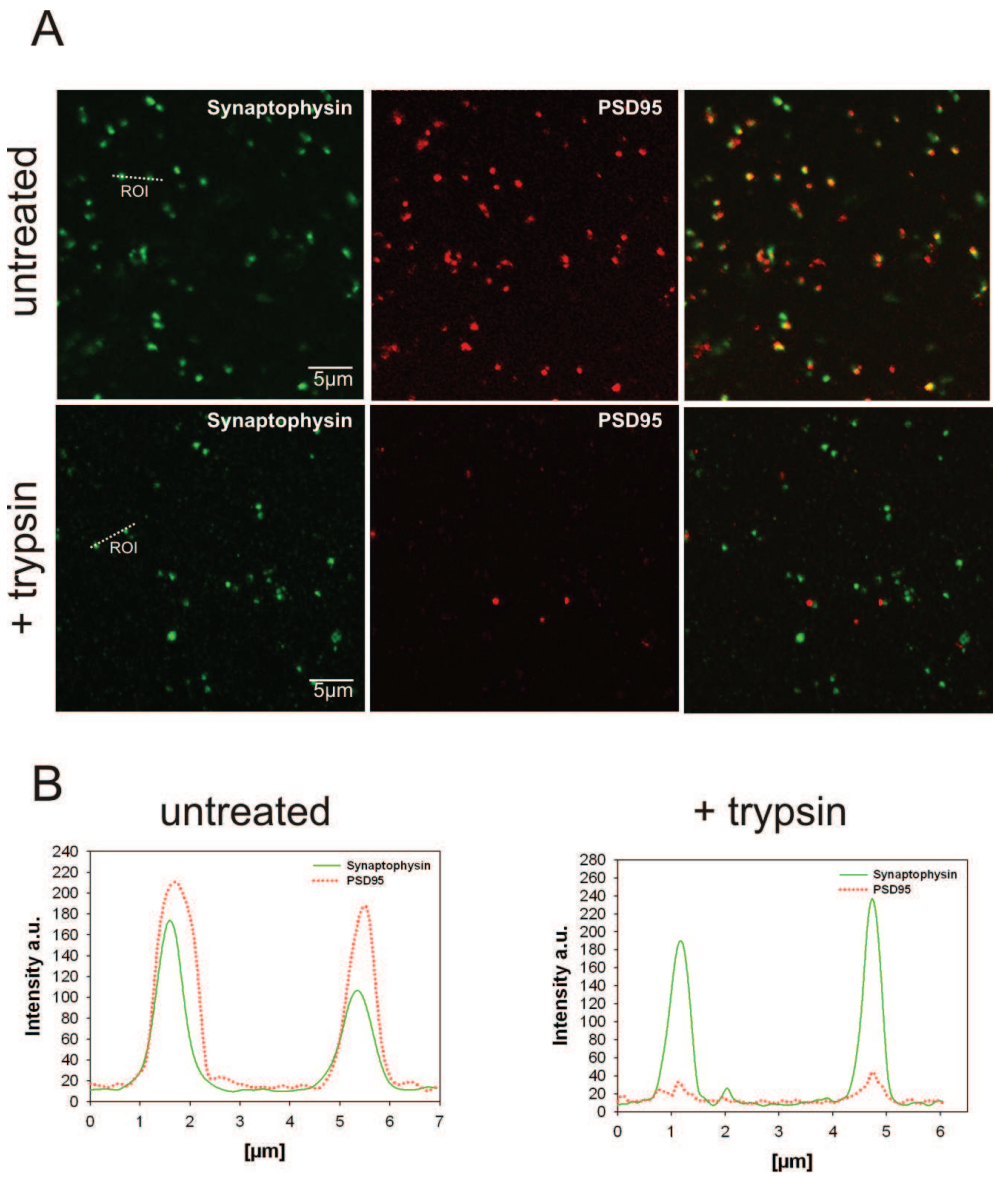

Figure 3.5: (A) Synaptosomal fractions at 1.2 M sucrose in the gradient was pelleted on coverslips and pre- and postsynaptic specializations visualized by immuno-fluorescent staining with antibodies against synaptophysin (green) and PSD95 (red). Protease treatment reduced the detected postsynaptic signal while the presynaptic signal did not change. (B) Linescans showing co-localization of pre- and postsynaptic signal in untreated synaptosomes. Trypsinized samples were devoid of any postsynaptic signal.

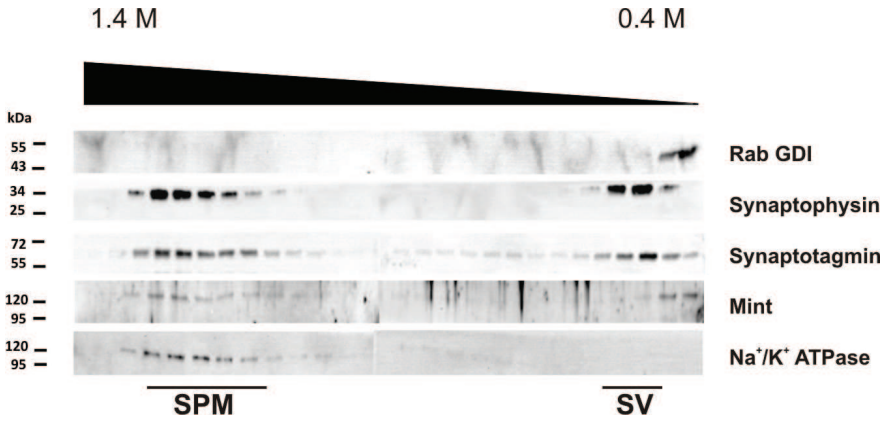

Figure 3.6: Gradient centrifugation of trypsinized and lysed synaptosomes displayed two synaptic vesicle populations. Docked vesicle co-migrated with active zone and plasma membrane marker.

blot analysis of the gradient fractions additionally revealed that the SPM fraction also contained components of the active zone (Mint, Munc13) and mitochondria (SDHA) (Fig. **??**) . These proteins were greatly reduced or absent in the SV fractions. Thus, these data confirms that in addition to the attached vesicles, the presynaptic machinery remains coupled to the plasma membrane following hypotonic lysis.

Mitochondrial contamination in synaptic preparations has been an issue for several decades. A complete separation of these components according to their equilibrium buoyant densities is almost impossible. In the early seventies several groups published different protocols addressing this issue. Davis and Bloom increased the density of mitochondria by histochemically changing the succinic dehydrogenase with tetrazolium [174]. They could show a reduction of mitochondrial contamination of synaptic membranes, but the disadvantage of this protocol is that the procedure might change the stability of the synaptic complexes as it involves additional treatments and elevated temperatures. Another method to improve purity was published by Jones and Matus. They introduced a simultaneous sedimentation and flotation centrifugation step to separate mitochondria from synaptic membranes. Lysed synaptosomes were suspended in sucrose of intermediate density between both buoyant densities, resulting in flotation of SPM and a sedimentation of mitochondria [175]. Although being a true separation based on density, this protocol is limited with respect to the aim of this study, because separation of docked vesicles and free vesicles was not achieved. One of the earliest methods published is based on the pH during lysis. Cotman and Matthews showed that carrying out osmotic shock at alkaline pH greatly enhanced SPM purity [176]. However, these findings could not be reproduced in this work. As shown in fig. 3.7A, varying the pH from 7.5 to 8.5 did not change the distribution of mitochondria in the gradient. Under all conditions tested, the mitochondrial

marker SDHA remained enriched in the SPM fractions. To evaluate if mitochondria in fact only co-migrate in the gradient or are actually an essential part of exocytotic sites at the plasma membrane, the isolated SPM fraction was analyzed for co-localization by immunofluorescent staining (Fig3.7B). Images showed a significant overlap of the presynaptic active zone marker piccolo with the plasma membrane SNARE syntaxin 1. Interestingly, staining of syntaxin 1 appeared to be more dense than piccolo. This indicates that there are stretches of plasma membrane that contain SNAREs but no attached active zone. Based on the observed signals for piccolo and synaptotagmin, the abundance of active zone components to synaptic vesicles was comparable and the proteins were in close proximity as exemplified by the high degree of co-localization of these proteins. In contrast, signals for mitochondria and active zone proteins did not show any significant co-localization. Moreover, mitochondria were present in very high amounts. This supports the idea that mitochondria are only co-migrating with synaptic membranes as a consequence of the closeness of their sedimentation factors and are therefore heavily contaminating these fractions. Thus, additional purification steps for isolating docked vesicles were necessary.

3.1.2.2 Immunoisolation of docked vesicles

To simultaneously minimize mitochondrial contamination and concentrate docked vesicles, a immunoaffinity purification step was added to the existing protocol. The feasibility of this approach has been previously demonstrated [173], but has been modified in this study. Eupergit C1Z beads covalently conjugated to antibodies specific for synaptophysin were used to isolate docked vesicle or free vesicles. Several buffer conditions including variations in salt concentration and supplements were tested to optimize yield while minimizing non-specific attachment of proteins. The best results were achieved using phosphate buffered saline (PBS) supplemented with bovine serum albumin (BSA) as a stabilizer (see Fig. 3.8, first panel). Under these conditions vesicles could be purified from the SPM fractions together with parts of the plasma membrane (as exemplified by the $\mathrm{Na^+/K^+ATPase}$) and components of the active zone e.g. Munc13. Unfortunately, mitochondria were still present in the immunoisolates. Surprisingly, SDHA was also detected in the immunoisolates of control beads either coupled to the amino acid glycine (G) or to unspecific anti-sheep IgG (IgG). This suggested that mitochondria might co-sediment as a result of the centrifugation step used to pellet the eupergit beads instead of actually being co-purified. To a lesser extent, unspecific binding of the vesicle proteins synaptophysin and synaptobrevin were observed. To test this hypothesis, the *g* force of the centrifugation steps was reduced from 3400 *g* (6000 rpm)to 400 *g* (2000 rpm). With IgG or glycine coupled beads, unspecific binding of synaptophysin and synaptobrevin was almost

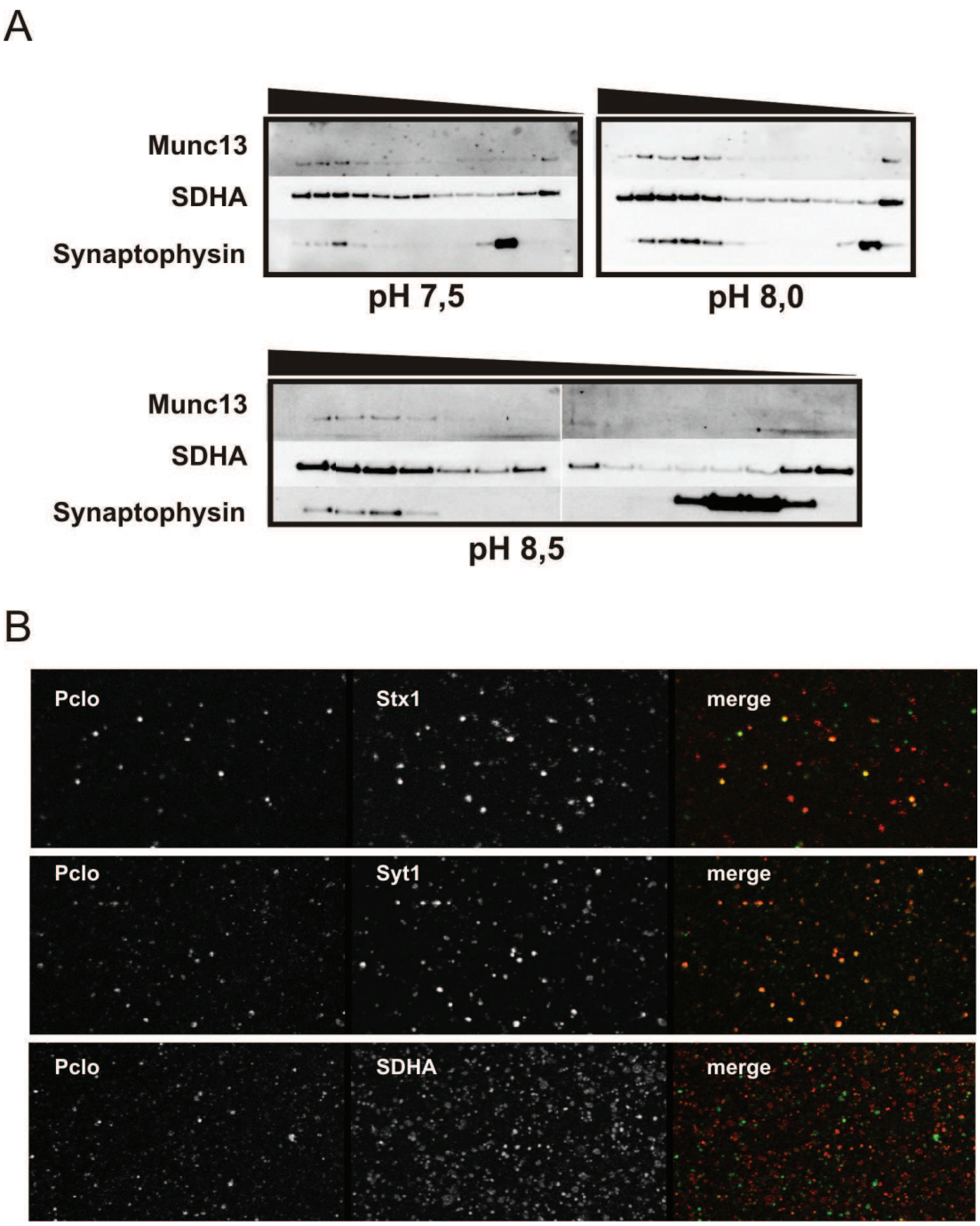

Figure 3.7: (A) Co-migration of mitochondria and docked vesicles in a sucrose gradient is not pH dependant. Synaptosomes were osmotically lysed at pH 7.5, pH 8.0 or pH 8.5 and its components separated on a 0.4.-1.3M continuous sucrose geradient. Migration patterns for mitochondria and synaptic plasma membranes did not change despite varying the pH used during the lysis. (B) Immunofluorescent staining of SPM fractions. The active zone protein piccolo showed a high co-localization with the synaptic vesicle protein synaptotagmin. Partial overlap of piccolo with the plasma membrane SNARE syntaxin 1 was also observed. Fractions were heavily contaminated with mitochondria.

completely abolished and the signal for SDHA was greatly diminished. Nevertheless, similar amounts of mitochondria were still co-purified with beads immobilized to the antibody for synaptophysin (Fig. 3.8, 2nd panel). Maybe mitochondria are attached to the synaptic plasma membrane by other forces such as lipid-lipid interactions. Because the mitochondrial proteome is well characterized, it allowed to eliminate mitochondrial contamination from the generated data.

Free synaptic vesicles could be isolated from the corresponding fractions using the same protocol (Fig. 3.8, 3rd panel). As expected, only vesicle proteins were purified (VGlut1 , synaptophysin and synaptobrevin). Neither the plasma membrane ATPase nor active zone components were detected in the immunoisolates. Mitochondrial contamination was still observed, but to a significantly lesser extent than in docked vesicles. In this work quantitative mass spectrometry was used to compare the protein composition of docked and free vesicles. Importantly, the amount of immunoisolated vesicles from the docked and free vesicle fraction were required to be approximately equal. This allows proteins enriched in the docked fraction to be confidently identified while the ratios of SV proteins in both fractions to be 1:1. To achieve this, input amounts of docked and free vesicle fractions were adjusted according to the chemiluminescence signal intensity of synaptophysin, synaptobrevin and VGlut1 in the immunoisolates (Fig. 3.8, last panel). Using twice the amount of the docked vesicle fraction compared to free vesicles as a starting material resulted in approximately same amount of synaptophysin, synaptobrevin and VGlut1.

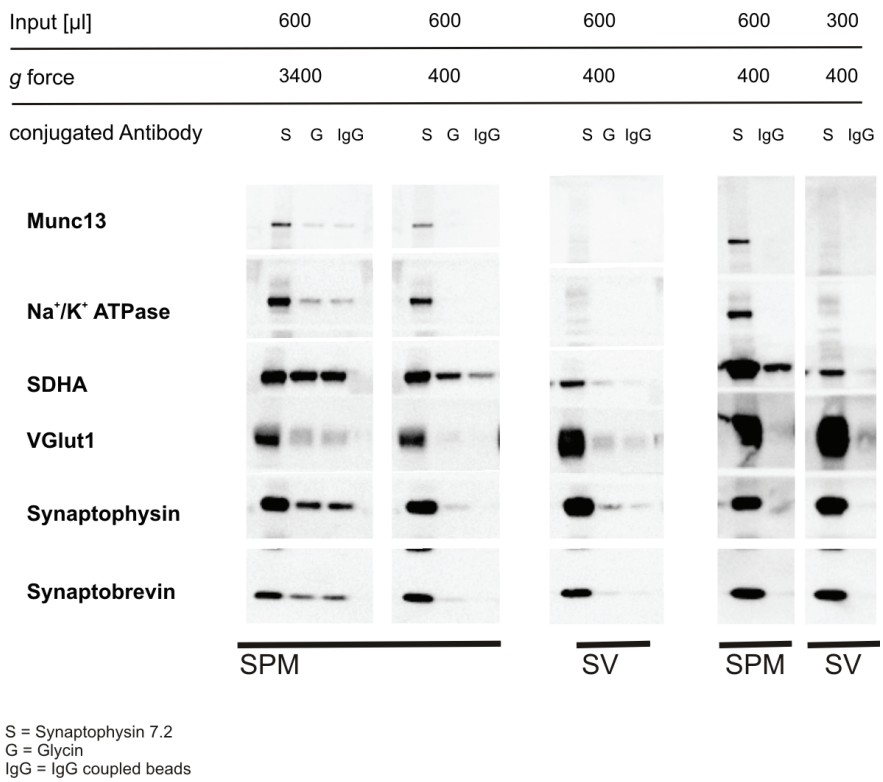

Figure 3.8: Docked vesicles (SPM) and free vesicles (SV) were immunoisolated from the corresponding fractions of the sucrose gradient using Eupergit C1Z beads comjugated to antibodies specific for synaptophysin. For unspecific binding controls, Eupergit C1Z were coupled to anti-sheep IgG or inactivated by glycine. SPM immunoisolates contained in addition to synaptic vesicles plasma membrane proteins ($\mathrm{Na}^{+}/\mathrm{K}^{+}\mathrm{ATPase}$) and active zone components (Munc13). Low speed centrifugation minimized unspecific background but did not remove mitochondrial contamination. Input of SPM and SV were adjusted to similar amounts of synaptic vesicle proteins detected in the immunoisolates.

3.2 Quantitative comparison of a docked and free vesicle proteome

The proteomes of the immunoisolates containing free and docked vesicle fractions were compared using an isobaric tag for relative and absolute quantification (iTRAQ) in combination with tandem mass spectrometry (LC-MS/MS). This quantitation method was developed by Ross et al. and it is designed to compare relative protein amounts in complex mixtures [141]. In detail, the iTRAQ reagent places an isobaric mass tag to reactive amino groups of the tryptic peptides generated after solubilisation and digestion of the sample. In this case, the docked vesicle fraction was labeled with a tag of *m/z 117* and free vesicles with *m/z 116*. Both samples were combined after the labeling and analyzed. The labeled peptides are chromatographically indistinguishable, but upon peptide fragmentation during the MS/MS analysis they yield different reporter ions of the masses *m/z 117* and *m/z 116*. The intensity of these reporter ions can be used to calculate the relative abundance of individual proteins. To reduce the complexity of the sample, the digested samples were pre-fractionated by strong cation exchange chromatography using increasing salt concentration steps. Afterwards the fractions were separately analyzed by reverse phase LC-MS/MS (see Fig. 3.9A).

In total, 506 proteins were identified from both fractions. Not surprisingly, a substantial portion of 217 proteins (42%) originated from the mitochondria according to NCBI and MitoCarta [177]. These proteins were not considered in the following analysis and are listed in the appendix. The remaining 289 proteins were investigated in greater detail and sorted into different functional groups according to their subcellular localization or molecular function (Fig.3.9B). The clustering of functional groups reflect the existence of several molecular mechanisms participating in the regulation of synaptic transmission.

Remarkably, only three exclusively postsynaptic proteins were identified (PSD, syngap 1, kalirin). Furthermore, in addition to mitochondria (as mentioned above), only minor contamination of other membranous organelles was detected. This minor contamination includes molecules involved in nucleotide metabolism, protein synthesis, metabolic enzymes, chaperones and proteins located at centrosomes, ER or Golgi (see appendix).

More than 30 hitherto uncharacterized proteins were detected, many of which are integral membrane proteins while others are identified purely by gene prediction. One of these proteins has been characterized in some detail in 3.4.

In summary, the proteome presented in this work provides detailed insights into the molecular composition of synaptic vesicle docking sites and the plasma membrane underlying these sites. A static picture of a synapse assembled by the proteins identified in this screen is presented at the end of this section (Fig. 3.10).

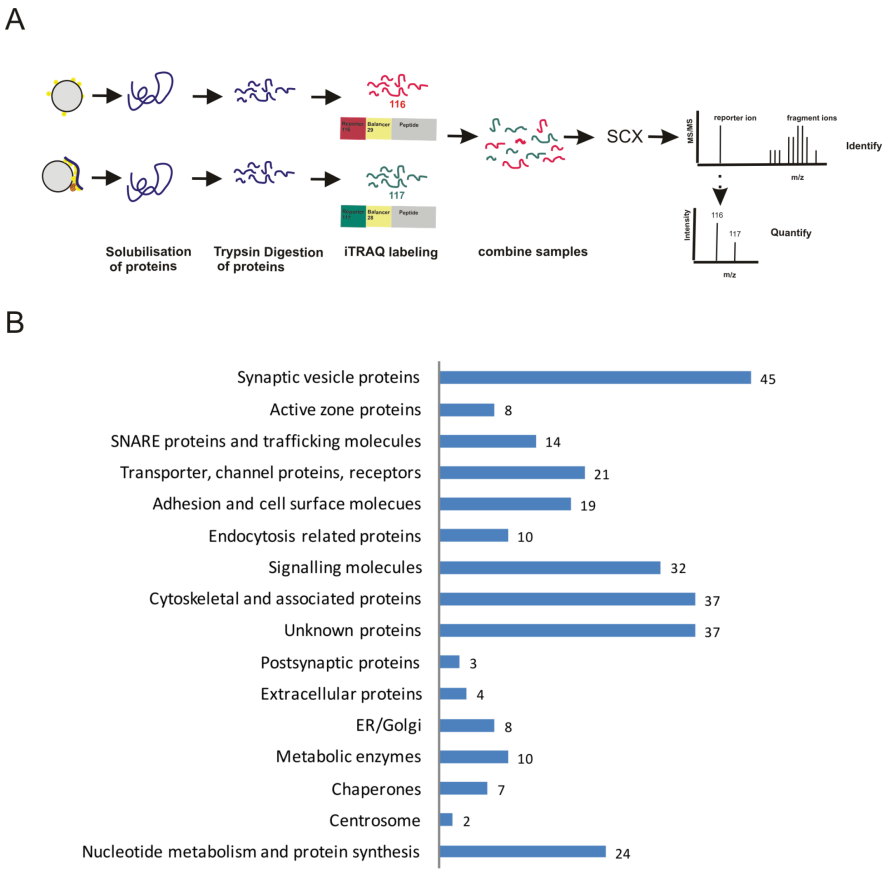

Figure 3.9: (A) Schematic overview of the iTRAQ experiment. (B) Proteins identified by iTRAQ analysis of docked and free vesicles were grouped according to their subcellular localization or molecular function.

3.2.1 Synaptic vesicle proteins

Synaptic vesicle proteins constitute the largest group of proteins identified. These proteins were detected in same amounts in both fractions as evidenced by a 1:1 ratio of the reporter ions *m/z 117* and *m/z 116*. Synaptic vesicles are one of the best characterized organelles in biology. A complete quantitative description of the protein composition of purified SVs has already been published [138] and was used as a reference for the analyzed data. The vacuolar ATPase, which is essential for the acidification of synaptic vesicles, has been determined to be present in one or two copies per vesicle [138, 137]. The vATPase is a large multi-subunit complex, the peripheral membrane domain V1 is about 640 kDa in size. Due to its enormous size, great variations in the abundance of the vATPase on SVs are unlikely. Therefore, the iTRAQ protein ratio was calculated by normalizing the amount of the vATPase in the docked vesicle fraction against the amount in the free vesicle fraction. As shown in table 3.1, all major synaptic

vesicle proteins were identified. This includes neurotransmitter transporters such as VGlut1, VGlut2 and VGAT, integral SV proteins like synaptophysin, the synaptotagmins (1,2,5), SV2a and b, and membrane associated proteins such as synapsins (1,3) as well as a number of Rab GTPases. Mover [178] and MAL2 [130] (proteins only recently identified as synaptic vesicle components) were detected. Importantly, almost all vesicle proteins were present in equal amounts in both fraction as exemplified by an iTRAQ ratio in the range of 1. Taking a twofold increase in the ratio as a cut off for enrichment, only Rab proteins showed a slight enrichment in the docked vesicle fraction. Rab GTPases are molecular switches that cycle between an active membrane attached state, in this case synaptic vesicles, and the cytosol depending on the bound nucleotide (for review see [179]). Unlike docked vesicles that require a membrane bound active Rab GTPase, not all free vesicles might contain a bound Rab protein. In fact, Pavlos et al. showed that Rab

The Rab family consists of over 60 members and a great number of Rab proteins were originally found on purified SVs that are involved in completely different trafficking pathways [138]. Recently, Pavlos et al. could determine the core Rab machinery using a quantitative analysis of synaptic vesicle Rabs [21]. Rab27b and the Rab3 isoforms are the major exocytotic, while Rab4b, Rab5a/b, Rab11 and Rab14 represent the endocytotic Rabs of synaptic vesicles. In line with this findings, the Rab proteins identified in this work represent the core Rab machinery. However, Rab proteins are very redundant in their sequence. Therefore only unique peptides were used for protein quantification.

3.2.2 Active zone proteins

In contrast to the SV proteins, active zone components were highly enriched in the docked vesicle fraction. Indeed, these proteins exhibited iTRAQ ratios of greater than six-fold (as seen for bassoon and Rim1) or were exclusively found in the SPM fraction.

Almost all established active zone components were detected in the docked vesicle fraction. Importantly, the identification of these proteins validated our purification approach as being appropiate for the analyses of the presynaptic release machinery. The AZ proteins identified included the multidomain scaffolding proteins piccolo, bassoon and CASK , the cytomatrix organizer ERC2 and proteins of the liprin family. Among the identified active zone proteins, a distinctive network of protein-protein interactions exists (as described in the introduction 1.2). Of the core active zone proteins, only Munc13, MALS and Mint1 could not be identified by mass spectrometry. However, the presence of Munc13 in these fractions has been proven by immunoblotting (see Fig.3.8). Munc13 appears to be difficult to analyze by mass spectrometry as noticed in other proteomic approaches [173, 180]. This "loss" of Munc13 might result from

Synaptic vesicle proteins

GI number	*Gene symbol*	*Name*	*#*	*iTRAQ ratio*	*std*
gi|16758202	Rab27b	RAB27B	2	2.6	0.6
gi|16758368	Rab14	RAB14	3	2.5	0.7
gi|45433570	Rab1a	RAB1A	3	2.3	0.1
gi|61556789	Rab35	RAB35	3	2.2	0.2
gi|61098195	Rab3a	RAB3A	3	2.2	0.3
gi|13929006	Rab2a	RAB2A	3	2.2	0.4
gi|9507159	Syn1	synapsin I isoform a	3	1.9	0.9
gi|8394389	Syn3	synapsin III	2	1.8	0.0
gi|158749626	Scamp1	secretory carrier membrane protein 1	3	1.8	1.2
gi|61889071	Rab10	RAB10, member RAS oncogene family	3	1.7	0.1
gi|13592037	Rab3b	RAB3B, member RAS oncogene family	2	1.7	0.5
gi|77404242	Syn2	synapsin II isoform 1	3	1.6	0.2
gi|74271849	Slc6a17	neurotramsmitter transporter NTT4	3	1.5	0.2
gi|109499663	Atp8a1	Aminophospholipid transporter (APLT) 8A, member 1	3	1.4	0.1
gi|6981624	Syt2	synaptotagmin II	3	1.4	0.2
gi|9507171	Syt5	synaptotagmin V	2	1.3	0.2
gi|148356226	Syt1	synaptotagmin 1	3	1.1	0.1
gi|109465077	Scamp3	Secretory carrier membrane protein 3	2	1.1	0.1
gi|13162361	Dnajc5	cysteine string protein	3	1.1	0.1
gi|40786463	Atp6v1d	ATPase, H+ transporting, lysosomal V1 subunit D	3	1.1	0.0
gi|16758754	Atp6v1f	ATPase, H transporting, lysosomal V1 subunit F	3	1.0	0.1
gi|58865560	Atp6v1c1	ATPase, H+ transporting, lysosomal V1 subunit C1	3	1.0	0.2
gi|38454230	Atp6v1e1	vacuolar H+ ATPase E1	3	1.0	0.1
gi|58865424	Atp6v0d1	ATPase, H+ transporting, lysosomal 38kDa, V0 subunit d1	3	0.9	0.0
gi|77627990	Atp6v0a1	ATPase, H+ transporting, lysosomal V0 subunit a1	3	0.9	0.0
gi|62078587	Atp6v1h	ATPase, H+ transporting, lysosomal V1 subunit H	3	0.9	0.0
gi|109493234	Atp6v1a1	ATPase, H+ transporting, V1 subunit A, isoform 1	3	0.9	0.0
gi|47059104	Atp6v1g2	ATPase, H+ transporting, lysosomal V1 subunit G2	3	0.9	0.1
gi|17105370	Atp6v1b2	vacuolar H+ATPase B2	3	0.9	0.0
gi|13929110	Atp6ap1	ATPase, H+ transporting, lysosomal accessory protein 1	3	0.9	0.0
gi|16758166	Slc17a6	VGlut2	3	0.9	0.1
gi|16758726	Slc17a7	VGlut1	3	0.9	0.1
gi|17105360	Sv2b	synaptic vesicle glycoprotein 2b	3	0.9	0.1
gi|148747227	Sv2a	synaptic vesicle glycoprotein 2a	3	0.8	0.0
gi|160333093	Tprgl	mover	3	0.8	0.2
gi|13929106	Slc32a1	VGat	3	0.8	0.1
gi|61557417	Slc30a3	zinc transporter ZnT-3	3	0.8	0.0
gi|77157795	Mal2	MAL2 proteolipid protein	3	0.8	0.0
gi|13027428	Synpr	synaptoporin	2	0.8	0.2
gi|18677757	Atp6v0c	ATPase, H+ transporting, lysosomal 16kDa, V0 subunit c	3	0.7	0.1
gi|6981622	Syp	synaptophysin	3	0.7	0.0
gi|13929020	Scamp5	secretory carrier membrane protein 5	3	0.6	0.0
gi|9507167	Syngr1	synaptogyrin 1	3	0.6	0.0
gi|157819371	Syngr3	synaptogyrin 3	3	0.5	0.0

Table 3.1: The table shows the synaptic vesicle proteins identified in the docked and free vesicle fraction. # indicates the number of times the protein was detected in 3 biological replicates. The iTRAQ ratio was calculated as *m/z*117 divided by *m/z*116 (docked/free vesicles).

Active zone proteins

GI number	*Gene symbol*	*Name*	*#*	*iTRAQ ratio*	*std*
gi|11559947	Cask	calcium/calmodulin-dependent serine protein kinase	2	SPM	
gi|25140983	Erc2	ELKS/RAB6-interacting/CAST family member 2	3	SPM	
gi|109497902	Ppfia4	Liprin-α4	3	SPM	
gi|10048483	Pclo	piccolo isoform 1	2	SPM	
gi|157824053	PPFIA2	Liprin-α 2	2	SPM	
gi|158749559	Bsn	Bassoon	3	7.4	0.8
gi|16306470	Rims1	RIM 1	3	6.3	0.4
gi|213972596	Ppfibp2	Liprin-β 2	3	0.4	0.1

Table 3.2: Active zone proteins identified in the iTRAQ analysis. Proteins with an iTRAQ ratio of "SPM" have only been identified in the docked vesicle fraction and could therefore not be quantified.

the high insolubility of Munc13 in detergents other than SDS or from a masking of the peptides in the MS spectrum by other more abundant peptides.

In our proteomic analysis, neither Mint1 nor MALS could be identified. They may have been missed for the same reasons as for Munc13 or they are really absent in this fraction. Genetic studies of MALS showed, that knock out of this protein results in aberrant EPSC amplitudes and an accelerated synaptic depression after high frequency stimulation. This lead to the assumption that this complex is involved in replenishing the readily releasable pool from the reserve pool [112]. In this respect, the complex possibly disassembles after docking of the vesicle to the plasma membrane and as a consequence is not detected here.

Along with the α-liprins, also the less characterized isoform liprin-β2 was detected, but did not show an enrichment in the docked vesicle fraction (iTRAQ ratio of 0.5). Thus, this protein appears to have a different localization as α-liprins and presumably is not involved in docking of vesicles to the plasma membrane

3.2.3 SNARE proteins and trafficking molecules

In addition to synaptic vesicles and active zone components, all known components of the neuronal fusion machinery were identified with this approach.

Vesicle fusion in general is mediated by different groups of proteins. SNARE proteins form the minimal machinery for membrane fusion and SM proteins bind trans-SNARE complexes thereby regulating their fusogenic activity. In addition complexin is thought to neurotransmitter release by grappling zippered SNARE complexes and releasing them upon calcium influx. In agreement with current literature it was shown here that the neuronal t-SNAREs SNAP25 and

syntaxin 1a and b were enriched in the SPM fraction, whereas the v-SNAREs Vamp1 and Vamp2 had iTRAQ ratios of approximately 1 and are localized to synaptic vesicles (see table 3.3). Furthermore the synaptic SM protein Munc18 and complexin are enriched in the docked vesicle fraction.

Interestingly, a component of the SNARE recycling machinery was found as well. NSF, a member of the AAA family of ATPases, takes action after the fusion event and disassembles *cis*-SNARE complexes. However, the NSF adaptor protein α-SNAP was not detected.

Apart from the neuronal SNAREs, only one non-neuronal SNARE was detected. Syntaxin 16 and its associated SM protein vps45 were enriched in the docked vesicle fraction. Synatxin 16 is ubiquitously expressed, but mainly localizes at the trans-Golgi network [181].

SNARE proteins and trafficking molecules

GI number	*Gene symbol*	*Name*	*#*	*iTRAQ ratio*	*std*
gi|109471437	Stx16	Syntaxin-16 (Syn16) isoform 1	2	SPM	
gi|25742604	Vps45	vacuolar protein sorting 45 homolog	2	SPM	
gi|9507127	Snip	SNAP25-interacting protein	3	5.9	1.9
gi|12408324	Cplx1	complexin 1	2	5.3	2.3
gi|13591882	Snap25	synaptosomal-associated protein 25	3	4.2	0.1
gi|6981600	Stx1b2	syntaxin 1B2	3	3.4	0.1
gi|13489067	Nsf	N-ethylmaleimide-sensitive factor	3	3.3	1.6
gi|33667087	Stx1a	syntaxin 1A (brain)	3	3.0	0.1
gi|219275534	Vps13a	vacuolar protein sorting 13 homolog A	2	2.8	0.1
gi|13027430	Wdr7	rabconnectin 3 beta	2	2.5	
gi|6981602	Stxbp1	Munc18-1	3	2.3	0.2
gi|62079163	Atg9a	ATG9 autophagy related 9 homolog A	3	1.2	0.5
gi|76443677	Vamp1	vesicle-associated membrane protein 1	3	0.9	0.1
gi|6981614	Vamp2	Synaptobrevin	3	0.7	0.0

Table 3.3: The neuronal fusion machinery consisting of the SNAREs syntaxin 1a/b, SNAP25 and Vamp2, Munc18 and complexin was identified in the analyzed fractions. All proteins except for the v-SNAREs Vamp1 and Vamp2 were enriched in the docked vesicle fraction.

3.2.4 Transporter, channel proteins and receptors

The presynaptic membrane contains an extensive array of molecules that are involved in the signaling process across the synapse. Here we showed that the stretches of the plasma membrane purified with the docked vesicles contain a number of transporters and channels that are involved in calcium homeostasis, modulation of synaptic strength, pH maintenance and neurotransmitter clearance at the nerve terminal.

Transporter, channel proteins, receptors

GI number	*Gene symbol*	*Name*	*#*	*iTRAQ ratio*	*std*
gi|31542335	Cacna2d1	calcium channel, voltage-dependent, $\alpha 2/\delta$ subunit 1	2	SPM	
gi|6978583	Cacnb3	calcium channel, voltage-dependent, β 3 subunit	2	SPM	
gi|16758108	Hcn1	hyperpolarization-activated cyclic nucleotide-gated potassium channel 1	2	SPM	
gi|13929184	Kcnma1	potassium large conductance calcium-activated channel, subfamily M, alpha member 1	2	SPM	
gi|155369700	Tlr8	toll-like receptor 8	2	SPM	
gi|6981558	Slc9a1	sodium/hydrogen exchanger Nhe1	2	SPM	
gi|62644838	Slc27a4	fatty acid transporter, member 4	3	SPM	
gi|157817045	Clcn6	chloride channel 6	2	SPM	
gi|13242269	Slc6a1	GABA transporter protein	2	SPM	
gi|9507115	Slc1a3	EAAT1	2	SPM	
gi|78126161	Slc1a2	EAAT2	2	8.9	1.9
gi|148747253	Atp1b1	Na+/K+ -ATPase beta 1 subunit	3	8.4	1.2
gi|6978543	Atp1a1	Na+/K+ -ATPase alpha 1 subunit	3	7.8	0.7
gi|6978547	Atp1a3	Na+/K+ -ATPase alpha 3 subunit	3	7.3	0.6
gi|55925610	Itpr1	inositol 1,4,5-triphosphate receptor, type 1	3	6.9	1.0
gi|16758008	Atp2b1	plasma membrane calcium ATPase 1	3	6.3	2.8
gi|6978557	Atp2b2	plasma membrane calcium ATPase 2	2	6.2	3.9
gi|148747140	Slc2a3	glucose transporter GLUT3	2	4.7	0.3
gi|17530967	Slc8a2	sodium/calcium exchanger Ncx2	3	4.6	1.1
gi|19705463	Slc12a5	Neuronal potassium-chloride transporter	3	4.2	1.2
gi|47576439	Olr1589	olfactory receptor Olr1589	2	2.1	

Table 3.4: The docked vesicle fraction contains transporters and channels proteins that are involved in calcium homeostasis, modulation of synaptic strength, pH maintenance and neurotransmitter clearance at the nerve terminal.

Voltage-gated calcium channels initiate the release of neurotransmitters at the presynaptic nerve terminal. Mainly N-type and P/Q-type calcium channels are responsible for presynaptic calcium influx at conventional synapses. Calcium channels are composed of a poreforming $\alpha 1$ subunit that determines the pharmacological classification, and four distinct auxilliary subunits: an intracellular β-subunit, a disulfide linked complex of $\alpha 2\delta$ and a γ-subunit. In this work, the subunits β and $\alpha 2\delta$ were detected, but not the transmembrane $\alpha 1$ subunit. This made it impossible to distinguish between L-, N- and P/Q-type calcium channels.

Second, calcium-dependent potassium channels (also known as BK channels) modulate synaptic transmission by altering the duration of presynaptic action potentials [182]. The BK channel Kcnma1 which localizes at presynaptic terminals [183, 184] was identified in this analysis as well as the hyperpolarization-activated cyclic nucleotide-gated potassium channel (HCN1). HCN1 recently was reported to be present at active zones of asymmetric synapses [185].

Importantly, calcium has to be actively removed from the cell after neuronal excitation. Both of the calcium clearance systems were enriched in our docked vesicle fraction. The plasma membrane $Ca^{2+} - ATPase$ (PMCA) and the plasma membrane Na^{+}/Ca^{2+} exchanger (NCX) exchanger extrude calcium from the cell and have been previously reported to enrich in synaptic plasma membrane preparations. In fact, PMCA is known to cluster to neurotransmitter release sites [186].

In addition to the calcium and calcium-dependent machinery, presynaptic terminals require a pH regulatory system to control intra- and extracellular pH-changes. Here, we identified the sodium/hydrogen exchanger NHE1. NHE1 removes H^{+} from synaptosomes [187] and its inhibition changes neurotransmitter release in dissociated hippocampal neurons [188].

Finally, also components of the neurotransmitter recycling machinery were found in the SPM fraction. GAT1 is the predominant transporter responsible for the re-uptake of GABA from the synaptic cleft, and is localized on presynaptic terminals of GABAergic inhibitory neurons [189]. Furthermore, the sodium-dependent glutamate transporters EAAT1 and EAAT2 were detected. Although these transporters are mainly distributed on glial plasma membranes [190], these transporters are also detected in synaptosomes and appear to directly associate with the $Na^{+}/K^{+}ATPase$ [191].

3.2.5 Adhesion and cell surface molecules

Synaptosomes were treated with proteases during the purification process resulting in a digestion of proteins on the surface of the plasma membrane. This makes the identification of adhesion and cell surface molecules difficult and possibly incomplete. Nevertheless, cell adhesion molecules usually contain an intracellular domain that is expected to be protected from proteases. Therefore, several known plasma membrane proteins and adhesion molecules bridging the synaptic cleft were found in the docked vesicle fractions (see table 3.5).

Proteins involved in neurite formation and neuronal morphology were detected. The neuronal Growth-Associated Protein 43 (GAP43) plays a role in neuronal development [192] and is one of the most abundant proteins in growth cones [193]. Glycoproteins M6a and M6b are related proteolipid proteins. M6a is an axonal component of glutamatergic neurons with a suggested role in neurite outgrowth and stress response [194, 195]. Also Thy-1 enriches in synaptosomes [196] and modulates neurite outgrowth, but it additionally requires calcium influx through both N- and L-type calcium channels [197].

Among the identified synaptic adhesion molecules were NCAM , Neurexin4, CAM3, neuroplastin, sirpa and CD47. The latter finding is consistent with sirpa having a role in organizing the clustering vesicles mediated by its interaction with CD47 [198]. Although synaptic

Adhesion and cell surface molecules

GI number	*Gene symbol*	*Name*	*#*	*iTRAQ ratio*	*std*
gi|14091742	Cntnap1	Neurexin 4	2	SPM	
gi|157817081	Ctnna2	catenin alpha 2	2	SPM	
gi|157820047	Ctnnd1	catenin delta 1	2	SPM	
gi|109464562	Ctnnd2	Neurojungin	3	SPM	
gi|109478967	Crim1	Cysteine-rich motor neuron 1 protein	2	SPM	
gi|30017437	Gpm6a	glycoprotein m6a	3	SPM	
gi|20301986	Gpm6b	glycoprotein m6b	2	SPM	
gi|8850221	Hpca	hippocalcin	2	SPM	
gi|157817019	Pkp4	plakophilin 4	2	9.7	1.1
gi|8393415	Gap43	growth associated protein 43	3	8.9	1.3
gi|46048609	Ctnnb1	catenin beta 1	3	8.4	3.4
gi|13928706	Ncam1	neural cell adhesion molecule 1	2	7.9	0.7
gi|114052921	Cadm3	cell adhesion molecule 3	2	7.0	0.1
gi|9506469	Cd47	Cd47 molecule	2	6.7	2.0
gi|9507073	Nptn	neuroplastin	3	5.8	0.2
gi|31543529	Sirpa	signal-regulatory protein alpha	2	5.3	0.6
gi|61557326	Reep6	receptor accessory protein 6	3	4.8	0.6
gi|8393864	Hpcal1	hippocalcin-like 1	3	4.3	0.1
gi|6981654	Thy1	Thy-1 cell surface antigen	3	3.9	0.3

Table 3.5: Identification of synaptic plasma membrane proteins involved in neurite formation and neuronal morphology (GAP43, M6a/b, Thy-1) and adhesion molecules (NCAM, Neurexin, CAM3, neuroplastin, sirpa and CD47).

N-cadherins could not be identified, its intracellular binding partners α- and β-catenins were present. α-catenin directly binds to the filamentous actin, linking the adhesion complex of Cadherin/catenins to the actin cytoskeleton [199].

3.2.6 Endocytosis related proteins

Because exocytotic and endocytic sites are suggested to be in close proximity at the plasma membrane, the discovery of proteins belonging to endocytic pathways was not surprising. However, proteins involved in clathrin-mediated endocytosis are not enriched in the docked vesicle fraction, except for clathrin itself (iTRAQ ratio 5.8) 3.6. Components of the AP2-complex and endophilin were equally distributed in both fractions. This indicates that the free vesicle fraction is a mixture of the reserve and recycling pool of vesicles. Presumably only uncoated or partially uncoated vesicles could be immunoisolated with an antibody against synaptophysin. This would explain the enrichment of clathrin in the docked vesicle fraction but not in free vesicle immunoisolates. However, a 1:1 ratio for endophilin was surprising, because endophilin is suggested to function at endocytotic retrieval sites, presumably as a membrane

bending molecule. But in line with our data, a recent study could show that despite acting at the plasma membrane, the majority of endophilin is targeted to the SV pool [200].

Interestingly, proteins of clathrin-independent flotillin endocytotic pathway were also identified. Flotillin 1/2 oligomerizes in distinct membrane microdomains [201], but have been initially described as regeneration molecules in axons of goldfish retinal ganglion cells [202]. Related to this, flotillin microdomains have been reported to associate with Thy-1 (see section adhesion and cell surface molecules) suggesting a role of flotillin/Thy-1 in neurite outgrowth and axon regeneration [203].

Endocytosis related proteins

GI number	*Gene symbol*	*Name*	*#*	*iTRAQ ratio*	*std*
gi|158636004	Flot1	flotillin 1	3	SPM	
gi|13929186	Flot2	flotillin 2	3	SPM	
gi|9506497	Cltc	clathrin, heavy chain (Hc)	3	5.8	1.6
gi|13928818	Ptprn2	protein tyrosine phosphatase (Phogrin)	3	2.0	0.6
gi|57527421	Sh3glb2	endophilin B2	3	1.4	1.0
gi|18034787	Ap2b1	adaptor-related protein complex 2, beta 1 subunit	3	0.8	0.2
gi|157823677	Ap2a1	adaptor-related protein complex 2, alpha 1 subunit	3	0.7	0.1
gi|162138932	Ap2a2	adaptor-related protein complex 2, alpha 2 subunit	3	0.7	0.1
gi|16758938	Ap2m1	adaptor-related protein complex 2, mu 1 subunit	3	0.6	0.0
gi|56961624	Ap2s1	adaptor-related protein complex 2, sigma 1 subunit	3	0.6	0.1

Table 3.6: Components of the clathrin-dependent and the flotillin-dependent endocytic pathway could be identified, but only flotillins are enriched in the docked vesicle fraction.

3.2.7 Cytoskeletal and associated proteins

Cytoskeletal elements are essential for synapse morphology, stabilization of the active zone and vesicular transport in neurons. Also the high morphological plasticity of the synapse requires a dynamic cytoskeleton. Consequently, we identified a wide range of cytoskeletal components, which are known to play a role in the synapse.

Actin and its motor protein myosin were detected. Actin is a major structural component of active zones, where it recruits vesicles to the docking sites and associates with synapsin [125]. Among the identified myosins, myosin 5 interacts with syntaxin1a in a Ca^{2+}-dependent manner [204]. Very recently, myosin 5a has been shown to directly associate with Rab3a in its active GTP-bound form, implicating a role in the transport of neuronal vesicles [205]. Another motor protein found in the docked vesicle fraction, myosin 10, has been proposed to have a role

in neurite outgrowth [206]. Similarly, the microtubule cytoskeleton and specifically the kinesin motor KIF1b is involved in long distance axonal transport of synaptic vesicle precursors [207].

Another component of the presynaptic cytomatrix are septins. Septins are large filamentous proteins and suggested to be part of the filamentous mesh of the active zone that is observed by electron microscopy [55]. They might play a role in positioning SVs at the active zone. In particular septin5, which is detected here, seems to be crucial for the proximity of SVs and active zone elements in the priming/docking stage [208]. Septin5 additionally binds to syntaxin1 in the SNARE complex, competing with SNAP25 [209]. Also septin3 is identified in the docked vesicle fraction, a septin isoform that is exclusively expressed in neurons, enriches in presynaptic terminals and co-localizes with SV markers [210].

Furthermore parts of the spectrin-based membrane skeleton were found. Spectrins and the associated ankyrins interact with with membrane channels and adhesion molecules, including the $\mathrm{Na}^{+}/\mathrm{K}^{+}\mathrm{ATPase}$ [211], the sodium-calcium exchanger NCX [212], and cadherins [213].

3.2.8 Signaling molecules

Signaling at the synapse is very complex and only poorly understood. Therefore, a detailed analysis of the identified signalling proteins was not performed. Nevertheless, many G-proteins (guanine nucleotide binding-proteins) were found in the docked vesicle fraction. G-proteins, especially Gnaq and Gnao, are involved in modulating neurotransmitter release (for review see [214]).

Not surprisingly, also 14-3-3 proteins are present in this fraction as they comprise about 1% of the total soluble brain proteins. They are involved in many signaling processes, but in the context of synaptic vesicle docking it is worthwhile mentioning that they have been shown to interact with Rim [215] and presynaptic calcium channels [216].

Also CaMKII was detected in our proteomic analysis. CaMKII is a large complex with a well established role in postsynaptic signalling, but is also present in presynaptic terminals [217], associates with vesicles [218] and may have a role in modulating synaptic strength and plasticity. Interestingly, in *C. elegans* presynaptic CaMKII activates BK channels at the neuromuscular junction [219].

Cytoskeletal and associated proteins

GI number	*Gene symbol*	*Name*	*#*	*iTRAQ ratio*	*std*
gi|109472192	Dnahc6	dynein, axonemal, heavy chain 6	3	SPM	
gi|109488370	Dnah2	dynein, axonemal, heavy chain 2	3	SPM	
gi|13591902	Actn1	actinin, alpha 1	2	SPM	
gi|29789307	Kif1b	kinesin family member 1B	2	SPM	
gi|13928704	Myh10	myosin, heavy chain 10, non-muscle	3	SPM	
gi|6981236	Myh9	myosin, heavy chain 9, non-muscle	3	SPM	
gi|72255527	Stoml2	stomatin (Epb7.2)-like 2	3	SPM	
gi|109474612	Rp1	Oxygen-regulated protein 1	2	SPM	
gi|6981696	Utrn	utrophin	2	SPM	
gi|157817598	Invs	inversin	3	SPM	
gi|109467596	Ank2	ankyrin 2, neuronal	2	SPM	
gi|9507085	Sept3	neuronal-specific septin-3	2	SPM	
gi|16758016	Dynll1	dynein, cytoplasmic, light peptide	3	9.9	
gi|31543764	Sptan1	spectrin alpha chain, brain	3	7.3	0.0
gi|61557085	Sptbn1	spectrin beta chain, brain 1	2	6.1	2.0
gi|13592133	Actb	actin, beta	3	5.2	2.4
gi|13540714	Plec	plectin 1	3	5.0	1.6
gi|90577179	Sept5	septin 5	3	4.7	1.3
gi|157819689	Sept8	septin 8	3	4.5	1.3
gi|57164143	Actr2	ARP2 actin-related protein 2 homolog	2	4.0	1.4
gi|9506371	Acta1	actin, alpha 1, skeletal muscle	2	3.7	0.8
gi|166091429	Sept7	septin 7 isoform a	2	3.6	0.4
gi|109464350	Kif2	Kinesin-like protein KIF2	2	3.3	1.2
gi|11560133	Tuba1a	tubulin, alpha 1A	3	3.3	3.0
gi|47058982	Septb	spectrin, beta, erythrocytic	2	3.2	3.2
gi|112984124	Tuba1b	tubulin, alpha 1B	3	3.1	2.6
gi|11559935	Myo5a	myosin Va	2	2.7	0.2
gi|158262004	Tubb4	tubulin, beta 4	3	2.1	0.9
gi|27465535	Tubb5	tubulin, beta 5	3	2.1	1.0
gi|145966774	Tubb3	tubulin, beta 3	3	1.9	1.0
gi|55741524	Tuba4a	tubulin, alpha 4A	2	1.7	0.8
gi|109495859	Dnah10	dynein, axonemal, heavy polypeptide 10	3	1.2	1.0
gi|164698508	Sept9	septin 9 isoform 2	3	1.0	0.4
gi|109508026	Sntb2	Beta-2-syntrophin (Syntrophin 3)	2	1.0	0.2
gi|148491097	Dync1h1	cytoplasmic dynein 1 heavy chain 1	2	0.9	0.4
gi|188595680	Sphkap	A-kinase anchor protein SPHKAP	2	0.9	0.1
gi|109480041	RGD1308350	similar to hypothetical protein MGC13251	3	0.7	0.1

Table 3.7: Components of the actin and microtubule cytoskeleton, septins and spectrins/ankyrins are present in the docked vesicle fraction.

Signaling molecules

GI number	*Gene symbol*	*Name*	*#*	*iTRAQ ratio*	*std*
gi|109475021	Cdk5rap2	CDK5 regulatory subunit associated protein 2	2	SPM	
gi|13592021	Pde2a	phosphodiesterase 2A, cGMP-stimulated isoform 2	2	SPM	
gi|155369271	Prkaca	protein kinase, cAMP-dependent, catalytic, alpha	2	SPM	
gi|8394267	Shh	sonic hedgehog	2	SPM	
gi|157822659	Riok3	RIO kinase 3	2	SPM	
gi|132626321	Slk	STE20-like kinase	2	SPM	
gi|6981712	Ywhaq	14-3-3 theta	2	SPM	
gi|25742825	Pi4k	phosphatidylinositol 4-kinase a	2	SPM	
gi|157818451	Arl8a	ADP-ribosylation factor-like 8A	2	SPM	
gi|109507443	Gnal	Guanine nucleotide-binding protein G(olf), alpha	2	SPM	
gi|13592039	Rala	v-ral simian leukemia viral oncogene homolog A	2	SPM	
gi|157821177	Trio	triple functional domain (PTPRF interacting)	3	SPM	
gi|109458044	Nlrp12	NACHT, LRR and PYD domains-containing protein 12	2	SPM	
gi|13591957	Gnaq	guanine nucleotide binding protein, alpha q	2	SPM	
gi|9507061	Pcsk1	Neuroendocrine convertase 1	3	SPM	
gi|9506737	Gnas	GNAS complex locus gnas1-a	2	SPM	
gi|157820415	Rasal1	RAS protein activator like 1 (GAP1 like)	3	9.0	0.8
gi|19424316	Camkg	calcium/calmodulin-dependent protein kinase II γ	3	8.2	1.7
gi|148747524	Gnb1	guanine nucleotide-binding protein, beta-1 subunit	3	8.0	1.5
gi|108796657	Camkb	calcium/calmodulin-dependent protein kinase II β	3	7.9	1.0
gi|29789261	Gnb2	guanine nucleotide-binding protein, beta 2	2	7.5	1.7
gi|6978593	Camka	calcium/calmodulin-dependent protein kinase II α	3	7.3	1.6
gi|8394152	Gnao1	GTP-binding protein alpha o	3	6.7	1.8
gi|6980962	Gnai1	guanine nucleotide binding protein α inhibiting 1	2	6.7	0.9
gi|6978595	Camkd	calcium/calmodulin-dependent protein kinase II δ	2	6.1	2.3
gi|19173774	Rap2b	RAP2B	2	5.7	0.7
gi|62990183	Ywhaz	14-3-3 zeta	2	4.9	0.4
gi|12408298	Dpp6	dipeptidylpeptidase 6	2	4.5	0.2
gi|6981400	Prkcg	protein kinase C, gamma	2	2.7	0.1
gi|109464256	Cmya5	Myospyn	3	1.2	0.6
gi|42476092	Gps1	G protein pathway suppressor 1	2	1.1	0.0
gi|109487963	Dock2	dedicator of cyto-kinesis 2	3	0.8	0.2

Table 3.8: Signaling at the active zone includes G-proteins, members of the 14-3-3 family and CaMKII.

3.2.9 Unknown proteins

More than 30 unknown proteins were identified by our analysis of the docked vesicle fraction. These proteins are predicted to be mostly transmembrane proteins and have either an unknown function or localization. Some are indeed novel proteins. Considering the low amount of contaminations and the specificity of the proteins described above, the chance that many of these proteins are in fact associated with the presynaptic membrane is rather high.

Hypothetical proteins and transmembrane proteins with unknown function or localisation

GI number	*Gene symbol*	*Name*	*#*	*iTRAQ ratio*	*std*
gi|157822793	Ccdc109a	coiled-coil domain containing 109A	3	SPM	
gi|56090369	Tmx2	thioredoxin-related transmembrane protein 2	2	SPM	
gi|109484624	LOC683941	transmembrane protease, serine 4	3	SPM	
gi|62651891	RGD1309995	CG13957-PA	2	SPM	
gi|62660468	Wdr19	WD repeat-containing protein 19	2	SPM	
gi|62718819	LOC501488	rCG41835-like	2	SPM	
gi|157819311	RGD1308226	hypothetical protein LOC296968	2	SPM	
gi|56605740	Wdfy1	WD repeat and FYVE domain containing 1	2	SPM	
gi|109478621	Setd3	SET domain containing 3	2	SPM	
gi|109492012	Prp2l1	proline-rich protein isoform 1	2	SPM	
gi|109461608	LOC687472	rCG54054-like	2	SPM	
gi|62078483	OCIAD1	OCIA domain containing 1	2	SPM	
gi|62079059	Cend1	BM88 antigen	3	SPM	
gi|157822273	RGD1309188	hypothetical protein LOC315463	3	SPM	
gi|62079015	RGD1309676	hypothetical protein LOC361118	2	SPM	
gi|157821195	LOC362419	hypothetical protein LOC362419	2	SPM	
gi|157821401	LOC683512	hypothetical protein LOC683512	3	SPM	
gi|158262028	RGD1302996	hypothetical protein MGC15854	3	SPM	
gi|68342019	Lrrc17	leucine rich repeat containing 17	2	SPM	
gi|109499872	Fam193a	Hypothetical protein	2	SPM	
gi|109510841	ApoO	hypothetical protein Apolipoprotein O	3	SPM	
gi|109512114	RGD1562521	Similar to Ppnx	2	SPM	
gi|71361663	Fam162a	family with sequence similarity 162, member A	3	8.4	5.7
gi|157819829	RGD1565496	hypothetical protein LOC300783	2	4.8	
gi|109481310	LOC681219	hypothetical protein LOC681219	2	4.8	
gi|66730294	Abhd12	abhydrolase domain containing 12	2	4.4	2.5
gi|62641302	RGD1564195	similar to hypothetical protein	2	3.7	0.1
gi|109473862	LOC686590	IQ motif and Sec7 domain 1 isoform 2	3	3.5	1.4
gi|51948472	Tmem30a	transmembrane protein 30A	3	2.6	0.6
gi|61557143	Scrn3	secernin 3	2	2.2	
gi|62078999	Traf3ip3	TRAF3 interacting protein 3	2	1.3	
gi|67846010	Rogdi	rogdi homolog	2	1.2	0.5
gi|189011652	Tmprss13	transmembrane protease, serine 13	3	1.1	0.1
gi|56605828	Trappc3	trafficking protein particle complex 3	3	0.6	0.1
gi|109483746	RGD1307365	protein QN1 homolog	3	0.5	0.2
gi|157786666	RGD1560058	hypothetical protein LOC287559	3	0.5	0.3
gi|109464586	Lrrcc1	leucine rich repeat and coiled-coil containing 1	3	0.3	0.1

Table 3.9: Proteins identified with unknown function or localization. Some of them are novel, predicted proteins.

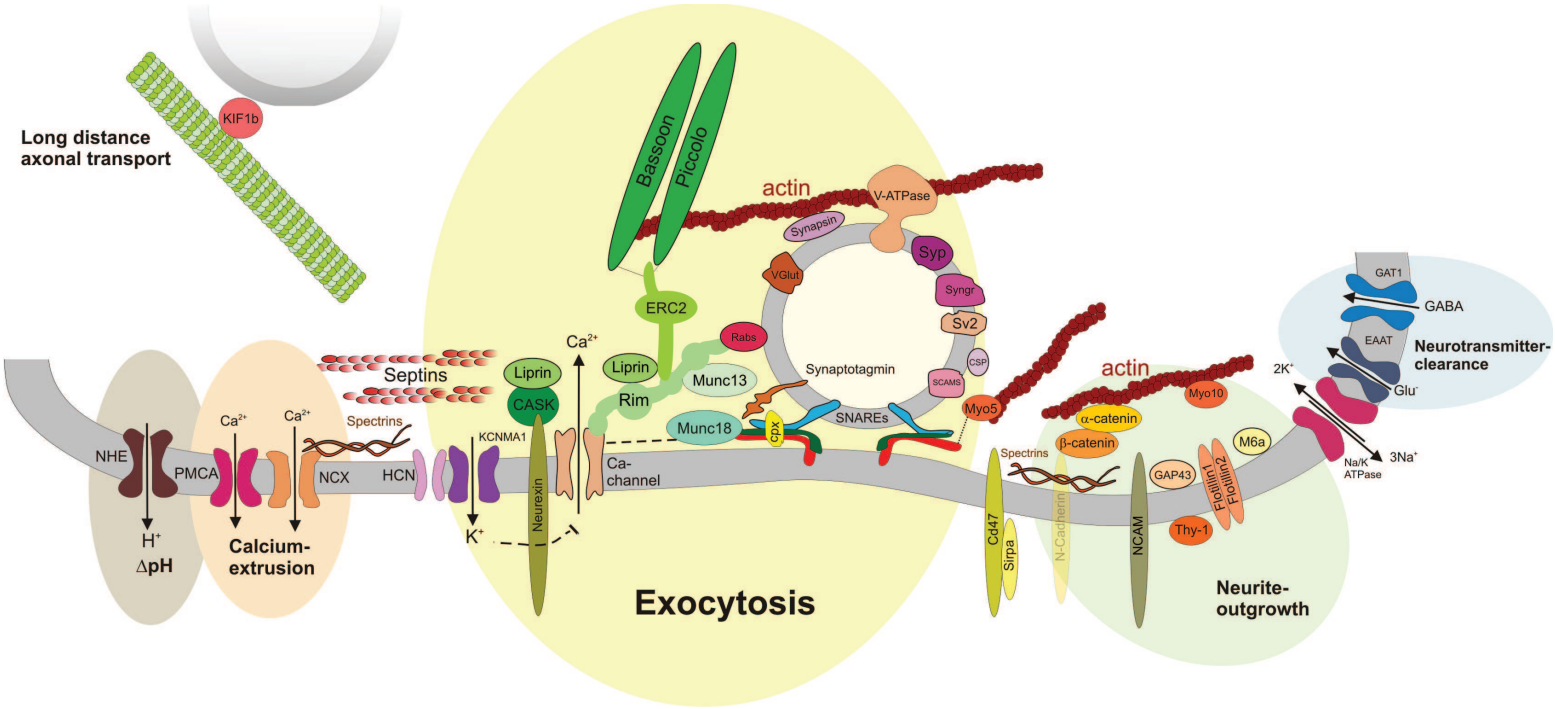

Figure 3.10: Schematic overview of the identified proteins. Proteins were arranged according to their function and interaction partners. Note, that cytoskeletal components were only indicated to avoid overcrowding of the illustration.

3.3 Effect of the Rab GTPase modulator GDI on synaptic vesicle docking

The access to a defined docked vesicle fraction presents an excellent basis to investigate changes in the presynaptic proteome in response to different treatments. We decided to use this fraction to investigate the effect of the Rab effector GDP dissociation inhibitor (GDI) on the organization of the presynapse. Rab GTPases are molecular switches, they cycle between a GTP-bound active state and a GDP-bound inactive state. In the GTP-bound state, Rab proteins are localized to their target membrane, mediating membrane attachment and specifying intracellular membrane fusion reactions. They are bound to synaptic vesicles and have a substantial role in neuronal exocytosis [20]. For instance, Rab3 dissociates from synaptic vesicles after stimulation [149]. A removal of Rab3 from synaptic vesicles can also be induced by GDI. In general, GDI retrieves GDP-bound inactive Rabs from the membrane upon GTP-hydrolysis and forms a soluble cytosolic complex until Rab proteins are actived again and recruited to the membrane [220, 221]. Interestingly, Rab3 proteins can assemble into tripartite complexes with Rim and Munc13 that have been postulated to tether synaptic vesicles to the active zone [68]. Indeed, reduced synaptic vesicle docking is observed in Rab3 mutant mice [222] and *C. elegans* [79]. In this context, it was examined, whether a GDI-induced extraction of Rab3 from the SV has an effect of vesicle attachment to the plasma membrane or of the protein composition at the active zone.

3.3.1 Removal of Rab3 from the vesicle membrane does not alter vesicle attachment to the plasma membrane

The GDI dissociation protocol was adapted from [170]. Briefly, samples were incubated for 30 minutes at $37\,^{\circ}\mathrm{C}$ with purified GDI [0.5 μM] in the presence of excess GDP or the non-hydrolytic GTP analogon GTPγS [0.5 mM]. GTPγS locks Rab3 in the active membrane-bound state and thus prevents membrane extraction by GDI. A His-tagged version of GDI from rat species was recombinantly expressed and purified according to [223]. GDI can be introduced at two stages in the established purification procedure (see Fig. 3.11 A) and both possibilities were examined.

The earliest possible step at which GDI incubation could be applied is after synaptosomal lysis prior to the gradient centrifugation step. Following treatment, the fractions were collected and the migration pattern of docked and free vesicles compared by Western blot. As seen in Fig. 3.11 B, no change in the distribution of the vesicle marker synaptobrevin was observed even though GDI/GDP dependent Rab3 removal was successful. Samples treated with GDI/GDP

showed two vesicle populations in the same fractions and in the same intensity as untreated samples or samples incubated with GDI/GTPγS or only GDP. Thus, despite the removal of Rab3 from the membrane, GDI incubation appears to have no effect on the attachment of vesicles in this fraction. Clearly, a significant reduction in docked vesicles, as hypothesized, was not seen.

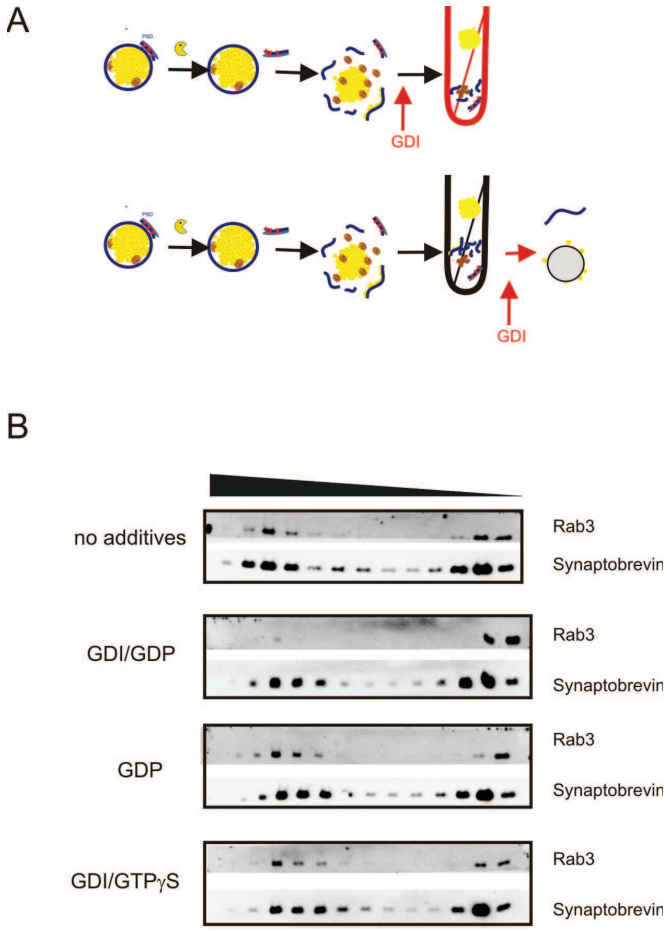

Figure 3.11: (A) Schematic overview of GDI experiments. GDI was added to lysed synaptosomes or directly to the docked vesicle fraction. (B) GDI/GDP, GDI/GTPγS, GDP were added to lysed synaptosomes. Samples were incubated for 30 minutes at 37 °C, followed by a sucrose gradient centrifugation step as in Fig. 3.1. Western blot analysis of gradient fractions showed that Rab3 was removed efficiently from the SPM, but GDI did not alter the migration of docked vesicles.

The next plausible step to add GDI is the docked vesicle fraction. SPM fractions from the gradient were incubated with GDI and GDP, or GTPγS, followed by the immunoisolation of synaptic vesicles. If synaptic vesicles are released from the plasma membrane, the immunoisolates should be devoid of or be reduced in synaptic membrane components. As before,

Rab3 was efficiently extracted from the membranes, but the immunoisolates still contained the plasma membrane marker $\mathrm{Na^+/K^+ATPase}$ and components of the active zone (see Fig. 3.12 A). Thus, synaptic membranes appear to remain attached to SVs. Despite the absence of changes when selected proteins were analyzed after GDI treatment, a possibility remains that only a release of few synaptic vesicles has occured that could not be revealed with this method. Few attached vesicle could remain sufficient to immunoisolate the complete docking site.

To investigate smaller changes in vesicle release, we examined vesicle docking by floatation assay and analyzed if a floatation of released synaptic vesicles has occured after treatment with GDI/GDP or GDP. Following GDI incubation, samples were overlaid with an discontinuous sucrose density gradient [SPM, 0.7 M, 0.32 M sucrose] and centrifuged for 3 hours. Fractions were collected and analyzed by Western blotting. The distribution of the material showed no difference between GDI/GDP and GDP treated samples. In both treated and control samples a minor floatation of membranous material was detected at the 0.7M sucrose/SPM interface. However, these likely do not respond to released synaptic vesicles since parts of the plasma membrane were still present evidenced by the presence of the $\mathrm{Na^+/K^+ATPase}$. More likely this membranous material may represent a less dense portion of docked synaptic vesicles (Fig. 3.12 B).

This flotation assay has been systematically changed to improve the separation of the material, parameters e.g. different sucrose densities, sample densities or sample conditions were tested. However, neither reducing the sucrose density overlaying the sample nor diluting the sample itself showed any effect in the distribution in the detected signal of synaptic marker proteins (data not shown). Changes in the GDI assay, such as adding salt, pre-incubation with nucleotides or varying incubation time and temperature did not influence the observed vesicle docking, suggesting that under all conditions, synaptic vesicles remain attached to the plasma membrane. Thus, at the stage where vesicle are already docked, Rab3 extraction does not influence the adherence to the membrane.

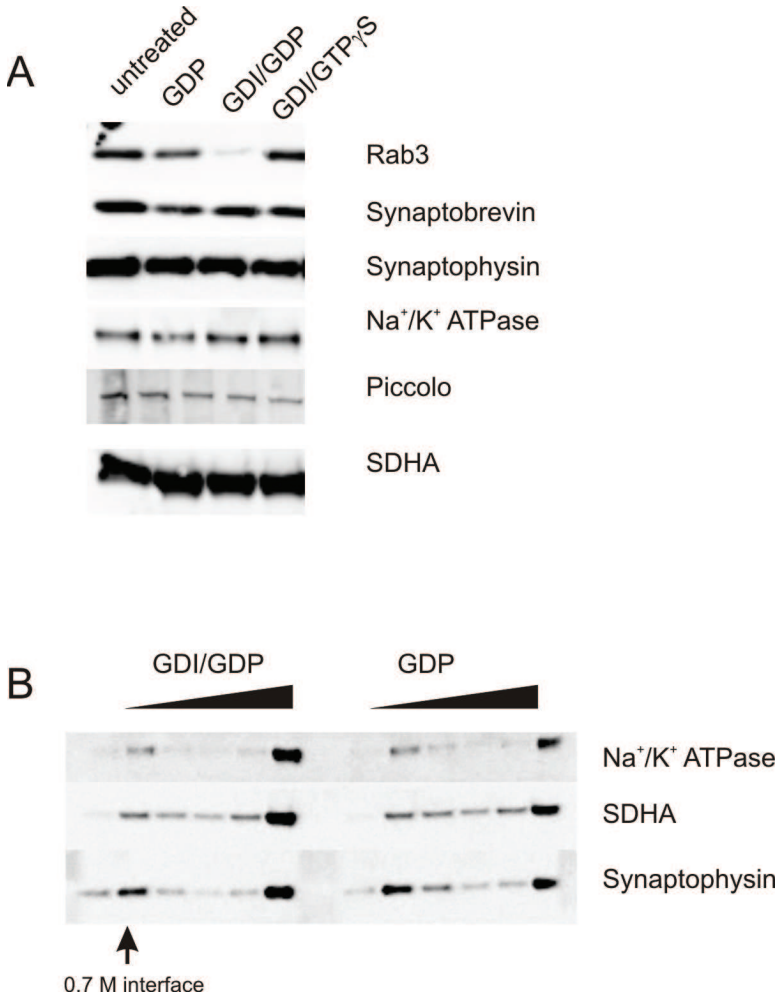

Figure 3.12: (A) Immunoisolation of a docked vesicle fraction after treatment with purified GDI for 30 minutes at 37 °C. Western blot analysis showed that in the GDI/GDP treated docked vesicle fraction, immunoisolated synaptic vesicles are devoid of Rab3 but appear to remain attached to the plasma membrane. (B) Floatation assay of GDI treated docked vesicles. Following GDI treatment, samples were subjected to discontinuous floatation gradient centrifugation. Fractions were collected and analyzed by Western blot. Membranous material was detected at the 0.7 M sucrose interface in all samples, but GDI-dependent vesicle release from the membrane was not observed.

3.3.2 GDI treatment does not remodel the protein composition of the active zone

Rab3 null mutants in *D. melanogaster*, exhibit defetcs in the distribution of active zone components. This indicated that that Rab3 plays and important role in regulating the protein composition at vesicle release sites [224]. To determine whether removal of Rabs by GDI-treatment also induced a change in already assembled mammalian active zones, we decided to look at changes in the GDI treated samples using iTRAQ analyses. Similar to the previous described comparison of docked and free vesicle (see section 3.2), immunoisolates of untreated, GDI/GDP, GDI/GTPγS and GDP incubated SPM fractions were labeled in parallel, combined, purified, and analyzed. Because direct comparison is limited to two samples within the iTRAQ analysis, all modified samples were compared to the untreated immunoisolates. In order to display enrichment and de-enrichment, a log2 scale was used in the Y-axes of the graphs to allow changes in ratios to be easily compared. With this, evenly distributed proteins have a value of zero, a two-fold change is illustrated as a value of one and was set as the cut-off value in this experiments.

In line with the previous Western blot analyses, addition of recombinant GDI led to a significant decrease in the amount of Rab proteins detected in the presence of excess GDP. Among the group of Rab proteins, members of the Rab3 family showed the highest reduction as exemplified by log2 = 1.5 which is equal to a 3-fold reduction. As an indication of the specificity of the assay, no changes were observed in the levels of Rab27. Rab27, a recently identified member of the exocytotic Rabs is known to be resistant to GDI-membrane extraction [21]. Strikingly, except for the Rab proteins and GDI, no other component of the docked vesicle fraction was significantly altered (Fig. 3.13 C).

Importantly, treatment with GDP alone or GDI in combination with the inextractable Rab3-GTPγS, also did not change the proteome of the docked vesicle fraction. In the GDP alone negative control, none of the over 500 identified proteins were significantly reduced or enriched compared to untreated symaples. Samples treated with GDI/GTPγS exhibited only an enrichment of GDI among all detected proteins. These data indicate that removal of Rab3 does not remodel the active zone at an assembled stage. More importantly, they also demonstrate that the fraction (or the protocol) can be used to investigate other manipulations on changes in the presynapse.

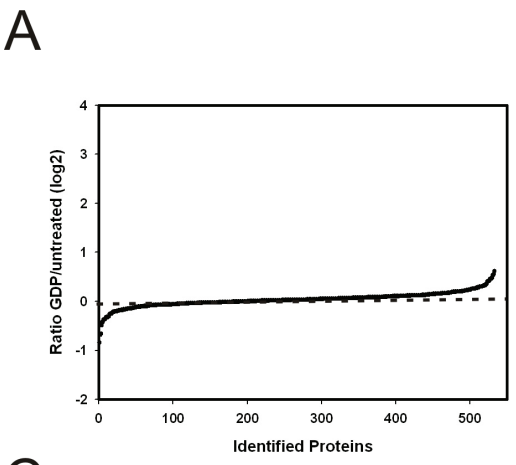

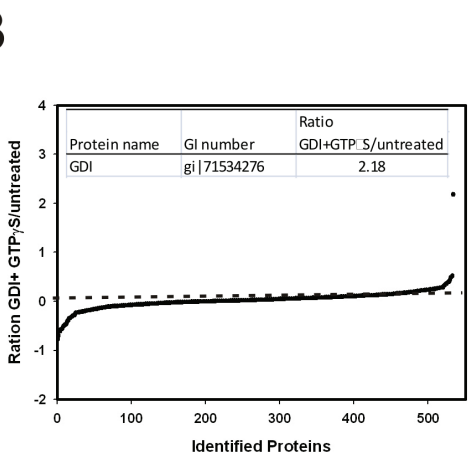

Protein name	GI number	Ratio GDI+GTPγS/untreated
GDI	gi|71534276	2.18

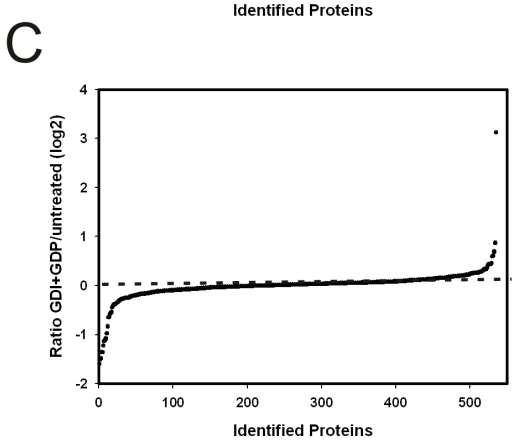

Protein name	GI number	Ratio GDI+GDP/untreated
RAB3B	gi|13592037	-1.60
RAB7A	gi|13027392	-1.50
RAB3A	gi|61098195	-1.49
RAB6A	gi|213972608	-1.36
RAB39	gi|157822741	-1.36
RAB14	gi|16758368	-1.23
RAB10	gi|61889071	-1.14
Rab-1B	gi|109463007	-1.12
RAB1	gi|45433570	-1.08
RAB35	gi|61556789	-1.08
GDI	gi|71534276	3.12

Figure 3.13: Following incubation with GDI/GDP, GDI/GTPγS or GDP, SPM fractions were immunoisolated and analyzed by ITRAQ analysis as in 3.2. Peptides were labeled with iTRAQ reagents 114-117 and ratios generated as treated/untreated sample. Data are illustrated on a log2 scale. A value of 0 equals a 1:1 ratio showing that no change had occured. (A) Incubation only with GDP did not result in any changes in the proteome of the docking sites. (B) When retaining Rab3 in its membrane bound state with GTPγS, GDI treatment showed no effect except for an enrichment of GDI itself. (C) GDI/GDP incubation successfully removed Rab proteins, but no other components were affected. The levels of Rab27, which is not extractable by GDI, was unchanged.

3.4 JB1 is a novel transmembrane protein localized at presynaptic nerve terminals

As previous mentioned in 3.2.9, a large number of unknown proteins were present in the docked vesicle fraction. To facilitate selection of the most interesting candidates, proteins were ranked according to their mRNA expression level in the brain, domains composition and extent of evolutionary conservation. Using this strategy, five proteins were chosen for further characterization. Of the five, one of them, JB1, shows much promise as a novel integral member of the presynaptic membrane.

3.4.1 Identification and characterization of JB1

JB1 was exclusively found in the SPM (Table 3.9). Officially named hypothetical protein LOC315463 by NCBI, this protein is largely uncharacterized and its function unknown. It is 267 amino acids long and has a predicted molecular weight of 30kDa.

Using the SMART (Simple Modular Architecture Research Tool) program [225, 226], a web-based tool for the study of genetically mobile domains , JB1 was predicted to contain a domain of unknown function (DUF2366) and a transmembrane domain near the N-terminus (Fig. 3.14 A). However, the reliability of the transmembrane domain prediction is uncertain. The transmembrane helix probability was close to the threshold. Additional analyses using other public available computational programs were done to confirm the predicted transmembrane domain. Unfortunately, theses transmembrane prediction analyses yielded conflicting results: The number of identified transmembrane segments varied between 0 (TMHMM [227]), 1 (HMMTOP [228]) and 2 transmembrane helices (DAS [229], TMPRED [www.ch.embnet.org]). A potential transmembrane domain can be supported by sequence coverage of the identified iTRAQ peptides which exclude the predicted transmembrane segment (see Fig. 3.14 B). Transmembrane sequences seldom contain the positively charged tryptic cleavage sites and are therefore rarely detected.

Next, sequences homologous to JB1 were identified using BLAST (Basic Local Alignment Search Tool) . The identified sequences were then aligned using the program T-Coffee [230]. As seen in Fig. 3.14 B, JB1 is highly conserved among mammals, but orthologes are also found in *D. rerio*, *D. melanogaster* and *C. elegans*. Even in these model organisms, JB1 function is unknown.

To investigate JB1 transcript distribution in the brain, we made use of the Allen Mouse Brain Atlas, an open interactive, genome-wide image database of gene expression [231]. The online available data are obtained by RNA in situ hybridization of tissues derived from 8-week

old male mouse brains and are integrated into a detailed digital reference atlas. As shown in Fig. 3.14 C, JB1 transcripts were present in the brain with a particularly high level of expression in the hippocampus.

To enable further characterization of JB1, a rabbit polyclonal antibody was generated against recombinant full length JB1 protein. In immunoblots, anti-JB1 antibody recognised a single 30 kDa protein band in crude synaptosomes in excellent agreement with the predicted size of JB1 (Fig. 3.15 A). Lysates of HEK293 cells overexpressing a JB1-GFP fusion protein additionally confirmed the specificity of the anti-JB1 antibody. Immunoblots with anti-JB1 and anti-GFP antibody both recognized the fusion protein at approximately 55 kDa. Lysates of untransfected HEK293 cells did not show chemiluminescence indicating that these cells don not express endogenous JB1 (Fig. 3.15 B).

3.4.2 JB1 is a transmembrane synaptic protein

To determine if JB1 indeed contains a transmembrane region, we used a panel of detergents to analyze the behavior of endogenous JB1 following detergent extraction. JB1 was completely extractable from crude synaptosomal membranes by the non-ionic detergent Triton-X 100, partially soluble with zwitterionic detergent CHAPS and insoluble when treated with alkaline Na_2CO_3. Alkaline Na_2CO_3 releases peripheral membrane proteins by converting the membrane into flat sheets [232]. The solubility pattern of JB1 resembled the single transmembrane domain-containing SNARE syntaxin1A (Fig. 3.15 C). In contrast, the multispanning transmembrane receptor NR1 remained insoluble in all conditions. Thus, these studies indicate that JB1 indeed contains a bona fide transmembrane domain.

To determine the expression profile of JB1, multiple tissues were dissected from a 6-week old male wistar rat, homogenized and membrane fractions enriched using a Triton-X-114 phase partitioning assay [166]. The highest amounts of JB1 were observed in brain tissues (cortex, cerebellum, spinal cord), supporting that the main function of this protein might be neuronal (Fig. 3.15 D). JB1 is also present in heart and to a lesser extent in kidney and pancreas. Interestingly JB1 was absent in skeletal muscle tissue, although both cardiac and skeletal muscle coordinate excitation-contraction coupling. In the pancreas, the antibody detected 3 protein bands at 30 kDa, 35 kDa, and a major band at 50 kDa, respectively. The larger polypeptides might indicate the existence of different splice variants in pancreas. To exclude detection biases due to sample preparation, tissues were additionally probed for the ubiquitously expressed mitochondrial protein SDHA as well as the Golgi SNARE syntaxin6. These proteins were detected in all tissues.

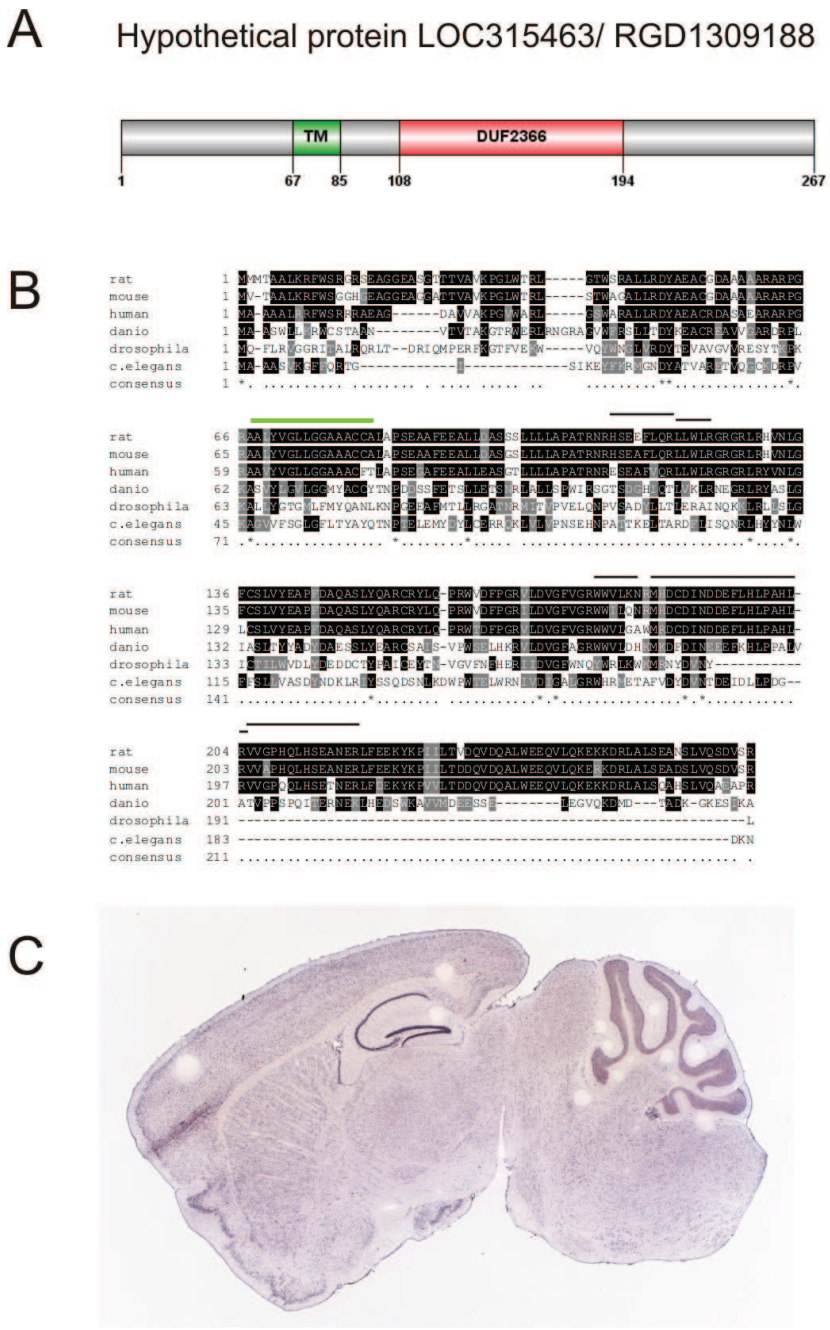

Figure 3.14: (A) Hypothetical protein LOC315463 (JB1) has one potential transmembrane domain and a domain of unknown function (DUF2366). Data were obtained using the online tool SMART. (B) Amino acid sequences of JB1. Sequences were deduced from sequence analysis of rat, mouse, human, zebrafish, fly and worm. Black lines denote peptides identified by iTRAQ. The green line highlights the putative TM domain. (C) JB1 transcript distribution in mouse brain. Strongest expression was observed in the hippocampal CA3 region and in the dentate gyrus. Data were obtained from the Allen Mouse Brain Atlas (accesion number NM178619).

Next the subcellular distribution of JB1 was analyzed by Western blotting. JB1 is strongly enriched in the synaptosomal fraction P2' and the presynaptic plasma membrane fraction LP1. Importantly, it is completely absent from synaptic vesicles (see Fig.3.15 E). Because in this experiment synaptosomes were not protease treated, the LP1 fraction still contained parts of the postsynaptic density exemplified by the immunoreactivity of PSD95. PSD95 exhibited a strong co-enrichment with JB1. The SV protein synaptobrevin is diminished in the LP1 fraction and highly enriched in the synaptic vesicle fraction. These data agree with the iTRAQ result of JB1 being only present in the docked vesicle fraction and essentially identifies JB1 as a novel synaptic protein. However, attention should be paid to a remaining possibility of JB1 being a postsynaptic component. Although the low postsynaptic contamination detected in the iTRAQ data point to a presynaptic role of JB1, the employed subfractional analysis is not sufficient to completely exclude a postsynaptic localization.

3.4.3 JB1 is associated with presynaptic structures

To exclude the possibility that JB1 is a postsynaptic contaminant, the developed validation assay for the removel of postsynaptic components (see section 3.1.1.2) was applied to verify the indicated presynaptic localization of JB1. Trypsinized and untreated synaptosomes were immunofluorescently labeled with a combination of antibodies against JB1 and synaptotagmin or JB1 and PSD95 and the distribution of the detected signals analyzed by confocal microscopy. As shown in Fig 3.16 A, signals observed for JB1 (green) and synaptotagmin (red) co-localize extensively in untreated synaptosomes. Linescans drawn across the puncta showed overlapping signal intensity peaks for both proteins. This co-localization did not change in trypsinized samples. Neither the signal intensity nor the number of puncta observed for JB1 was affected as is observed for synaptotagmin. In contrast to this, in the samples co-stained with PSD95, the extent of co-localization significantly decreased in trypsinized synaptosomes. Moreover, the number of PSD95 puncta was greatly diminished compared to untreated synaptosomes while the amount of observed JB1 puncta appear to stay constant. Linescans verified that the remaining JB1 puncta were devoid of any postsynaptic signal.

The immunofluorescent images represented only a small fraction of the total population of synaptosomes. To analyze the total protein amount in the sample, the same fractions were additionally compared by Western blotting (Fug. 3.16 B). As expected, JB1 is not degraded by protease treatment.The detected signal was comparable to untreated synaptosomes, whereas PSD95 levels was reduced significantly upon trypsin digestion.

Finally, we compared the endogenous distribution pattern of JB1 in rat hippocampal neurons with synaptotagmin and PSD95. Hippocampal neurons were fixed at 14 DIV and immuno-

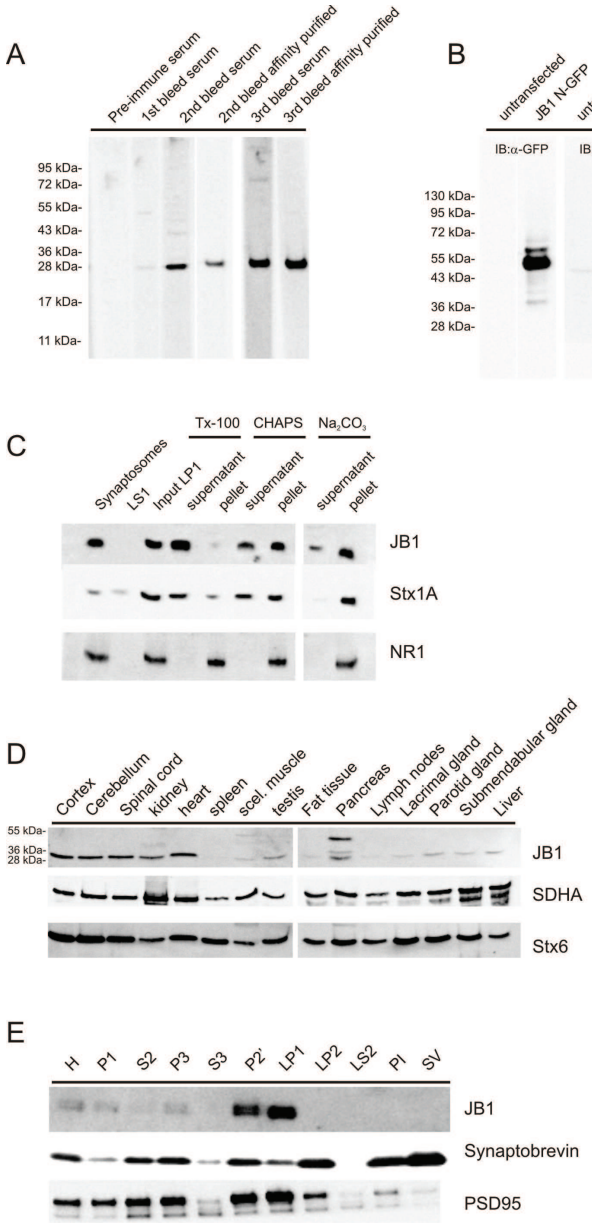

Figure 3.15: (A) Characterization of antiseren showed that JB1 is present in synaptosomes. 22μg synaptosomes per lane were resolved by SDS-PAGE and transferred to a nitrocellulose membrane. Different batches of serum (1:2000) or affinity purified (1:500) anti-JB1 rabbit polyclonal antibody were tested for their efficacy to recognise endogenous JB1. A single protein band corresponding to the predicted molecular weight was detected since the second bleeding. (B) Immunoblot of untransfected and transfected HEK293 lysates overexpressing a JB1-GFP fusion protein. HEK293 cells were transiently transfected and harvested after 24 h. JB1-GFP was detected with anti-GFP antibody (left) and anti-JB1 antibody (right). (C) Solubility of JB1 from pelleted synaptic plasma membrane fractions (LP1). LP1 pellets were resuspended in 1% Tx-100, 1% CHAPS or 100mM sodium carbonate pH 11.4 and incubated for 30 minutes at $4\,^{\circ}\mathrm{C}$. The remaining insoluble parts were re-pelleted for 30 minutes at 100 000 *g*. Solubility of JB1 resembled that of syntaxin 1. (D) Expression of JB1 in different tissues. 1 mg of each tissue homogenate was subjected to membrane extraction with Triton-X-114 and equal volumes loaded per lane. (E) Western blot analysis of subcellular fractions from the rat brain. 10μg of homogenate (H), nuclear and large membrane pellet (P1), crude brain cytosol and small organelles (S2), small cell organelles (P3), brain cytosol (S3), crude synaptosomes (P2'), presynaptic plasma membrane (LP1), crude synaptic vesicles (LP2), synaptic cytosol (LS2), (P1) and pure synaptic vesicles (SV) was loaded and probed for JB1, a postsynaptic marker JB1 and the SV protein synaptobrevin. JB1 is strongly enriched in synaptosomes and presynaptic membrane fraction.

A

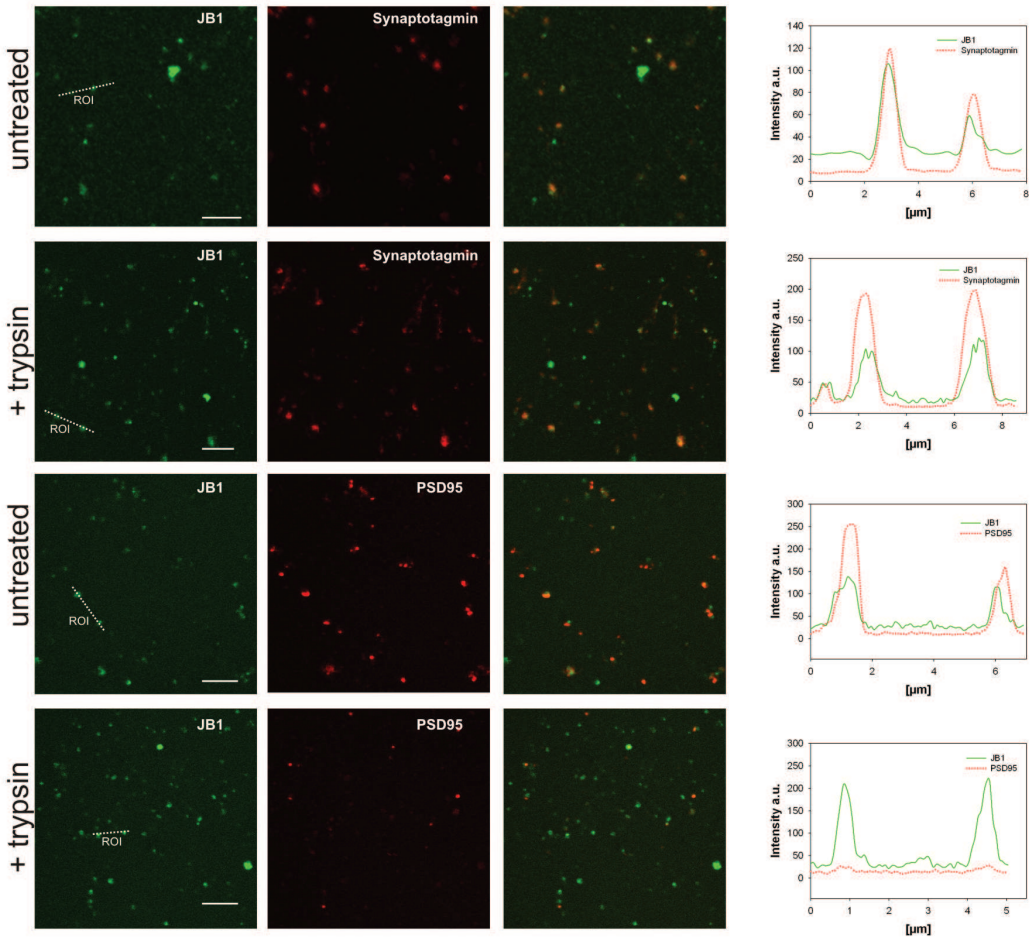

B

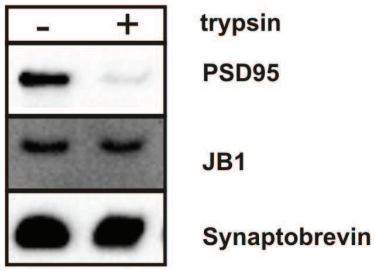

Figure 3.16: (A) Immunofluorescent staining of synaptosomes. Protease treated and untreated synaptosomes prepared as in 3.1.1.2 were co-labeled with antibodies directed against JB1 (green) and synaptotagmin (red) or JB1 and PSD95. JB1 puncta were resistant to protease treatment. (B) Western blot analysis of the total protein in the fraction confirmed that JB1 remains present in shaved synaptosomes, whereas levels of PSD95 are depleted.

labeled with antibodies against JB1 and synaptotagmin or PSD95. As seen in Fig. 3.17, JB1 labeling showed a punctate staining in neuronal processes. A closer examination of synaptic nerve terminals revealed that these puncta partially overlapped with the synaptic vesicle protein synaptotagmin (see arrowheads). In contrast to this, no overlap was detected with the dendritic protein PSD95. Moreover, JB1 puncta appeared to be localized juxtaposed to the postsynaptic density (see arrowheads).

In summary, the accumulated data agree with the iTRAQ results and demostrates that JB1 is a bona fide novel presynaptic protein.

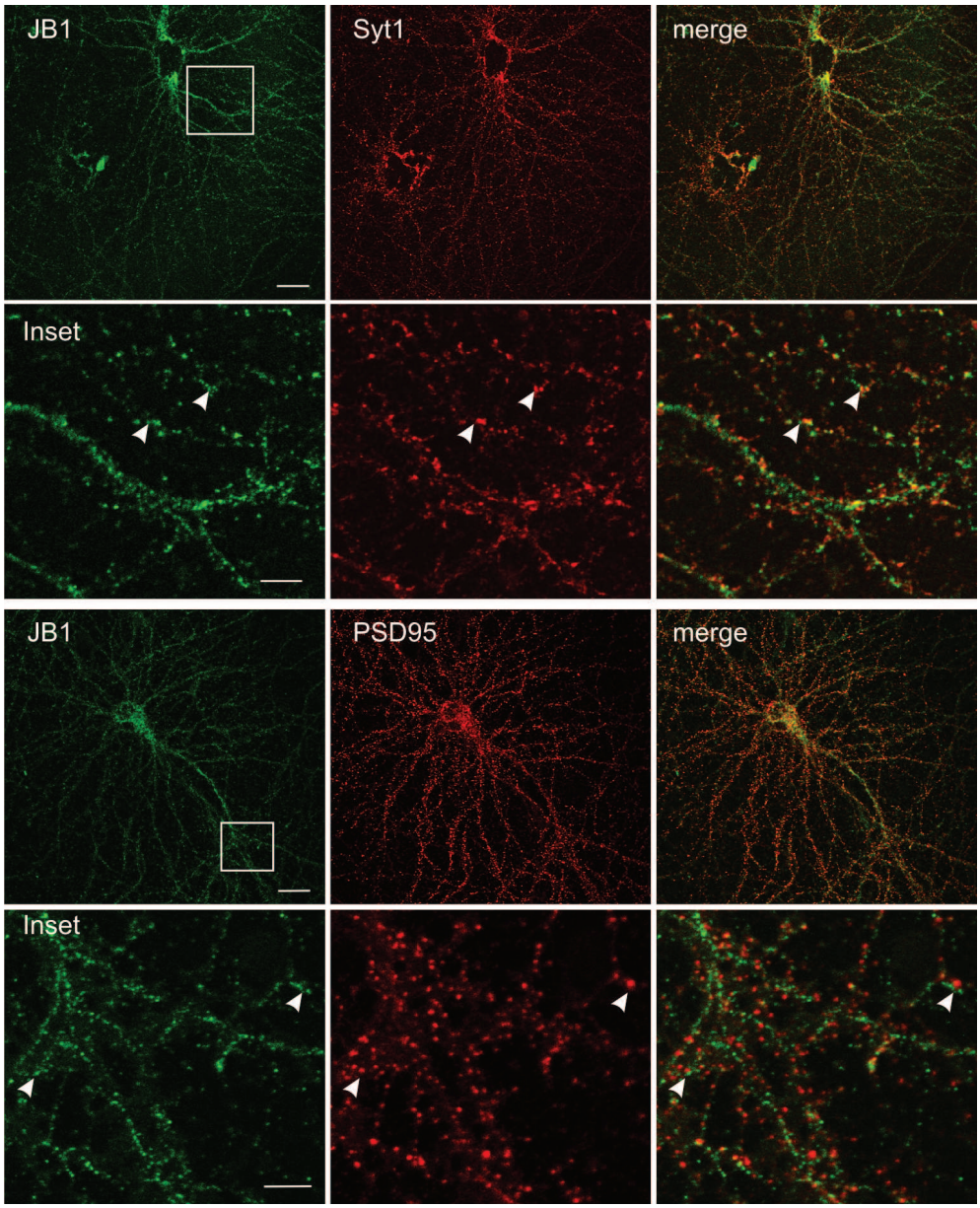

Figure 3.17: Hippocampal neurons DIV14 were double labeled with antibodies against JB1 and synaptotagmin or JB1 and PSD95. Immunostaining for JB1 (green) was observed in neuronal processes. Magnified views (boxed) revealed a punctate staining for JB1 with a partial colocalization with the synaptic vesicle protein synatotagmin in contrast to the postsynaptic protein PSD95. Arrowheads highlight co-labeled structures.

4 Discussion

4.1 A novel protocol to separate pre- and postsynaptic compartments

As outlined in the introduction, excitatory synapses are characterized by their asymmetric organization with a presynaptic nerve terminal containing synaptic vesicles and the presynaptic machinery, a synaptic cleft, and a postsynaptic signaling complex called the postsynaptic density (PSD). Postsynaptic densities can be isolated from synaptosomes by non-ionic detergents that solubilize the presynaptic, but not the postsynaptic specialization [172]. These PSD fractions have been characterized extensively by proteomic approaches, revealing a large number of proteins that are bona fide postsynaptic proteins ([233, 133, 135, 234]). However, these preparations are not exclusively postsynaptic as they also contain a number of presynaptic proteins exemplified by the discovery of bassoon [97].

On the other side, the isolation of presynaptic specializations has been addressed for years, but compared to the large number of postsynaptic density constituents, comparatively few presynaptic components have been identified. Core active zone proteins have been mainly found by low-throughput approaches such as yeast-two-hybrid screens: Rim [78], ERCs 1 and 2 [88], CASK [117] and Mint [120]. These systems are very useful in the detection of pairwise protein interactions, but cannot reveal the global constituents of the presynaptic nerve terminal. Thus, it is commonly believed that the molecular composition of the presynaptic site is incompletely characterized. The identification of presynaptic protein components is mainly limited by difficulties in obtaining a sufficiently active zone-enriched fraction that is devoid of postsynaptic contamination. Unfortunately, plasma membrane fractions isolated by density gradient centrifugation still exhibit intact pre- and postsynaptic adhesion [172]. Consequently, no satisfactory and comprehensive characterization of the presynaptic proteome was previously available, although a number of proteomic studies have been performed to profile synaptic protein constituents:

- In 2001 and more comprehensively in 2005, Phillips and co-workers reported a detergent based isolation of a presynaptic particle fraction [152, 151]. This protocol is based on a sequential pH-dependent Triton-X-100 extraction of synaptosomes. A first extraction with 1% Triton-X-100 in Tris pH 6.0 solubilizes the plasma membrane but paired pre- and postsynaptic structures remain in the insoluble pellet. A second extraction step with an elevated pH 8.0 solubilizes only the presynaptic network that is collected and repelleted after a dialysis back to pH 6.0. This was the first attempt to separate the presynaptic- from the postsynaptic compartment, allowing the identification of proteins from an isolated presynaptic fraction. Characterizing both fractions using MudPIT, they could show that the presynaptic proteins dynamin, clathrin heavy chain, syntaxin1, SNAP25 and Munc18 are present in the presynaptic particle fraction, but controversially, bassoon, piccolo, Rim and synaptotagmin were exclusively found in the postsynaptic fraction. Other known active zone components, e.g. Munc13, ERC2 or Liprins could not be identified.

- A different approach to obtain the presynaptic fraction, that did not address a separation of pre- and postsynaptic compartments, but included an affinity purification step of a docked vesicle fraction was developed by Morciano and co-workers in 2005 and 2009 [173, 153]. Briefly, synaptosomes were osmotically lysed, synaptic plasma membranes fractionated by gradient centrifugation an immunoisolated with an antibody specific for the synaptic vesicle protein SV2. The analyzed immunoisolates contained synaptic vesicle proteins, cytoskeletal elements, active zone molecules, plasma membrane components, mitochondrial proteins and metabolic enzymes. However, active zone proteins were mostly identified by additional Western blotting and some major components such as Liprins, CASK and ERC2 remain undetected. Notably, an examination for PSD contamination was omitted.

- Using the protocol developed by Philipps and co-workes, Abul-Husn et al. systematically approached the presynaptic proteome by generating a comprehensive list of presynaptic proteins [235] by including known protein interactions derived from literature mining and combining them with their own data, the data from Phillips et al. [151], and Morciano et al [173]. The final "presynaptic core list" of 117 proteins in total included only proteins identified two or more times in their MS analyses and contained largely synaptic vesicle proteins, plasma membrane components and cytoskeletal elements. Strikingly, active zone proteins are completely absent from this list.

Here I have established a novel protocol that permits the immunoisolation of a presynaptic compartment from proteolytically "shaved" synaptosomes. From this fraction I was able to

generate the first global protein composition of presynaptic docking sites using quantitative mass spectrometry. Using this strategy, I was able to identify novel components of the presynapse and characterize one of them in detail. Additionally, I showed that proteolytically treated synaptosomes/immunoisolated presynaptic AZ fractions can be used to study global changes in their proteome following external manipulations. In the following, the new procedure described in this work will be compared to the existing studies in relation to sample preparation and analysis, and data quantity and quality.

4.1.1 Method

Two fundamental problems currently limit the characterization of the presynaptic proteome: Sample complexity and the dynamic range of the analytes. Due to the large number of proteins and the heterogeneity, proteins in low abundance have a high chance of being obscured by those of high abundance. Also highly hydrophobic proteins such as channels and transporters remain challenging, because these proteins cannot be properly solubilized and are consequently difficult to identify.

By removing the postsynaptic density (whicht itself contains several hundred proteins [133, 135, 234]) is not only important to ascertain presynaptic localization of the identified proteins, but is also the most effective step to reduce the complexity of the sample. This strategy has already been adressed by two groups, but a satisfactory separation of pre- and postsynaptic compartments could not be achieved so far:

- The detergent based protocol reported by Philipps and coworkers depends on differential solubilities of the proteins in the sample to achieve separation of both synaptic compartments [152]. However, transmembrane proteins and also scaffolding proteins like bassoon, piccolo and Rim have a tendency to be difficult to extract and thus could explain their existence in the detergent resistent postsynaptic pellet [236].

- A detergent-independent approach using a denaturing protocol was reported by Berninghausen et al. By combining urea and DTT to disassemble the connection of pre- and postsynaptic membranes, they enriched bassoon and piccolo in a presynaptic membrane fraction together with syntaxin, SNAP25 and synaptotagmin while postsynaptic preoteins like NR1, GluR1 and PSD95 are diminished. They could provide a calculated 3.2-fold enrichment, but did not achieve homogeneity of the pre-and postsynaptic membranes [237].

In this study the postsynaptic membrane was almost quantitatively removed from synaptosomes after a protease treatment step. Western blotting and immunofluorescence microscopy con-

firmed that trans- and postsynaptic components such as Neuroligin, NR1, GluR1 and PSD95 were successfully removed while presynaptic components and synaptic vesicle proteins remained intact. I further combined this depletion strategy with an enrichment of presynaptic proteins (affinity purification of a docked vesicle fraction). A separation with such a high degree of efficiency has not been achieved before.

However, the novel protocol developed in this study is based on the proteolytic cleavage of the synaptic cleft. Unlike a detergent based strategy, using proteases entails the risk of unwanted protein degradation in the presynaptic compartment. Therefore, proteolytic conditions were carefully tested and optimized to minimize presynaptic protein degradation, but still provide sufficient proteolytic activity to cleave the trans-synaptic connections. Importantly, trypsin activity could be immediately stopped at the desired time by adding an irreversible serine protease inhibitor. Furthermore, one need to keep in mind that the elevated temperature incubation at $30\,^{\circ}\mathrm{C}$ might cause an increase of endogenous protease reactivity.

In contrast to the other separation strategies, the extracellular domains of presynaptic transmembrane proteins and adhesion molecules are removed resulting in a potential loss of function of these proteins. Therefore studies of these proteins are limited with this method. Additionally, synaptic adhesion molecules have been proposed to have a role in the organization and modulation of synaptic structure ([238, 239, 240]). Thus, a possible effect on protein stability induced by the removal of these proteins cannot be completely excluded. However, the large number and identity of the detected proteins did not support a change in the protein composition as a consequence of protease usage. Even intracellular proteins prone for degradation like the 500 kDa protein piccolo or synapsin did not show major degradation after protease treatment. This indicates that the presynaptic proteins inside of the membrane remain preserved.

Despite the successful removal of the postsynaptic density and a subsequent immunoisolation step, the presynaptic docked vesicle fraction remains a biological complex sample. Sample complexity often exceeds the capability of mass spectrometers although a continuous improvement in accuracy and throughput has taken place. This not only leads to a loss in information, it can also produce sample bias towards proteins with high abundance. In comparison to other proteomic analyses [153], we additionally employed an upstream peptide fractionation by strong cation exchange chromatography (SCX) prior to LC-MS/MS analysis. Such a fractionation increases resolution and minimize ion suppression effects by separating tryptic peptides according to charge and hydrophobicity prior to the MS analysis. When analyzing samples with large amounts and a diverse heterogeneity of proteins, this method has succeeded conventional 1D SDS-PAGE protein separation [241], which is often limited by an unavoidable band overlap due to the large protein amounts. Conventional 2D-gel electrophoresis, separating in the first dimension by isoelectric focusing point (IEF) and in the second dimension by mass,

has major problems resolving hydrophobic proteins [242] and is therefore limited for the use of membrane proteins [243]. An alternative gel-based 2D-electrophoretic separation method named BAC/SDS-PAGE has been applied by Morciano et al. [173]. This separation improves the resolution of membrane proteins [244, 245], but might be biased against hydrophilic proteins.

The SCX fractionation method has already been proven to be a good choice for synaptic plasma membrane preparations [246]. By doing a comprehensive study on the mass spectrometric side of the analysis of crude synaptic plasma membranes, this group showed that a comparable amount of sequencing information could be obtained from each SCX fraction as to the one-dimensional analysis of whole digest sample. This improvement allowed for an identification of a large number of proteins that have been underrepresented in other studies, in particular active zone components and transmembrane channels [151, 153]. Another advantage of a SCX purification is its ability to remove excess labeling chemicals and other substrates that possibly interfere with MS analysis.

Finally, unlike previous proteomic studies of the presynapse, I have applied a quantitative mass spectrometric strategy by using the stable isotope labeling reagent iTRAQ. A relative quantitation comparing the immunoisolates from the docked vesicle fraction and free vesicles was done to enrich for presynaptic proteins and distinguish SV proteins.

4.1.2 Presynaptic proteome

What constitutes the proteome of presynaptic preparations? Clearly, presynaptic signature molecules and organelles such as synaptic vesicles, active zone components and presynaptic channels have to be present. For the first time, with this novel protocol, we could identify almost all active zone proteins and a large number of transmembrane channels by mass spectrometric analysis. In addition, synaptic vesicle proteins (SCAMPs, SV2s and neurotransmitter transporters) that remained unidentified in the presynaptic particle fraction [152, 151], or were only detected by Western blotting [153], were identified and quantified in this preparation, providing a comprehensive list of SV proteins.

A good presynaptic proteome needs to be additionally devoid of postsynaptic contamination. As a result of the successful removal of the postsynaptic density, the final immunoisolates only exhibit three remaining proteins exclusively localized to the postsynaptic density among 500 identified proteins. Interestingly, in the immunoisolated docked vesicles of synaptosomes that have not been addressed for PSD removal as done by [173, 153], PSD components were also not detected by mass spectrometry. But unfortunately, the authors did not additionally

test for postsynaptic contamination as it has been done for the undetected presynaptic proteins [153].

In this study we have performed the first correlation profiling of presynaptic proteins contained in the docked synaptic vesicle and free synaptic vesicle fractions using iTRAQ quantification. Originally established as a label-free approach to characterize the human centrosome [139] or map whole organelles [247], protein correlation profiling simplifies the analysis of complex samples that can only be enriched by fractionation but not completely purified to homogeneity. In our study, this strategy was used to discriminate genuine presynaptic proteins from synaptic vesicle constituents. It assumes that proteins which are contained in the synaptic vesicle would have the same degree of enrichment, whereas proteins involved in attaching the SV to the plasma membrane or residing in the presynaptic membrane are thought to have a different degree of enrichment. Indeed, all detected proteins that have been reported to be localized to synaptic vesicles [138] were additionally confirmed as such by a non-enrichment in the iTRAQ ratio.

However, some contaminants may behave biochemically similar and therefore may co-purify with the docked vesicle fraction. An example could be the persisting detection of mitochondria in this study. However, this hypothesis remains debatable and mitochodondria might also represent integral components of the active zone. Although the immunofluorescent images of the docked vesicle fraction did not show significant overlap between mitochondria and the active zone protein piccolo, other studies suggest a direct attachment of this organelle to nerve terminals via syntaphilin [248, 249]. Syntaphilin was not detected in this study, but a possible association at close sites at the plasma membrane but not directly at the active zone cannot be excluded. In fact, electron tomography showed evidence for a cytoskeletal structure that connects mitochondria to the presynaptic membrane near active zones [250]. This supports the idea that mitochondrial localization at active zones is essential to regulate the calcium concentration and metabolic demand of synaptic transmission.At the neuromuscular junction of *D. melanogaster*, an additional role for mitochondria in the assembly of the actin cytoskeleton within presynaptic boutons [251] and mobilization of synaptic vesicle from the reserve pool to the readily releasable pool [252] has been proposed.

In conclusion, the identification and quantification of the presynaptic signature molecules together with a low detection of contaminants proves a high quality for this presynaptic preparation. As a consequence, the remaining proteins that were identified raised in interest. In this study we could identify 506 proteins in the docked vesicle fraction. After a subtraction of 217 mitochondrial localized proteins, 289 proteins remain associated to the presynaptic compartment. Strikingly, compared to the existing presynaptic proteomic studies, the amount of detected proteins has doubled [153] or tripled [151]. A graphical description and comparison

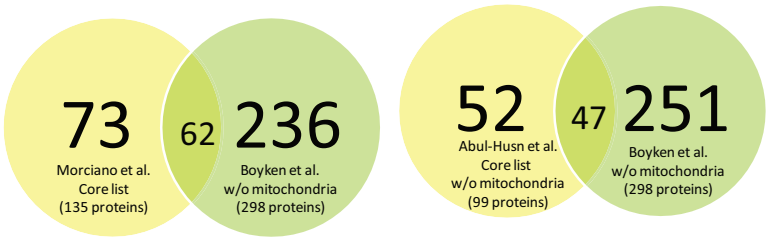

Figure 4.1: A significant overlap between the dataset of Morciano et al., Abul-Husn et al. and the data obtained in this work was observed. Mitochondrial proteins are substracted from all data.

of the data obtained by the different proteomic approaches [153, 235] is illustrated in Fig. 4.1. An overlap between proteins that were identified in this study was observed. This overlapping proteins include synaptic vesicle proteins, high abundant plasma membrane molecules and cytoskeletal components. A complete list of proteins detected in both approaches can be found in the appendix.

Among the proteins that were identified by Morciano et al. but were not detected in this study are dynamin 1/2, SNAP (α, β, γ), several Rab proteins (1b, 11, 3D, 5A, 6B, 7A), GTP-binding proteins (GNA11, GNAI2, GNAZ, GNG3), additional isoforms of 14-3-3 (eta and epsilon) and the plasma membrane calcium ATPase (PMCA3 and PMCA4). Their data also include other adhesion molecules (NCAM2, N-CAM L1, contactin-1, hepaCAM) and cytoskeletal components (actin and tubulin). Also the glial protein MBP was found. Similarly, the presynaptic core list generated by Abul-Husn et al. contained more endocytic related proteins such as dynamin, clathrin light chain and synaptojanin. This list also included additional signaling proteins (calmodulin, MAPK, LYN, protein phosphatase 2B, phospholipase C), other adhesion molecules (L1CAM, contactin 1) and cytoskeletal components (MAP2, actinin 2/3, tropomyosin, tubulin 6) that were not identified in this study. This list also contained the glial protein MBP.

What are these 298 proteins? For the first time, this study presents a global view on the molecular architecture of the presynapse. The data proves evidence that similar to the PSD, neurotransmitter releasing sites exhibit a number of functionally different protein groups that all together form a highly organized network to ensure precise synaptic transmission. Aside from the proteins responsible for regulating exocytosis, this includes a large number of cytoskelatal elements and proteins involved in the mechanisms of calcium extrusion and neurotransmitter clearance as well as neurite outgrowth. Many of these proteins have already been reported to be localized to synaptosomes or synaptic plasma membrane fractions by other non-proteomic approaches. For example, the plasma membrane $\mathrm{Ca}^{2+} - \mathrm{ATPase}$ [186] or EAAT1 and EAAT2 [191] were detected in synaptosomes by Western Blotting. However, these prepa-

rations have contained pre- and postsynaptic compartments. With this study we can not only additionally validate the presence of these proteins by mass spectrometry, we can further prove their localization to the presynaptic membrane. However, a dual existence of these proteins on both sides of the synaptic cleft cannot be excluded, because the postsynaptic membrane was removed in this approach. Although the number of identified proteins could be increased to almost 300 (500 with mitochondria), some known presynaptic proteins remain underrepresented. For example presynaptic receptors such as kainate [253, 254] and Eph [255], were not identified in this study. This lack of identification may have been caused by the tryptic cleavage of molecules exposed to the synaptic cleft, but it also implies that the presynaptic proteome generated in this study, although being very comprehensive, remains incomplete.

4.1.3 Identification of novel proteins

Coming back to the belief that the knowledge of the presynaptic proteome is limited, for many proteins the detection at presynaptic sites was a novelty. Some of these proteins are already characterized but have not been assigned to a presynaptic function, making them interesting candidates that are worthwhile to be investigated in more detail. Strikingly, also more than 30 novel (predicted) proteins could be identified and enriched among the presynaptic proteins. Considering the quality of the preparation, these novel molecules have a high chance of being true bona fide presynaptic constituents. One of these novel proteins, termed JB1, was further characterized and shown to be localized to presynaptic membranes. This makes it a novel presynaptic protein of unknown function. JB1 shows no resemblance to other neuronal proteins and apart from a potential transmembrane region does not contain any known domains. Thus hypothesizing a function in synaptic transmission is difficult without additional studies. Nevertheless, JB1 is conserved and RNAi interference in *C.elegans* is embryonic lethal, suggesting this protein plays an important role. A specific expression in excitatory tissues such as brain and heart indicates a role in excitatory processes. Interestingly, although expressed in cardiac muscle, JB1 could not be detected in skeletal muscle. In contrast to skeletal muscle, cardiac muscles require extracellular calcium for normal excitation-contraction to occur. But implicating a calcium dependent role for JB1 only based on this is pure speculation and needs to be further elucidated. A continuation of the characterization will hopefully reveal its synaptic contribution.

4.1.4 Versatility/usage of the method

The methods developed so far have been mainly used to identify and localize synaptic proteins. A broader application of these protocols in combination with other techniques is limited.

The use of detergents limits many methods. For proteomic applications, there are three major disadvantages: First, a complete solubilization of all proteins contained in the sample cannot be guaranteed. The proteomic data obtained by [237] is indicative of this limitation. Second, all detergents interfere with mass spectrometry to some extent when they are present at high concentrations. Triton-X-100 has a low critical micellar concentration (CMC) [256] and thus cannot be removed by dialysis. This also effects the identification of protein complexes, because other detergents can only be used in addition, but not as an alternative. The Phillips protocol [152] is additionally based on a Tris-buffered system. Thus, quantitative labeling strategies that involve reactive amine groups (such as iTRAQ) cannot be applied. Furthermore many functions of membrane proteins can only be studied in a lipid bilayer, which is perturbed or lost in detergents. Also spectophotometric monitoring can be ineligibly to some extent, because detergents such as Triton-X-100 strongly absorb UV light.

Urea, as used in the denaturing protocol [237], is a chaotropic reagent that denatures proteins at high concentrations (4-8 M). Even at low concentrations (1 M) it can perturb protein structure and alter protein function [257]. Due to the heterogeneity of the proteins in synaptosomes, the probability that the stability of some proteins is affected is rather high. In addition urea causes extensive changes in the behavior of the solvent environment that in turn weakens or disrupts native protein complexes. Repetitive freeze/thaw cycles additionally affects protein stability.

The protocol developed in this study provides the broadest application range. The use of trypsin as a protease does not interfere with subsequent mass spectrometric applications. The protocol is also compatible with immunofluroscence microscopy. Additionally, molecular complexes are retained and can be isolated at a later stage by subsequent immunoisolation strategies. But most important, proteins remain active within the synaptosomal membrane and can be functionally addressed. This, in combination with the applied iTRAQ quantification, allows to study proteomic changes and protein interactions by targeting specific proteins with effectors that promote or inhibit its function.

4.2 Investigation of proteomewide changes in synaptic vesicle docking site upon treatment with effectors

An example of this application is shown by the removal of Rab proteins from synaptic vesicles by GDI. A hypothesis that Rab3 plays an important role in synaptic vesicle recruitment rather than docking has emerged over the years [258]. Although Rab3 have a suggested role in regulating dense core vesicle docking [16, 15], the precise function of Rab3 in synaptic trans-

mission is still not fully understood. Rab3 directly interacts with the active zone scaffolding protein Rim [75] providing a physical link between synaptic vesicles and the presynaptic active zone [68]. Additionally, a similar reduction of docked vesicles in Rab3-, Rim- or Rab3/Rim-double mutants in *C. elegans* were observed, assuming that this interaction might be crucial for the tethering of synaptic vesicles [79]. On the other hand, a recent study showed that Rab3 directly associates with the tail of the actin motor protein myosin5a. supporting a role of Rab3 in the transport of neuronal vesicles rather than the attachment to the plasma membrane [205]. However, as outlined in the introduction 1.1.1, docking is mainly defined as a morphological observation of vesicles located in close proximity to the plasma membrane. This only provides a static picture at a given time point and does not reflect the dynamic actions of docked vesicles that constantly undergo association and dissociation from the plasma membrane [259]. This is further supported by the relative high amount of synaptic vesicles observed in the docked vesicle fraction compared to the free vesicle fraction. Such a high number of vesicles does not reflect the morphologically observed low number of vesicles attached to the plasma membrane.

Here, alterations in the docked vesicle fraction were analyzed as a consequence of a GDI induced removal of Rab proteins from synaptic vesicles. The effect of GDI treatment on the attachment of SVs as well as global changes in the presynaptic proteome as a consequence of GDI incubation were examined using the iTRAQ based quantitation. In this study, addition of recombinant GDI only led to a significant decrease in the amount of Rab proteins in the presence of excess GDP, but synaptic vesicles remained attached to the plasma membrane. This provides direct evidence that Rab3 is not required for attaching synaptic vesicles to the plasma membrane after docking had taken place. However, docking might not be determined by a single protein-protein interaction. In fact, deletion of a large number of proteins (Munc18, Munc13, Rim [260], synaptotagmin [47], syntaxin [2]) result in changes in the amount of vesicles attached to the plasma membrane, indicating that docking is possibly mediated by a series of protein-protein interactions. Thus, Rab3 might only contribute to docking as a transient contact between vesicle and active zone, that is followed by additional factors that determine the attachment of vesicles to the plasma membrane.

- Munc18 has been shown to promote docking *in vivo* [4, 7, 6], possibly mediated by binding to the "closed" conformation of synatxin 1 [8, 9]. But at this stage it remains elusive if the attached vesicles are only docked or already primed. Therefore, it is also possible that Munc18 binds to the "open" synatxin 1, stabilizing the SNARE acceptor complex [261] and thus facilitating SNARE assembly [262, 263]. On the vesicular side synaptotagmin seems to be the prime candidate for docking aside from its function as the neuronal calcium sensor. In chromaffin cells, synaptotagmin has been shown bind

to the SNARE acceptor complex, anchoring vesicles and promoting SNARE assembly [261, 47]. However, docking mechanisms in chromaffin cells might be different from neurons, as these cells do not contain many of the active zone proteins.

- The SNARE complex is very stable [264]. Assuming that SNARE proteins are already assembled at this stage (possibly as a consequence of Munc18), this interaction itself might be sufficient to keep vesicles attached.

- Cytoskeletal components, in particular the F-actin network, might entrap synaptic vesicles in the subplasmalemmal cytoskeleton. Actin dynamics play an important role in in the presynaptic nerve terminal [265, 266] and interact with the vesicle protein synapsin [125]. Considering the large number of cytoskeletal components identified in this study, I assume that the cytoskeletal network persists in the isolated docked vesicle fraction. Apart from a possible direct interaction between the cytoskeleton and synaptic vesicle, de-attachment of vesicles might just simply be abolished because these whole organelles get physically entangled in these network.

- It cannot be completely ruled out that the Rab3 mediated effect on docking is sufficiently compensated by Rab27b. These Rab proteins share common GEFs [267, 268] and appear to have overlapping functions in synaptic vesicle exocytosis [21]. Similar to Rab3, Rab27 has also been shown to influence docking [17, 18], but in contrast to Rab3, Rab27 is resistent to GDI-membrane retrieval [21]. Instead, inactive GDP-bound Rab27b has been suggested to persist on membrane as an inactive homodimer [269].

Strikingly, except for the reduction of Rab proteins, the molecular composition of the active zone remains constant. Precisely, the amount of more than 500 proteins that were identified were unchanged. Surprisingly, this included the Rab3 interacting protein Rim. Rim proteins are large multi-domain molecules that are proposed to function as central organizers interacting with multiple proteins [87, 67, 85]. However, the Rab3-binding site is localized to the N-terminus, whereas other parts of Rim mediate different functions. For example, the central PDZ domain interacts with calcium channels, localizing them to the active zone [84]. Importantly, these domains appear to act autonomously[270]. Thus, a disruption of the Rab3-Rim-interaction does not interfere with Rim function in tethering calcium channels to release sites. This possibly accounts for Rim localization at the active zone. Taken together I hypothesize that Rab3 is possibly involved in the first contact of synaptic vesicles with the presynaptic active zone via its interaction with Rim and thus might initiate the attachment of vesicles to the plasma membrane, but it does not restrict the diffusion of these vesicles after docking.

4.3 Conclusion and outlook

Proteomic analysis of subcellular compartments have a tremendous potential to help understanding complex processes such as synaptic transmission. Addressing the emerging need to comprehensively profile the presynaptic proteome, this thesis describes the establishment and use of a new proteolytic protocol that can immunoisolate active zones including a step that efficiently removes the postsynaptic density from synaptosomes. This study identified more than 500 proteins in a presynaptic docked vesicle fraction. In addition to the entire active zone, synaptic vesicle constituents, previously reported synaptic proteins, molecules with a hitherto unidentified synaptic function and novel proteins were detected. This work also uncovered a novel presynaptic protein, JB1. However, its precise function remains to be elucidated. Ongoing knock-down and over-expression studies in *D. melanogaster* and rat hippocampal neurons will hopefully shed some light on its neuronal function. Nevertheless, the gathered presynaptic proteome only represents an average molecular composition of all synapse types in cortical and hippocampal neurons and cannot distinguish between excitatory and inhibitory synapses.

The established protocol allowed to measure quantitative changes in the protein composition at these synapses. As an example, I analyzed the docked vesicle proteome downstream of Rab3 removal by GDI treatment. Our results prove evidence that Rab3 alone does not mediate this attachment. Moreover, Rab3 removal after SV docking does not change the protein composition of active zones components, suggesting that the main role of Rab3 role is targeting synaptic vesicles to the active zone. The feasibility of this protocol provides a powerful basis to further dissect molecular interactions and mechanisms at the presynaptic active zone. For example, a quantitative comparison of immunoisolated docked vesicles from glutamatergic excitatory and GABAergic inhibitory synapses would significantly account for the understanding of the molecular heterogeneity of central synapses.

References

[1] J. J. Chua, S. Kindler, J. Boyken, and R. Jahn, "The architecture of an excitatory synapse," *J Cell Sci*, vol. 123, no. Pt 6, pp. 819–23, 2010. 1

[2] M. Hammarlund, M. T. Palfreyman, S. Watanabe, S. Olsen, and E. M. Jorgensen, "Open syntaxin docks synaptic vesicles," *PLoS Biol*, vol. 5, no. 8, p. e198, 2007. 2, 3, 82

[3] T. Schikorski and C. F. Stevens, "Morphological correlates of functionally defined synaptic vesicle populations," *Nat Neurosci*, vol. 4, no. 4, pp. 391–5, 2001. 2

[4] T. Voets, R. F. Toonen, E. C. Brian, H. de Wit, T. Moser, J. Rettig, T. C. Sudhof, E. Neher, and M. Verhage, "Munc18-1 promotes large dense-core vesicle docking," *Neuron*, vol. 31, no. 4, pp. 581–91, 2001. 2, 82

[5] R. F. Toonen, O. Kochubey, H. de Wit, A. Gulyas-Kovacs, B. Konijnenburg, J. B. Sorensen, J. Klingauf, and M. Verhage, "Dissecting docking and tethering of secretory vesicles at the target membrane," *EMBO J*, vol. 25, no. 16, pp. 3725–37, 2006. 2

[6] R. F. Toonen, K. Wierda, M. S. Sons, H. de Wit, L. N. Cornelisse, A. Brussaard, J. J. Plomp, and M. Verhage, "Munc18-1 expression levels control synapse recovery by regulating readily releasable pool size," *Proc Natl Acad Sci U S A*, vol. 103, no. 48, pp. 18332–7, 2006. 2, 82

[7] R. M. Weimer, J. E. Richmond, W. S. Davis, G. Hadwiger, M. L. Nonet, and E. M. Jorgensen, "Defects in synaptic vesicle docking in unc-18 mutants," *Nat Neurosci*, vol. 6, no. 10, pp. 1023–30, 2003. 2, 82

[8] H. de Wit, L. N. Cornelisse, R. F. Toonen, and M. Verhage, "Docking of secretory vesicles is syntaxin dependent," *PLoS One*, vol. 1, p. e126, 2006. 2, 3, 82

[9] A. Gulyas-Kovacs, H. de Wit, I. Milosevic, O. Kochubey, R. Toonen, J. Klingauf, M. Verhage, and J. B. Sorensen, "Munc18-1: sequential interactions with the fusion machinery stimulate vesicle docking and priming," *J Neurosci*, vol. 27, no. 32, pp. 8676–86, 2007. 2, 82

[10] H. de Wit, A. M. Walter, I. Milosevic, A. Gulyas-Kovacs, D. Riedel, J. B. Sorensen, and M. Verhage, "Synaptotagmin-1 docks secretory vesicles to syntaxin-1/snap-25 acceptor complexes," *Cell*, vol. 138, no. 5, pp. 935–46, 2009. 2

[11] E. Chieregatti, J. W. Witkin, and G. Baldini, “Snap-25 and synaptotagmin 1 function in ca2+-dependent reversible docking of granules to the plasma membrane,” *Traffic*, vol. 3, no. 7, pp. 496–511, 2002. 2

[12] N. E. Reist, J. Buchanan, J. Li, A. DiAntonio, E. M. Buxton, and T. L. Schwarz, “Morphologically docked synaptic vesicles are reduced in synaptotagmin mutants of drosophila,” *J Neurosci*, vol. 18, no. 19, pp. 7662–73, 1998. 2

[13] E. M. Jorgensen, E. Hartwieg, K. Schuske, M. L. Nonet, Y. Jin, and H. R. Horvitz, “Defective recycling of synaptic vesicles in synaptotagmin mutants of caenorhabditis elegans,” *Nature*, vol. 378, no. 6553, pp. 196–9, 1995. 2

[14] M. Fukuda, J. E. Moreira, V. Liu, M. Sugimori, K. Mikoshiba, and R. R. Llinas, “Role of the conserved whxl motif in the c terminus of synaptotagmin in synaptic vesicle docking,” *Proc Natl Acad Sci U S A*, vol. 97, no. 26, pp. 14715–9, 2000. 2

[15] J. R. van Weering, R. F. Toonen, and M. Verhage, “The role of rab3a in secretory vesicle docking requires association/dissociation of guanidine phosphates and munc18-1,” *PLoS One*, vol. 2, no. 7, p. e616, 2007. 2, 81

[16] A. M. Martelli, G. Baldini, G. Tabellini, D. Koticha, and R. Bareggi, “Rab3a and rab3d control the total granule number and the fraction of granules docked at the plasma membrane in pc12 cells,” *Traffic*, vol. 1, no. 12, pp. 976–86, 2000. 2, 81

[17] H. Gomi, K. Mori, S. Itohara, and T. Izumi, “Rab27b is expressed in a wide range of exocytic cells and involved in the delivery of secretory granules near the plasma membrane,” *Mol Biol Cell*, vol. 18, no. 11, pp. 4377–86, 2007. 2, 83

[18] K. Kasai, M. Ohara-Imaizumi, N. Takahashi, S. Mizutani, S. Zhao, T. Kikuta, H. Kasai, S. Nagamatsu, H. Gomi, and T. Izumi, “Rab27a mediates the tight docking of insulin granules onto the plasma membrane during glucose stimulation,” *J Clin Invest*, vol. 115, no. 2, pp. 388–96, 2005. 2, 83

[19] M. Geppert, V. Y. Bolshakov, S. A. Siegelbaum, K. Takei, P. De Camilli, R. E. Hammer, and T. C. Sudhof, “The role of rab3a in neurotransmitter release,” *Nature*, vol. 369, no. 6480, pp. 493–7, 1994. 2

[20] O. M. Schluter, F. Schmitz, R. Jahn, C. Rosenmund, and T. C. Sudhof, “A complete genetic analysis of neuronal rab3 function,” *J Neurosci*, vol. 24, no. 29, pp. 6629–37, 2004. 2, 59

[21] N. J. Pavlos, M. Gronborg, D. Riedel, J. J. Chua, J. Boyken, T. H. Kloepper, H. Urlaub, S. O. Rizzoli, and R. Jahn, "Quantitative analysis of synaptic vesicle rabs uncovers distinct yet overlapping roles for rab3a and rab27b in ca2+-triggered exocytosis," *J Neurosci*, vol. 30, no. 40, pp. 13441–53, 2010. 2, 46, 63, 83

[22] E. A. Neale, L. M. Bowers, M. Jia, K. E. Bateman, and L. C. Williamson, "Botulinum neurotoxin a blocks synaptic vesicle exocytosis but not endocytosis at the nerve terminal," *J Cell Biol*, vol. 147, no. 6, pp. 1249–60, 1999. 2

[23] L. von Ruden and E. Neher, "A ca-dependent early step in the release of catecholamines from adrenal chromaffin cells," *Science*, vol. 262, no. 5136, pp. 1061–5, 1993. 3

[24] T. Voets, E. Neher, and T. Moser, "Mechanisms underlying phasic and sustained secretion in chromaffin cells from mouse adrenal slices," *Neuron*, vol. 23, no. 3, pp. 607–15, 1999. 3

[25] U. Becherer and J. Rettig, "Vesicle pools, docking, priming, and release," *Cell Tissue Res*, vol. 326, no. 2, pp. 393–407, 2006. 3

[26] H. Plattner, A. R. Artalejo, and E. Neher, "Ultrastructural organization of bovine chromaffin cell cortex-analysis by cryofixation and morphometry of aspects pertinent to exocytosis," *J Cell Biol*, vol. 139, no. 7, pp. 1709–17, 1997. 3

[27] K. Broadie, A. Prokop, H. J. Bellen, C. J. O'Kane, K. L. Schulze, and S. T. Sweeney, "Syntaxin and synaptobrevin function downstream of vesicle docking in drosophila," *Neuron*, vol. 15, no. 3, pp. 663–73, 1995. 3

[28] J. B. Sorensen, K. Wiederhold, E. M. Muller, I. Milosevic, G. Nagy, B. L. de Groot, H. Grubmuller, and D. Fasshauer, "Sequential n- to c-terminal snare complex assembly drives priming and fusion of secretory vesicles," *EMBO J*, vol. 25, no. 5, pp. 955–66, 2006. 3

[29] D. Fasshauer, W. K. Eliason, A. T. Brunger, and R. Jahn, "Identification of a minimal core of the synaptic snare complex sufficient for reversible assembly and disassembly," *Biochemistry*, vol. 37, no. 29, pp. 10354–62, 1998. 3

[30] G. Lonart and T. C. Sudhof, "Assembly of snare core complexes prior to neurotransmitter release sets the readily releasable pool of synaptic vesicles," *J Biol Chem*, vol. 275, no. 36, pp. 27703–7, 2000. 3

[31] I. Dulubova, M. Khvotchev, S. Liu, I. Huryeva, T. C. Sudhof, and J. Rizo, "Munc18-1 binds directly to the neuronal snare complex," *Proc Natl Acad Sci U S A*, vol. 104, no. 8, pp. 2697–702, 2007. 3

[32] J. Shen, D. C. Tareste, F. Paumet, J. E. Rothman, and T. J. Melia, "Selective activation of cognate snarepins by sec1/munc18 proteins," *Cell*, vol. 128, no. 1, pp. 183–95, 2007. 3

[33] T. Sollner, S. W. Whiteheart, M. Brunner, H. Erdjument-Bromage, S. Geromanos, P. Tempst, and J. E. Rothman, "Snap receptors implicated in vesicle targeting and fusion," *Nature*, vol. 362, no. 6418, pp. 318–24, 1993. 3

[34] R. B. Sutton, D. Fasshauer, R. Jahn, and A. T. Brunger, "Crystal structure of a snare complex involved in synaptic exocytosis at 2.4 a resolution," *Nature*, vol. 395, no. 6700, pp. 347–53, 1998. 3

[35] X. Chen, D. R. Tomchick, E. Kovrigin, D. Arac, M. Machius, T. C. Sudhof, and J. Rizo, "Three-dimensional structure of the complexin/snare complex," *Neuron*, vol. 33, no. 3, pp. 397–409, 2002. 3

[36] K. Reim, M. Mansour, F. Varoqueaux, H. T. McMahon, T. C. Sudhof, N. Brose, and C. Rosenmund, "Complexins regulate a late step in ca2+-dependent neurotransmitter release," *Cell*, vol. 104, no. 1, pp. 71–81, 2001. 3

[37] C. G. Giraudo, W. S. Eng, T. J. Melia, and J. E. Rothman, "A clamping mechanism involved in snare-dependent exocytosis," *Science*, vol. 313, no. 5787, pp. 676–80, 2006. 3, 4

[38] M. Xue, Y. Q. Lin, H. Pan, K. Reim, H. Deng, H. J. Bellen, and C. Rosenmund, "Tilting the balance between facilitatory and inhibitory functions of mammalian and drosophila complexins orchestrates synaptic vesicle exocytosis," *Neuron*, vol. 64, no. 3, pp. 367–80, 2009. 3

[39] U. Ashery, F. Varoqueaux, T. Voets, A. Betz, P. Thakur, H. Koch, E. Neher, N. Brose, and J. Rettig, "Munc13-1 acts as a priming factor for large dense-core vesicles in bovine chromaffin cells," *EMBO J*, vol. 19, no. 14, pp. 3586–96, 2000. 3

[40] I. Augustin, C. Rosenmund, T. C. Sudhof, and N. Brose, "Munc13-1 is essential for fusion competence of glutamatergic synaptic vesicles," *Nature*, vol. 400, no. 6743, pp. 457–61, 1999. 3, 5

[41] K. Broadie, H. J. Bellen, A. DiAntonio, J. T. Littleton, and T. L. Schwarz, "Absence of synaptotagmin disrupts excitation-secretion coupling during synaptic transmission," *Proc Natl Acad Sci U S A*, vol. 91, no. 22, pp. 10727–31, 1994. 3

[42] M. Geppert, Y. Goda, R. E. Hammer, C. Li, T. W. Rosahl, C. F. Stevens, and T. C. Sudhof, "Synaptotagmin i: a major ca2+ sensor for transmitter release at a central synapse," *Cell*, vol. 79, no. 4, pp. 717–27, 1994. 3

[43] J. T. Littleton, M. Stern, K. Schulze, M. Perin, and H. J. Bellen, "Mutational analysis of drosophila synaptotagmin demonstrates its essential role in ca(2+)-activated neurotransmitter release," *Cell*, vol. 74, no. 6, pp. 1125–34, 1993. 3

[44] B. A. Davletov and T. C. Sudhof, "A single c2 domain from synaptotagmin i is sufficient for high affinity ca2+/phospholipid binding," *J Biol Chem*, vol. 268, no. 35, pp. 26386–90, 1993. 4

[45] I. Fernandez, D. Arac, J. Ubach, S. H. Gerber, O. Shin, Y. Gao, R. G. Anderson, T. C. Sudhof, and J. Rizo, "Three-dimensional structure of the synaptotagmin 1 c2b-domain: synaptotagmin 1 as a phospholipid binding machine," *Neuron*, vol. 32, no. 6, pp. 1057–69, 2001. 4

[46] E. R. Chapman, P. I. Hanson, S. An, and R. Jahn, "Ca2+ regulates the interaction between synaptotagmin and syntaxin 1," *J Biol Chem*, vol. 270, no. 40, pp. 23667–71, 1995. 4, 17

[47] G. Schiavo, G. Stenbeck, J. E. Rothman, and T. H. Sollner, "Binding of the synaptic vesicle v-snare, synaptotagmin, to the plasma membrane t-snare, snap-25, can explain docked vesicles at neurotoxin-treated synapses," *Proc Natl Acad Sci U S A*, vol. 94, no. 3, pp. 997–1001, 1997. 4, 82, 83

[48] H. Dai, N. Shen, D. Arac, and J. Rizo, "A quaternary snare-synaptotagmin-ca2+-phospholipid complex in neurotransmitter release," *J Mol Biol*, vol. 367, no. 3, pp. 848–63, 2007. 4

[49] X. Yang, Y. J. Kaeser-Woo, Z. P. Pang, W. Xu, and T. C. Sudhof, "Complexin clamps asynchronous release by blocking a secondary ca(2+) sensor via its accessory alpha helix," *Neuron*, vol. 68, no. 5, pp. 907–20, 2010. 4

[50] R. Jahn and R. H. Scheller, "Snares–engines for membrane fusion," *Nat Rev Mol Cell Biol*, vol. 7, no. 9, pp. 631–43, 2006. 4

[51] T. Sollner, M. K. Bennett, S. W. Whiteheart, R. H. Scheller, and J. E. Rothman, “A protein assembly-disassembly pathway in vitro that may correspond to sequential steps of synaptic vesicle docking, activation, and fusion,” *Cell*, vol. 75, no. 3, pp. 409–18, 1993. 4

[52] E. G. Gray, “Electron microscopy of presynaptic organelles of the spinal cord,” *J Anat*, vol. 97, pp. 101–6, 1963. 4

[53] D. M. Landis, A. K. Hall, L. A. Weinstein, and T. S. Reese, “The organization of cytoplasm at the presynaptic active zone of a central nervous system synapse,” *Neuron*, vol. 1, no. 3, pp. 201–9, 1988. 4

[54] M. L. Harlow, D. Ress, A. Stoschek, R. M. Marshall, and U. J. McMahan, “The architecture of active zone material at the frog’s neuromuscular junction,” *Nature*, vol. 409, no. 6819, pp. 479–84, 2001. 4

[55] L. Siksou, P. Rostaing, J. P. Lechaire, T. Boudier, T. Ohtsuka, A. Fejtova, H. T. Kao, P. Greengard, E. D. Gundelfinger, A. Triller, and S. Marty, “Three-dimensional architecture of presynaptic terminal cytomatrix,” *J Neurosci*, vol. 27, no. 26, pp. 6868–77, 2007. 4, 54

[56] R. Fernandez-Busnadiego, B. Zuber, U. E. Maurer, M. Cyrklaff, W. Baumeister, and V. Lucic, “Quantitative analysis of the native presynaptic cytomatrix by cryoelectron tomography,” *J Cell Biol*, vol. 188, no. 1, pp. 145–56, 2010. 4

[57] S. Brenner, “The genetics of caenorhabditis elegans,” *Genetics*, vol. 77, no. 1, pp. 71–94, 1974. 5

[58] N. Brose, K. Hofmann, Y. Hata, and T. C. Sudhof, “Mammalian homologues of caenorhabditis elegans unc-13 gene define novel family of c2-domain proteins,” *J Biol Chem*, vol. 270, no. 42, pp. 25273–80, 1995. 5

[59] H. Koch, K. Hofmann, and N. Brose, “Definition of munc13-homology-domains and characterization of a novel ubiquitously expressed munc13 isoform,” *Biochem J*, vol. 349, no. Pt 1, pp. 247–53, 2000. 5

[60] C. Rosenmund, A. Sigler, I. Augustin, K. Reim, N. Brose, and J. S. Rhee, “Differential control of vesicle priming and short-term plasticity by munc13 isoforms,” *Neuron*, vol. 33, no. 3, pp. 411–24, 2002. 5

[61] F. Varoqueaux, A. Sigler, J. S. Rhee, N. Brose, C. Enk, K. Reim, and C. Rosenmund, "Total arrest of spontaneous and evoked synaptic transmission but normal synaptogenesis in the absence of munc13-mediated vesicle priming," *Proc Natl Acad Sci U S A*, vol. 99, no. 13, pp. 9037–42, 2002. 5, 9

[62] J. E. Richmond, W. S. Davis, and E. M. Jorgensen, "Unc-13 is required for synaptic vesicle fusion in c. elegans," *Nat Neurosci*, vol. 2, no. 11, pp. 959–64, 1999. 5

[63] B. Aravamudan, T. Fergestad, W. S. Davis, C. K. Rodesch, and K. Broadie, "Drosophila unc-13 is essential for synaptic transmission," *Nat Neurosci*, vol. 2, no. 11, pp. 965–71, 1999. 5

[64] S. Orita, A. Naito, G. Sakaguchi, M. Maeda, H. Igarashi, T. Sasaki, and Y. Takai, "Physical and functional interactions of doc2 and munc13 in ca2+-dependent exocytotic machinery," *J Biol Chem*, vol. 272, no. 26, pp. 16081–4, 1997. 5

[65] H. J. Junge, J. S. Rhee, O. Jahn, F. Varoqueaux, J. Spiess, M. N. Waxham, C. Rosenmund, and N. Brose, "Calmodulin and munc13 form a ca2+ sensor/effector complex that controls short-term synaptic plasticity," *Cell*, vol. 118, no. 3, pp. 389–401, 2004. 5

[66] G. Sakaguchi, S. Orita, A. Naito, M. Maeda, H. Igarashi, T. Sasaki, and Y. Takai, "A novel brain-specific isoform of beta spectrin: isolation and its interaction with munc13," *Biochem Biophys Res Commun*, vol. 248, no. 3, pp. 846–51, 1998. 5

[67] A. Betz, P. Thakur, H. J. Junge, U. Ashery, J. S. Rhee, V. Scheuss, C. Rosenmund, J. Rettig, and N. Brose, "Functional interaction of the active zone proteins munc13-1 and rim1 in synaptic vesicle priming," *Neuron*, vol. 30, no. 1, pp. 183–96, 2001. 5, 8, 83

[68] I. Dulubova, X. Lou, J. Lu, I. Huryeva, A. Alam, R. Schneggenburger, T. C. Sudhof, and J. Rizo, "A munc13/rim/rab3 tripartite complex: from priming to plasticity?," *EMBO J*, vol. 24, no. 16, pp. 2839–50, 2005. 5, 59, 82

[69] A. Betz, M. Okamoto, F. Benseler, and N. Brose, "Direct interaction of the rat unc-13 homologue munc13-1 with the n terminus of syntaxin," *J Biol Chem*, vol. 272, no. 4, pp. 2520–6, 1997. 5

[70] D. R. Stevens, Z. X. Wu, U. Matti, H. J. Junge, C. Schirra, U. Becherer, S. M. Wojcik, N. Brose, and J. Rettig, "Identification of the minimal protein domain required for priming activity of munc13-1," *Curr Biol*, vol. 15, no. 24, pp. 2243–8, 2005. 5

[71] J. Basu, N. Shen, I. Dulubova, J. Lu, R. Guan, O. Guryev, N. V. Grishin, C. Rosenmund, and J. Rizo, "A minimal domain responsible for munc13 activity," *Nat Struct Mol Biol*, vol. 12, no. 11, pp. 1017–8, 2005. 5

[72] C. Ma, W. Li, Y. Xu, and J. Rizo, "Munc13 mediates the transition from the closed syntaxin-munc18 complex to the snare complex," *Nat Struct Mol Biol*, vol. 18, no. 5, pp. 542–9, 2011. 5

[73] J. Lu, M. Machius, I. Dulubova, H. Dai, T. C. Sudhof, D. R. Tomchick, and J. Rizo, "Structural basis for a munc13-1 homodimer to munc13-1/rim heterodimer switch," *PLoS Biol*, vol. 4, no. 7, p. e192, 2006. 5

[74] O. H. Shin, J. Lu, J. S. Rhee, D. R. Tomchick, Z. P. Pang, S. M. Wojcik, M. Camacho-Perez, N. Brose, M. Machius, J. Rizo, C. Rosenmund, and T. C. Sudhof, "Munc13 c2b domain is an activity-dependent ca2+ regulator of synaptic exocytosis," *Nat Struct Mol Biol*, vol. 17, no. 3, pp. 280–8, 2010. 5

[75] Y. Wang, S. Sugita, and T. C. Sudhof, "The rim/nim family of neuronal c2 domain proteins. interactions with rab3 and a new class of src homology 3 domain proteins," *J Biol Chem*, vol. 275, no. 26, pp. 20033–44, 2000. 5, 82

[76] Y. Wang and T. C. Sudhof, "Genomic definition of rim proteins: evolutionary amplification of a family of synaptic regulatory proteins(small star, filled)," *Genomics*, vol. 81, no. 2, pp. 126–37, 2003. 5

[77] T. Coppola, S. Magnin-Luthi, V. Perret-Menoud, S. Gattesco, G. Schiavo, and R. Regazzi, "Direct interaction of the rab3 effector rim with ca2+ channels, snap-25, and synaptotagmin," *J Biol Chem*, vol. 276, no. 35, pp. 32756–62, 2001. 5

[78] Y. Wang, M. Okamoto, F. Schmitz, K. Hofmann, and T. C. Sudhof, "Rim is a putative rab3 effector in regulating synaptic-vesicle fusion," *Nature*, vol. 388, no. 6642, pp. 593–8, 1997. 5, 8, 73

[79] E. O. Gracheva, G. Hadwiger, M. L. Nonet, and J. E. Richmond, "Direct interactions between c. elegans rab-3 and rim provide a mechanism to target vesicles to the presynaptic density," *Neurosci Lett*, vol. 444, no. 2, pp. 137–42, 2008. 5, 6, 59, 82

[80] Y. Han, P. S. Kaeser, T. C. Sudhof, and R. Schneggenburger, "Rim determines ca(2)+ channel density and vesicle docking at the presynaptic active zone," *Neuron*, vol. 69, no. 2, pp. 304–16, 2011. 5

[81] C. Stigloher, H. Zhan, M. Zhen, J. Richmond, and J. L. Bessereau, "The presynaptic dense projection of the caenorhabditis elegans cholinergic neuromuscular junction localizes synaptic vesicles at the active zone through syd-2/liprin and unc-10/rim-dependent interactions," *J Neurosci*, vol. 31, no. 12, pp. 4388–96, 2011. 5, 7

[82] N. Calakos, S. Schoch, T. C. Sudhof, and R. C. Malenka, "Multiple roles for the active zone protein rim1alpha in late stages of neurotransmitter release," *Neuron*, vol. 42, no. 6, pp. 889–96, 2004. 5

[83] R. M. Weimer, E. O. Gracheva, O. Meyrignac, K. G. Miller, J. E. Richmond, and J. L. Bessereau, "Unc-13 and unc-10/rim localize synaptic vesicles to specific membrane domains," *J Neurosci*, vol. 26, no. 31, pp. 8040–7, 2006. 5

[84] P. S. Kaeser, L. Deng, Y. Wang, I. Dulubova, X. Liu, J. Rizo, and T. C. Sudhof, "Rim proteins tether ca2+ channels to presynaptic active zones via a direct pdz-domain interaction," *Cell*, vol. 144, no. 2, pp. 282–95, 2011. 5, 6, 8, 83

[85] S. Schoch, P. E. Castillo, T. Jo, K. Mukherjee, M. Geppert, Y. Wang, F. Schmitz, R. C. Malenka, and T. C. Sudhof, "Rim1alpha forms a protein scaffold for regulating neurotransmitter release at the active zone," *Nature*, vol. 415, no. 6869, pp. 321–6, 2002. 5, 7, 8, 83

[86] T. Shibasaki, Y. Sunaga, K. Fujimoto, Y. Kashima, and S. Seino, "Interaction of atp sensor, camp sensor, ca2+ sensor, and voltage-dependent ca2+ channel in insulin granule exocytosis," *J Biol Chem*, vol. 279, no. 9, pp. 7956–61, 2004. 5, 7

[87] T. Ohtsuka, E. Takao-Rikitsu, E. Inoue, M. Inoue, M. Takeuchi, K. Matsubara, M. Deguchi-Tawarada, K. Satoh, K. Morimoto, H. Nakanishi, and Y. Takai, "Cast: a novel protein of the cytomatrix at the active zone of synapses that forms a ternary complex with rim1 and munc13-1," *J Cell Biol*, vol. 158, no. 3, pp. 577–90, 2002. 5, 6, 8, 83

[88] Y. Wang, X. Liu, T. Biederer, and T. C. Sudhof, "A family of rim-binding proteins regulated by alternative splicing: Implications for the genesis of synaptic active zones," *Proc Natl Acad Sci U S A*, vol. 99, no. 22, pp. 14464–9, 2002. 5, 6, 73

[89] J. Lu, H. Li, Y. Wang, T. C. Sudhof, and J. Rizo, "Solution structure of the rim1alpha pdz domain in complex with an elks1b c-terminal peptide," *J Mol Biol*, vol. 352, no. 2, pp. 455–66, 2005. 5, 6

[90] L. Deng, P. S. Kaeser, W. Xu, and T. C. Sudhof, “Rim proteins activate vesicle priming by reversing autoinhibitory homodimerization of munc13,” *Neuron*, vol. 69, no. 2, pp. 317–31, 2011. 6

[91] T. Nakata, Y. Kitamura, K. Shimizu, S. Tanaka, M. Fujimori, S. Yokoyama, K. Ito, and M. Emi, “Fusion of a novel gene, elks, to ret due to translocation t(10;12)(q11;p13) in a papillary thyroid carcinoma,” *Genes Chromosomes Cancer*, vol. 25, no. 2, pp. 97–103, 1999. 6

[92] E. Takao-Rikitsu, S. Mochida, E. Inoue, M. Deguchi-Tawarada, M. Inoue, T. Ohtsuka, and Y. Takai, “Physical and functional interaction of the active zone proteins, cast, rim1, and bassoon, in neurotransmitter release,” *J Cell Biol*, vol. 164, no. 2, pp. 301–11, 2004. 6, 7, 8

[93] J. Ko, M. Na, S. Kim, J. R. Lee, and E. Kim, “Interaction of the erc family of rim-binding proteins with the liprin-alpha family of multidomain proteins,” *J Biol Chem*, vol. 278, no. 43, pp. 42377–85, 2003. 6, 7, 8

[94] E. Inoue, M. Deguchi-Tawarada, E. Takao-Rikitsu, M. Inoue, I. Kitajima, T. Ohtsuka, and Y. Takai, “Elks, a protein structurally related to the active zone protein cast, is involved in ca2+-dependent exocytosis from pc12 cells,” *Genes Cells*, vol. 11, no. 6, pp. 659–72, 2006. 6

[95] H. Nomura, T. Ohtsuka, S. Tadokoro, M. Tanaka, and N. Hirashima, “Involvement of elks, an active zone protein, in exocytotic release from rbl-2h3 cells,” *Cell Immunol*, vol. 258, no. 2, pp. 204–11, 2009. 6

[96] P. S. Kaeser, L. Deng, A. E. Chavez, X. Liu, P. E. Castillo, and T. C. Sudhof, “Elks2alpha/cast deletion selectively increases neurotransmitter release at inhibitory synapses,” *Neuron*, vol. 64, no. 2, pp. 227–39, 2009. 6

[97] S. tom Dieck, L. Sanmarti-Vila, K. Langnaese, K. Richter, S. Kindler, A. Soyke, H. Wex, K. H. Smalla, U. Kampf, J. T. Franzer, M. Stumm, C. C. Garner, and E. D. Gundelfinger, “Bassoon, a novel zinc-finger cag/glutamine-repeat protein selectively localized at the active zone of presynaptic nerve terminals,” *J Cell Biol*, vol. 142, no. 2, pp. 499–509, 1998. 7, 73

[98] S. D. Fenster, W. J. Chung, R. Zhai, C. Cases-Langhoff, B. Voss, A. M. Garner, U. Kaempf, S. Kindler, E. D. Gundelfinger, and C. C. Garner, “Piccolo, a presynaptic

zinc finger protein structurally related to bassoon," *Neuron*, vol. 25, no. 1, pp. 203–14, 2000. 7

[99] X. Wang, M. Kibschull, M. M. Laue, B. Lichte, E. Petrasch-Parwez, and M. W. Kilimann, "Aczonin, a 550-kd putative scaffolding protein of presynaptic active zones, shares homology regions with rim and bassoon and binds profilin," *J Cell Biol*, vol. 147, no. 1, pp. 151–62, 1999. 7

[100] C. Serra-Pages, Q. G. Medley, M. Tang, A. Hart, and M. Streuli, "Liprins, a family of lar transmembrane protein-tyrosine phosphatase-interacting proteins," *J Biol Chem*, vol. 273, no. 25, pp. 15611–20, 1998. 7

[101] S. Kim, J. Ko, H. Shin, J. R. Lee, C. Lim, J. H. Han, W. D. Altrock, C. C. Garner, E. D. Gundelfinger, R. T. Premont, B. K. Kaang, and E. Kim, "The git family of proteins forms multimers and associates with the presynaptic cytomatrix protein piccolo," *J Biol Chem*, vol. 278, no. 8, pp. 6291–300, 2003. 7

[102] S. D. Fenster, M. M. Kessels, B. Qualmann, W. J. Chung, J. Nash, E. D. Gundelfinger, and C. C. Garner, "Interactions between piccolo and the actin/dynamin-binding protein abp1 link vesicle endocytosis to presynaptic active zones," *J Biol Chem*, vol. 278, no. 22, pp. 20268–77, 2003. 7

[103] W. D. Altrock, S. tom Dieck, M. Sokolov, A. C. Meyer, A. Sigler, C. Brakebusch, R. Fassler, K. Richter, T. M. Boeckers, H. Potschka, C. Brandt, W. Loscher, D. Grimberg, T. Dresbach, A. Hempelmann, H. Hassan, D. Balschun, J. U. Frey, J. H. Brandstatter, C. C. Garner, C. Rosenmund, and E. D. Gundelfinger, "Functional inactivation of a fraction of excitatory synapses in mice deficient for the active zone protein bassoon," *Neuron*, vol. 37, no. 5, pp. 787–800, 2003. 7

[104] R. Zhai, G. Olias, W. J. Chung, R. A. Lester, S. tom Dieck, K. Langnaese, M. R. Kreutz, S. Kindler, E. D. Gundelfinger, and C. C. Garner, "Temporal appearance of the presynaptic cytomatrix protein bassoon during synaptogenesis," *Mol Cell Neurosci*, vol. 15, no. 5, pp. 417–28, 2000. 7

[105] M. Shapira, R. G. Zhai, T. Dresbach, T. Bresler, V. I. Torres, E. D. Gundelfinger, N. E. Ziv, and C. C. Garner, "Unitary assembly of presynaptic active zones from piccolo-bassoon transport vesicles," *Neuron*, vol. 38, no. 2, pp. 237–52, 2003. 7

[106] S. tom Dieck, W. D. Altrock, M. M. Kessels, B. Qualmann, H. Regus, D. Brauner, A. Fejtova, O. Bracko, E. D. Gundelfinger, and J. H. Brandstatter, "Molecular dissection of

the photoreceptor ribbon synapse: physical interaction of bassoon and ribeye is essential for the assembly of the ribbon complex," *J Cell Biol*, vol. 168, no. 5, pp. 825–36, 2005. 7

[107] O. Dick, S. tom Dieck, W. D. Altrock, J. Ammermuller, R. Weiler, C. C. Garner, E. D. Gundelfinger, and J. H. Brandstatter, "The presynaptic active zone protein bassoon is essential for photoreceptor ribbon synapse formation in the retina," *Neuron*, vol. 37, no. 5, pp. 775–86, 2003. 7

[108] S. Leal-Ortiz, C. L. Waites, R. Terry-Lorenzo, P. Zamorano, E. D. Gundelfinger, and C. C. Garner, "Piccolo modulation of synapsin1a dynamics regulates synaptic vesicle exocytosis," *J Cell Biol*, vol. 181, no. 5, pp. 831–46, 2008. 7

[109] K. Mukherjee, X. Yang, S. H. Gerber, H. B. Kwon, A. Ho, P. E. Castillo, X. Liu, and T. C. Sudhof, "Piccolo and bassoon maintain synaptic vesicle clustering without directly participating in vesicle exocytosis," *Proc Natl Acad Sci U S A*, vol. 107, no. 14, pp. 6504–9, 2010. 7

[110] E. Yeh, T. Kawano, R. M. Weimer, J. L. Bessereau, and M. Zhen, "Identification of genes involved in synaptogenesis using a fluorescent active zone marker in caenorhabditis elegans," *J Neurosci*, vol. 25, no. 15, pp. 3833–41, 2005. 7

[111] Y. Dai, H. Taru, S. L. Deken, B. Grill, B. Ackley, M. L. Nonet, and Y. Jin, "Syd-2 liprin-alpha organizes presynaptic active zone formation through elks," *Nat Neurosci*, vol. 9, no. 12, pp. 1479–87, 2006. 7

[112] O. Olsen, K. A. Moore, M. Fukata, T. Kazuta, J. C. Trinidad, F. W. Kauer, M. Streuli, H. Misawa, A. L. Burlingame, R. A. Nicoll, and D. S. Bredt, "Neurotransmitter release regulated by a mals-liprin-alpha presynaptic complex," *J Cell Biol*, vol. 170, no. 7, pp. 1127–34, 2005. 7, 8, 48

[113] M. Zhen and Y. Jin, "The liprin protein syd-2 regulates the differentiation of presynaptic termini in c. elegans," *Nature*, vol. 401, no. 6751, pp. 371–5, 1999. 7

[114] N. Kaufmann, J. DeProto, R. Ranjan, H. Wan, and D. Van Vactor, "Drosophila liprin-alpha and the receptor phosphatase dlar control synapse morphogenesis," *Neuron*, vol. 34, no. 1, pp. 27–38, 2002. 7

[115] S. M. Kaech, C. W. Whitfield, and S. K. Kim, "The lin-2/lin-7/lin-10 complex mediates basolateral membrane localization of the c. elegans egf receptor let-23 in vulval epithelial cells," *Cell*, vol. 94, no. 6, pp. 761–71, 1998. 7, 8

[116] S. Butz, M. Okamoto, and T. C. Sudhof, "A tripartite protein complex with the potential to couple synaptic vesicle exocytosis to cell adhesion in brain," *Cell*, vol. 94, no. 6, pp. 773–82, 1998. 7

[117] Y. Hata, S. Butz, and T. C. Sudhof, "Cask: a novel dlg/psd95 homolog with an n-terminal calmodulin-dependent protein kinase domain identified by interaction with neurexins," *J Neurosci*, vol. 16, no. 8, pp. 2488–94, 1996. 7, 8, 73

[118] K. Jo, R. Derin, M. Li, and D. S. Bredt, "Characterization of mals/velis-1, -2, and -3: a family of mammalian lin-7 homologs enriched at brain synapses in association with the postsynaptic density-95/nmda receptor postsynaptic complex," *J Neurosci*, vol. 19, no. 11, pp. 4189–99, 1999. 7

[119] M. Setou, T. Nakagawa, D. H. Seog, and N. Hirokawa, "Kinesin superfamily motor protein kif17 and mlin-10 in nmda receptor-containing vesicle transport," *Science*, vol. 288, no. 5472, pp. 1796–802, 2000. 7

[120] M. Okamoto and T. C. Sudhof, "Mints, munc18-interacting proteins in synaptic vesicle exocytosis," *J Biol Chem*, vol. 272, no. 50, pp. 31459–64, 1997. 8, 73

[121] M. B. Dalva, A. C. McClelland, and M. S. Kayser, "Cell adhesion molecules: signalling functions at the synapse," *Nat Rev Neurosci*, vol. 8, no. 3, pp. 206–20, 2007. 8

[122] M. Missler, W. Zhang, A. Rohlmann, G. Kattenstroth, R. E. Hammer, K. Gottmann, and T. C. Sudhof, "Alpha-neurexins couple ca2+ channels to synaptic vesicle exocytosis," *Nature*, vol. 423, no. 6943, pp. 939–48, 2003. 8

[123] K. Jungling, V. Eulenburg, R. Moore, R. Kemler, V. Lessmann, and K. Gottmann, "N-cadherin transsynaptically regulates short-term plasticity at glutamatergic synapses in embryonic stem cell-derived neurons," *J Neurosci*, vol. 26, no. 26, pp. 6968–78, 2006. 8

[124] C. Dillon and Y. Goda, "The actin cytoskeleton: integrating form and function at the synapse," *Annu Rev Neurosci*, vol. 28, pp. 25–55, 2005. 9

[125] N. Hirokawa, K. Sobue, K. Kanda, A. Harada, and H. Yorifuji, "The cytoskeletal architecture of the presynaptic terminal and molecular structure of synapsin 1," *J Cell Biol*, vol. 108, no. 1, pp. 111–26, 1989. 9, 53, 83

[126] E. G. Gray, "Axo-somatic and axo-dendritic synapses of the cerebral cortex: an electron microscope study," *J Anat*, vol. 93, pp. 420–33, 1959. 9, 34

[127] F. Varoqueaux, S. Jamain, and N. Brose, “Neuroligin 2 is exclusively localized to inhibitory synapses,” *Eur J Cell Biol*, vol. 83, no. 9, pp. 449–56, 2004. 9

[128] A. M. Craig, G. Banker, W. Chang, M. E. McGrath, and A. S. Serpinskaya, “Clustering of gephyrin at gabaergic but not glutamatergic synapses in cultured rat hippocampal neurons,” *J Neurosci*, vol. 16, no. 10, pp. 3166–77, 1996. 9

[129] D. Gitler, Y. Takagishi, J. Feng, Y. Ren, R. M. Rodriguiz, W. C. Wetsel, P. Greengard, and G. J. Augustine, “Different presynaptic roles of synapsins at excitatory and inhibitory synapses,” *J Neurosci*, vol. 24, no. 50, pp. 11368–80, 2004. 9

[130] M. Gronborg, N. J. Pavlos, I. Brunk, J. J. Chua, A. Munster-Wandowski, D. Riedel, G. Ahnert-Hilger, H. Urlaub, and R. Jahn, “Quantitative comparison of glutamatergic and gabaergic synaptic vesicles unveils selectivity for few proteins including mal2, a novel synaptic vesicle protein,” *J Neurosci*, vol. 30, no. 1, pp. 2–12, 2010. 9, 12, 46

[131] H. Husi, M. A. Ward, J. S. Choudhary, W. P. Blackstock, and S. G. Grant, “Proteomic analysis of nmda receptor-adhesion protein signaling complexes,” *Nat Neurosci*, vol. 3, no. 7, pp. 661–9, 2000. 10

[132] R. S. Walikonis, O. N. Jensen, M. Mann, J. Provance, D. W., J. A. Mercer, and M. B. Kennedy, “Identification of proteins in the postsynaptic density fraction by mass spectrometry,” *J Neurosci*, vol. 20, no. 11, pp. 4069–80, 2000. 10

[133] K. W. Li, M. P. Hornshaw, R. C. Van Der Schors, R. Watson, S. Tate, B. Casetta, C. R. Jimenez, Y. Gouwenberg, E. D. Gundelfinger, K. H. Smalla, and A. B. Smit, “Proteomics analysis of rat brain postsynaptic density. implications of the diverse protein functional groups for the integration of synaptic physiology,” *J Biol Chem*, vol. 279, no. 2, pp. 987–1002, 2004. 10, 73, 75

[134] K. Li, M. P. Hornshaw, J. van Minnen, K. H. Smalla, E. D. Gundelfinger, and A. B. Smit, “Organelle proteomics of rat synaptic proteins: correlation-profiling by isotope-coded affinity tagging in conjunction with liquid chromatography-tandem mass spectrometry to reveal post-synaptic density specific proteins,” *J Proteome Res*, vol. 4, no. 3, pp. 725–33, 2005. 10, 12

[135] J. Peng, M. J. Kim, D. Cheng, D. M. Duong, S. P. Gygi, and M. Sheng, “Semiquantitative proteomic analysis of rat forebrain postsynaptic density fractions by mass spectrometry,” *J Biol Chem*, vol. 279, no. 20, pp. 21003–11, 2004. 10, 12, 73, 75

[136] H. D. Coughenour, R. S. Spaulding, and C. M. Thompson, "The synaptic vesicle proteome: a comparative study in membrane protein identification," *Proteomics*, vol. 4, no. 10, pp. 3141–55, 2004. 10

[137] J. Burre, T. Beckhaus, H. Schagger, C. Corvey, S. Hofmann, M. Karas, H. Zimmermann, and W. Volknandt, "Analysis of the synaptic vesicle proteome using three gel-based protein separation techniques," *Proteomics*, vol. 6, no. 23, pp. 6250–62, 2006. 10, 45

[138] S. Takamori, M. Holt, K. Stenius, E. A. Lemke, M. Gronborg, D. Riedel, H. Urlaub, S. Schenck, B. Brugger, P. Ringler, S. A. Muller, B. Rammner, F. Grater, J. S. Hub, B. L. De Groot, G. Mieskes, Y. Moriyama, J. Klingauf, H. Grubmuller, J. Heuser, F. Wieland, and R. Jahn, "Molecular anatomy of a trafficking organelle," *Cell*, vol. 127, no. 4, pp. 831–46, 2006. 10, 11, 45, 46, 78

[139] J. S. Andersen, C. J. Wilkinson, T. Mayor, P. Mortensen, E. A. Nigg, and M. Mann, "Proteomic characterization of the human centrosome by protein correlation profiling," *Nature*, vol. 426, no. 6966, pp. 570–4, 2003. 10, 11, 78

[140] S. P. Gygi, B. Rist, S. A. Gerber, F. Turecek, M. H. Gelb, and R. Aebersold, "Quantitative analysis of complex protein mixtures using isotope-coded affinity tags," *Nat Biotechnol*, vol. 17, no. 10, pp. 994–9, 1999. 11

[141] P. L. Ross, Y. N. Huang, J. N. Marchese, B. Williamson, K. Parker, S. Hattan, N. Khainovski, S. Pillai, S. Dey, S. Daniels, S. Purkayastha, P. Juhasz, S. Martin, M. Bartlet-Jones, F. He, A. Jacobson, and D. J. Pappin, "Multiplexed protein quantitation in saccharomyces cerevisiae using amine-reactive isobaric tagging reagents," *Mol Cell Proteomics*, vol. 3, no. 12, pp. 1154–69, 2004. 12, 44

[142] S. A. Gerber, J. Rush, O. Stemman, M. W. Kirschner, and S. P. Gygi, "Absolute quantification of proteins and phosphoproteins from cell lysates by tandem ms," *Proc Natl Acad Sci U S A*, vol. 100, no. 12, pp. 6940–5, 2003. 12

[143] S. E. Ong, B. Blagoev, I. Kratchmarova, D. B. Kristensen, H. Steen, A. Pandey, and M. Mann, "Stable isotope labeling by amino acids in cell culture, silac, as a simple and accurate approach to expression proteomics," *Mol Cell Proteomics*, vol. 1, no. 5, pp. 376–86, 2002. 12

[144] R. P. Munton, R. Tweedie-Cullen, M. Livingstone-Zatchej, F. Weinandy, M. Waidelich, D. Longo, P. Gehrig, F. Potthast, D. Rutishauser, B. Gerrits, C. Panse, R. Schlapbach, and I. M. Mansuy, "Qualitative and quantitative analyses of protein phosphorylation in

naive and stimulated mouse synaptosomal preparations," *Mol Cell Proteomics*, vol. 6, no. 2, pp. 283–93, 2007. 13

[145] J. C. Trinidad, C. G. Specht, A. Thalhammer, R. Schoepfer, and A. L. Burlingame, "Comprehensive identification of phosphorylation sites in postsynaptic density preparations," *Mol Cell Proteomics*, vol. 5, no. 5, pp. 914–22, 2006. 13

[146] V. P. Whittaker, I. A. Michaelson, and R. J. Kirkland, "The separation of synaptic vesicles from nerve-ending particles ('synaptosomes')," *Biochem J*, vol. 90, no. 2, pp. 293–303, 1964. 13, 36

[147] J. W. Hell, P. R. Maycox, H. Stadler, and R. Jahn, "Uptake of gaba by rat brain synaptic vesicles isolated by a new procedure," *EMBO J*, vol. 7, no. 10, pp. 3023–9, 1988. 13

[148] M. L. Dustin and D. R. Colman, "Neural and immunological synaptic relations," *Science*, vol. 298, no. 5594, pp. 785–9, 2002. 13

[149] G. Fischer von Mollard, T. C. Sudhof, and R. Jahn, "A small gtp-binding protein dissociates from synaptic vesicles during exocytosis," *Nature*, vol. 349, no. 6304, pp. 79–81, 1991. 14, 23, 29, 30, 31, 59

[150] R. K. Carlin, D. J. Grab, R. S. Cohen, and P. Siekevitz, "Isolation and characterization of postsynaptic densities from various brain regions: enrichment of different types of postsynaptic densities," *J Cell Biol*, vol. 86, no. 3, pp. 831–45, 1980. 14, 34

[151] G. R. Phillips, J. K. Huang, Y. Wang, H. Tanaka, L. Shapiro, W. Zhang, W. S. Shan, K. Arndt, M. Frank, R. E. Gordon, M. A. Gawinowicz, Y. Zhao, and D. R. Colman, "The presynaptic particle web: ultrastructure, composition, dissolution, and reconstitution," *Neuron*, vol. 32, no. 1, pp. 63–77, 2001. 14, 74, 77, 78

[152] G. R. Phillips, L. Florens, H. Tanaka, Z. Z. Khaing, L. Fidler, r. Yates, J. R., and D. R. Colman, "Proteomic comparison of two fractions derived from the transsynaptic scaffold," *J Neurosci Res*, vol. 81, no. 6, pp. 762–75, 2005. 14, 74, 75, 77, 81

[153] M. Morciano, T. Beckhaus, M. Karas, H. Zimmermann, and W. Volknandt, "The proteome of the presynaptic active zone: from docked synaptic vesicles to adhesion molecules and maxi-channels," *J Neurochem*, vol. 108, no. 3, pp. 662–75, 2009. 14, 74, 76, 77, 78, 79

[154] R. Jahn, W. Schiebler, C. Ouimet, and P. Greengard, "A 38,000-dalton membrane protein (p38) present in synaptic vesicles," *Proc Natl Acad Sci U S A*, vol. 82, no. 12, pp. 4137–41, 1985. 17

[155] L. Edelmann, P. I. Hanson, E. R. Chapman, and R. Jahn, "Synaptobrevin binding to synaptophysin: a potential mechanism for controlling the exocytotic fusion machine," *EMBO J*, vol. 14, no. 2, pp. 224–31, 1995. 17

[156] N. Brose, A. G. Petrenko, T. C. Sudhof, and R. Jahn, "Synaptotagmin: a calcium sensor on the synaptic vesicle surface," *Science*, vol. 256, no. 5059, pp. 1021–5, 1992. 17

[157] N. Brose, G. W. Huntley, Y. Stern-Bach, G. Sharma, J. H. Morrison, and S. F. Heinemann, "Differential assembly of coexpressed glutamate receptor subunits in neurons of rat cerebral cortex," *J Biol Chem*, vol. 269, no. 24, pp. 16780–4, 1994. 17

[158] S. Takamori, J. S. Rhee, C. Rosenmund, and R. Jahn, "Identification of differentiation-associated brain-specific phosphate transporter as a second vesicular glutamate transporter (vglut2)," *J Neurosci*, vol. 21, no. 22, p. RC182, 2001. 17

[159] S. a. Russel, "Molecular cloning: A laboratory manual," *Cold Spring Harbor Laboratory Press*, vol. 1-3, 2001. 19

[160] F. Peter, C. Nuoffer, I. Schalk, and W. E. Balch, "Expression and purification of recombinant his6-tagged guanine nucleotide dissociation inhibitor and formation of its rab1 complex," *Methods Enzymol*, vol. 257, pp. 80–3, 1995. 19

[161] P. K. Smith, R. I. Krohn, G. T. Hermanson, A. K. Mallia, F. H. Gartner, M. D. Provenzano, E. K. Fujimoto, N. M. Goeke, B. J. Olson, and D. C. Klenk, "Measurement of protein using bicinchoninic acid," *Anal Biochem*, vol. 150, no. 1, pp. 76–85, 1985. 20

[162] P. J. Meberg and M. W. Miller, "Culturing hippocampal and cortical neurons," *Methods Cell Biol*, vol. 71, pp. 111–27, 2003. 20

[163] H. Schagger and G. von Jagow, "Tricine-sodium dodecyl sulfate-polyacrylamide gel electrophoresis for the separation of proteins in the range from 1 to 100 kda," *Anal Biochem*, vol. 166, no. 2, pp. 368–79, 1987. 22

[164] H. Schagger, "Tricine-sds-page," *Nat Protoc*, vol. 1, no. 1, pp. 16–22, 2006. 22

[165] H. Towbin, T. Staehelin, and J. Gordon, "Immunoblotting in the clinical laboratory," *J Clin Chem Clin Biochem*, vol. 27, no. 8, pp. 495–501, 1989. 22

[166] C. Bordier, “Phase separation of integral membrane proteins in triton x-114 solution,” *J Biol Chem*, vol. 256, no. 4, pp. 1604–7, 1981. 22, 66

[167] P. M. Burger, E. Mehl, P. L. Cameron, P. R. Maycox, M. Baumert, F. Lottspeich, P. De Camilli, and R. Jahn, “Synaptic vesicles immunoisolated from rat cerebral cortex contain high levels of glutamate,” *Neuron*, vol. 3, no. 6, pp. 715–20, 1989. 23

[168] K. W. Li, S. Miller, O. Klychnikov, M. Loos, J. Stahl-Zeng, S. Spijker, M. Mayford, and A. B. Smit, “Quantitative proteomics and protein network analysis of hippocampal synapses of camkiialpha mutant mice,” *J Proteome Res*, vol. 6, no. 8, pp. 3127–33, 2007. 25

[169] T. E. Thingholm and M. R. Larsen, “The use of titanium dioxide micro-columns to selectively isolate phosphopeptides from proteolytic digests,” *Methods Mol Biol*, vol. 527, pp. 57–66, xi, 2009. 26

[170] J. H. Chou and R. Jahn, “Binding of rab3a to synaptic vesicles,” *J Biol Chem*, vol. 275, no. 13, pp. 9433–40, 2000. 27, 59

[171] E. G. Gray and V. P. Whittaker, “The isolation of nerve endings from brain: an electron-microscopic study of cell fragments derived by homogenization and centrifugation,” *J Anat*, vol. 96, pp. 79–88, 1962. 29

[172] C. W. Cotman, G. Banker, L. Churchill, and D. Taylor, “Isolation of postsynaptic densities from rat brain,” *J Cell Biol*, vol. 63, no. 2 Pt 1, pp. 441–55, 1974. 34, 73

[173] M. Morciano, J. Burre, C. Corvey, M. Karas, H. Zimmermann, and W. Volknandt, “Immunoisolation of two synaptic vesicle pools from synaptosomes: a proteomics analysis,” *J Neurochem*, vol. 95, no. 6, pp. 1732–45, 2005. 36, 40, 46, 74, 77

[174] G. A. Davis and F. E. Bloom, “Subcellular particles separated through a histochemical reaction,” *Anal Biochem*, vol. 51, no. 2, pp. 429–35, 1973. 39

[175] D. H. Jones and A. I. Matus, “Isolation of synaptic plasma membrane from brain by combined flotation-sedimentation density gradient centrifugation,” *Biochim Biophys Acta*, vol. 356, no. 3, pp. 276–87, 1974. 39

[176] C. W. Cotman and D. A. Matthews, “Synaptic plasma membranes from rat brain synaptosomes: isolation and partial characterization,” *Biochim Biophys Acta*, vol. 249, no. 2, pp. 380–94, 1971. 39

[177] D. J. Pagliarini, S. E. Calvo, B. Chang, S. A. Sheth, S. B. Vafai, S. E. Ong, G. A. Walford, C. Sugiana, A. Boneh, W. K. Chen, D. E. Hill, M. Vidal, J. G. Evans, D. R. Thorburn, S. A. Carr, and V. K. Mootha, "A mitochondrial protein compendium elucidates complex i disease biology," *Cell*, vol. 134, no. 1, pp. 112–23, 2008. 44

[178] T. Kremer, C. Kempf, N. Wittenmayer, R. Nawrotzki, T. Kuner, J. Kirsch, and T. Dresbach, "Mover is a novel vertebrate-specific presynaptic protein with differential distribution at subsets of cns synapses," *FEBS Lett*, vol. 581, no. 24, pp. 4727–33, 2007. 46

[179] M. Zerial and H. McBride, "Rab proteins as membrane organizers," *Nat Rev Mol Cell Biol*, vol. 2, no. 2, pp. 107–17, 2001. 46

[180] C. Geumann, M. Gronborg, M. Hellwig, H. Martens, and R. Jahn, "A sandwich enzyme-linked immunosorbent assay for the quantification of insoluble membrane and scaffold proteins," *Anal Biochem*, vol. 402, no. 2, pp. 161–9, 2010. 46

[181] A. Simonsen, B. Bremnes, E. Ronning, R. Aasland, and H. Stenmark, "Syntaxin-16, a putative golgi t-snare," *Eur J Cell Biol*, vol. 75, no. 3, pp. 223–31, 1998. 49

[182] R. Robitaille, M. L. Garcia, G. J. Kaczorowski, and M. P. Charlton, "Functional colocalization of calcium and calcium-gated potassium channels in control of transmitter release," *Neuron*, vol. 11, no. 4, pp. 645–55, 1993. 50

[183] H. G. Knaus, C. Schwarzer, R. O. Koch, A. Eberhart, G. J. Kaczorowski, H. Glossmann, F. Wunder, O. Pongs, M. L. Garcia, and G. Sperk, "Distribution of high-conductance ca(2+)-activated k+ channels in rat brain: targeting to axons and nerve terminals," *J Neurosci*, vol. 16, no. 3, pp. 955–63, 1996. 50

[184] H. Hu, L. R. Shao, S. Chavoshy, N. Gu, M. Trieb, R. Behrens, P. Laake, O. Pongs, H. G. Knaus, O. P. Ottersen, and J. F. Storm, "Presynaptic ca2+-activated k+ channels in glutamatergic hippocampal terminals and their role in spike repolarization and regulation of transmitter release," *J Neurosci*, vol. 21, no. 24, pp. 9585–97, 2001. 50

[185] Z. Huang, R. Lujan, I. Kadurin, V. N. Uebele, J. J. Renger, A. C. Dolphin, and M. M. Shah, "Presynaptic hcn1 channels regulate ca(v)3.2 activity and neurotransmission at select cortical synapses," *Nat Neurosci*, 2011. 50

[186] M. Juhaszova, P. Church, M. P. Blaustein, and E. F. Stanley, "Location of calcium transporters at presynaptic terminals," *Eur J Neurosci*, vol. 12, no. 3, pp. 839–46, 2000. 51, 79

[187] T. Jean, C. Frelin, P. Vigne, P. Barbry, and M. Lazdunski, "Biochemical properties of the na+/h+ exchange system in rat brain synaptosomes. interdependence of internal and external ph control of the exchange activity," *J Biol Chem*, vol. 260, no. 17, pp. 9678–84, 1985. 51

[188] L. E. Trudeau, V. Parpura, and P. G. Haydon, "Activation of neurotransmitter release in hippocampal nerve terminals during recovery from intracellular acidification," *J Neurophysiol*, vol. 81, no. 6, pp. 2627–35, 1999. 51

[189] A. Minelli, N. C. Brecha, C. Karschin, S. DeBiasi, and F. Conti, "Gat-1, a high-affinity gaba plasma membrane transporter, is localized to neurons and astroglia in the cerebral cortex," *J Neurosci*, vol. 15, no. 11, pp. 7734–46, 1995. 51

[190] F. A. Chaudhry, K. P. Lehre, M. van Lookeren Campagne, O. P. Ottersen, N. C. Danbolt, and J. Storm-Mathisen, "Glutamate transporters in glial plasma membranes: highly differentiated localizations revealed by quantitative ultrastructural immunocytochemistry," *Neuron*, vol. 15, no. 3, pp. 711–20, 1995. 51

[191] E. M. Rose, J. C. Koo, J. E. Antflick, S. M. Ahmed, S. Angers, and D. R. Hampson, "Glutamate transporter coupling to na,k-atpase," *J Neurosci*, vol. 29, no. 25, pp. 8143–55, 2009. 51, 79

[192] L. Aigner and P. Caroni, "Depletion of 43-kd growth-associated protein in primary sensory neurons leads to diminished formation and spreading of growth cones," *J Cell Biol*, vol. 123, no. 2, pp. 417–29, 1993. 51

[193] J. H. Skene, R. D. Jacobson, G. J. Snipes, C. B. McGuire, J. J. Norden, and J. A. Freeman, "A protein induced during nerve growth (gap-43) is a major component of growth-cone membranes," *Science*, vol. 233, no. 4765, pp. 783–6, 1986. 51

[194] C. Lagenaur, V. Kunemund, G. Fischer, S. Fushiki, and M. Schachner, "Monoclonal m6 antibody interferes with neurite extension of cultured neurons," *J Neurobiol*, vol. 23, no. 1, pp. 71–88, 1992. 51

[195] B. Cooper, H. B. Werner, and G. Flugge, "Glycoprotein m6a is present in glutamatergic axons in adult rat forebrain and cerebellum," *Brain Res*, vol. 1197, pp. 1–12, 2008. 51

[196] W. Stohl and N. K. Gonatas, "Distribution of the thy-1 antigen in cellular and subcellular fractions of adult mouse brain," *J Immunol*, vol. 119, no. 2, pp. 422–7, 1977. 51

[197] P. Doherty, A. Singh, G. Rimon, S. R. Bolsover, and F. S. Walsh, "Thy-1 antibody-triggered neurite outgrowth requires an influx of calcium into neurons via n- and l-type calcium channels," *J Cell Biol*, vol. 122, no. 1, pp. 181–9, 1993. 51

[198] H. Umemori and J. R. Sanes, "Signal regulatory proteins (sirps) are secreted presynaptic organizing molecules," *J Biol Chem*, vol. 283, no. 49, pp. 34053–61, 2008. 51

[199] S. Yamada, S. Pokutta, F. Drees, W. I. Weis, and W. J. Nelson, "Deconstructing the cadherin-catenin-actin complex," *Cell*, vol. 123, no. 5, pp. 889–901, 2005. 52

[200] J. Bai, Z. Hu, J. S. Dittman, E. C. Pym, and J. M. Kaplan, "Endophilin functions as a membrane-bending molecule and is delivered to endocytic zones by exocytosis," *Cell*, vol. 143, no. 3, pp. 430–41, 2010. 53

[201] O. O. Glebov, N. A. Bright, and B. J. Nichols, "Flotillin-1 defines a clathrin-independent endocytic pathway in mammalian cells," *Nat Cell Biol*, vol. 8, no. 1, pp. 46–54, 2006. 53

[202] T. Schulte, K. A. Paschke, U. Laessing, F. Lottspeich, and C. A. Stuermer, "Reggie-1 and reggie-2, two cell surface proteins expressed by retinal ganglion cells during axon regeneration," *Development*, vol. 124, no. 2, pp. 577–87, 1997. 53

[203] S. O. Deininger, L. Rajendran, F. Lottspeich, M. Przybylski, H. Illges, C. A. Stuermer, and A. Reuter, "Identification of teleost thy-1 and association with the microdomain/lipid raft reggie proteins in regenerating cns axons," *Mol Cell Neurosci*, vol. 22, no. 4, pp. 544–54, 2003. 53

[204] M. Watanabe, K. Nomura, A. Ohyama, R. Ishikawa, Y. Komiya, K. Hosaka, E. Yamauchi, H. Taniguchi, N. Sasakawa, K. Kumakura, T. Ushiki, O. Sato, M. Ikebe, and M. Igarashi, "Myosin-va regulates exocytosis through the submicromolar ca2+-dependent binding of syntaxin-1a," *Mol Biol Cell*, vol. 16, no. 10, pp. 4519–30, 2005. 53

[205] T. Wollert, A. Patel, Y. L. Lee, J. Provance, D. W., V. E. Vought, M. S. Cosgrove, J. A. Mercer, and G. M. Langford, "Myosin5a tail associates directly with rab3a-containing compartments in neurons," *J Biol Chem*, vol. 286, no. 16, pp. 14352–61, 2011. 53, 82

[206] L. Zhu, R. Vranckx, P. Khau Van Kien, A. Lalande, N. Boisset, F. Mathieu, M. Wegman, L. Glancy, J. M. Gasc, F. Brunotte, P. Bruneval, J. E. Wolf, J. B. Michel, and X. Jeunemaitre, "Mutations in myosin heavy chain 11 cause a syndrome associating thoracic aor-

tic aneurysm/aortic dissection and patent ductus arteriosus," *Nat Genet*, vol. 38, no. 3, pp. 343–9, 2006. 54

[207] C. Zhao, J. Takita, Y. Tanaka, M. Setou, T. Nakagawa, S. Takeda, H. W. Yang, S. Terada, T. Nakata, Y. Takei, M. Saito, S. Tsuji, Y. Hayashi, and N. Hirokawa, "Charcot-marie-tooth disease type 2a caused by mutation in a microtubule motor kif1bbeta," *Cell*, vol. 105, no. 5, pp. 587–97, 2001. 54

[208] C. L. Beites, K. A. Campbell, and W. S. Trimble, "The septin sept5/cdcrel-1 competes with alpha-snap for binding to the snare complex," *Biochem J*, vol. 385, no. Pt 2, pp. 347–53, 2005. 54

[209] Y. M. Yang, M. J. Fedchyshyn, G. Grande, J. Aitoubah, C. W. Tsang, H. Xie, C. A. Ackerley, W. S. Trimble, and L. Y. Wang, "Septins regulate developmental switching from microdomain to nanodomain coupling of ca(2+) influx to neurotransmitter release at a central synapse," *Neuron*, vol. 67, no. 1, pp. 100–15, 2010. 54

[210] J. Xue, C. W. Tsang, W. P. Gai, C. S. Malladi, W. S. Trimble, J. A. Rostas, and P. J. Robinson, "Septin 3 (g-septin) is a developmentally regulated phosphoprotein enriched in presynaptic nerve terminals," *J Neurochem*, vol. 91, no. 3, pp. 579–90, 2004. 54

[211] W. J. Nelson and P. J. Veshnock, "Ankyrin binding to (na+ + k+)atpase and implications for the organization of membrane domains in polarized cells," *Nature*, vol. 328, no. 6130, pp. 533–6, 1987. 54

[212] Z. P. Li, E. P. Burke, J. S. Frank, V. Bennett, and K. D. Philipson, "The cardiac na+-ca2+ exchanger binds to the cytoskeletal protein ankyrin," *J Biol Chem*, vol. 268, no. 16, pp. 11489–91, 1993. 54

[213] K. Kizhatil, J. Q. Davis, L. Davis, J. Hoffman, B. L. Hogan, and V. Bennett, "Ankyrin-g is a molecular partner of e-cadherin in epithelial cells and early embryos," *J Biol Chem*, vol. 282, no. 36, pp. 26552–61, 2007. 54

[214] D. A. Brown and T. S. Sihra, "Presynaptic signaling by heterotrimeric g-proteins," *Handb Exp Pharmacol*, no. 184, pp. 207–60, 2008. 54

[215] L. Sun, M. A. Bittner, and R. W. Holz, "Rim, a component of the presynaptic active zone and modulator of exocytosis, binds 14-3-3 through its n terminus," *J Biol Chem*, vol. 278, no. 40, pp. 38301–9, 2003. 54

[216] Y. Li, Y. Wu, and Y. Zhou, "Modulation of inactivation properties of cav2.2 channels by 14-3-3 proteins," *Neuron*, vol. 51, no. 6, pp. 755–71, 2006. 54

[217] S. I. Walaas, F. S. Gorelick, and P. Greengard, "Presence of calcium/calmodulin-dependent protein kinase ii in nerve terminals of rat brain," *Synapse*, vol. 3, no. 4, pp. 356–62, 1989. 54

[218] C. C. Ouimet, T. L. McGuinness, and P. Greengard, "Immunocytochemical localization of calcium/calmodulin-dependent protein kinase ii in rat brain," *Proc Natl Acad Sci U S A*, vol. 81, no. 17, pp. 5604–8, 1984. 54

[219] Q. Liu, B. Chen, Q. Ge, and Z. W. Wang, "Presynaptic ca2+/calmodulin-dependent protein kinase ii modulates neurotransmitter release by activating bk channels at caenorhabditis elegans neuromuscular junction," *J Neurosci*, vol. 27, no. 39, pp. 10404–13, 2007. 54

[220] O. Ullrich, H. Stenmark, K. Alexandrov, L. A. Huber, K. Kaibuchi, T. Sasaki, Y. Takai, and M. Zerial, "Rab gdp dissociation inhibitor as a general regulator for the membrane association of rab proteins," *J Biol Chem*, vol. 268, no. 24, pp. 18143–50, 1993. 59

[221] S. Araki, A. Kikuchi, Y. Hata, M. Isomura, and Y. Takai, "Regulation of reversible binding of smg p25a, a ras p21-like gtp-binding protein, to synaptic plasma membranes and vesicles by its specific regulatory protein, gdp dissociation inhibitor," *J Biol Chem*, vol. 265, no. 22, pp. 13007–15, 1990. 59

[222] W. L. Coleman, C. A. Bill, and M. Bykhovskaia, "Rab3a deletion reduces vesicle docking and transmitter release at the mouse diaphragm synapse," *Neuroscience*, vol. 148, no. 1, pp. 1–6, 2007. 59

[223] F. Peter, C. Nuoffer, I. Schalk, and W. E. Balch, "Expression and purification of recombinant his6-tagged guanine nucleotide dissociation inhibitor and formation of its rab1 complex," *Methods Enzymol*, vol. 257, pp. 80–3, 1995. 59

[224] E. R. Graf, R. W. Daniels, R. W. Burgess, T. L. Schwarz, and A. DiAntonio, "Rab3 dynamically controls protein composition at active zones," *Neuron*, vol. 64, no. 5, pp. 663–77, 2009. 63

[225] J. Schultz, F. Milpetz, P. Bork, and C. P. Ponting, "Smart, a simple modular architecture research tool: identification of signaling domains," *Proc Natl Acad Sci U S A*, vol. 95, no. 11, pp. 5857–64, 1998. 65

[226] I. Letunic, T. Doerks, and P. Bork, "Smart 6: recent updates and new developments," *Nucleic Acids Res*, vol. 37, no. Database issue, pp. D229–32, 2009. 65

[227] A. Krogh, B. Larsson, G. von Heijne, and E. L. Sonnhammer, "Predicting transmembrane protein topology with a hidden markov model: application to complete genomes," *J Mol Biol*, vol. 305, no. 3, pp. 567–80, 2001. 65

[228] G. E. Tusnady and I. Simon, "The hmmtop transmembrane topology prediction server," *Bioinformatics*, vol. 17, no. 9, pp. 849–50, 2001. 65

[229] M. Cserzo, E. Wallin, I. Simon, G. von Heijne, and A. Elofsson, "Prediction of transmembrane alpha-helices in prokaryotic membrane proteins: the dense alignment surface method," *Protein Eng*, vol. 10, no. 6, pp. 673–6, 1997. 65

[230] C. Notredame, D. G. Higgins, and J. Heringa, "T-coffee: A novel method for fast and accurate multiple sequence alignment," *J Mol Biol*, vol. 302, no. 1, pp. 205–17, 2000. 65

[231] E. S. Lein, M. J. Hawrylycz, N. Ao, M. Ayres, A. Bensinger, A. Bernard, A. F. Boe, M. S. Boguski, K. S. Brockway, E. J. Byrnes, L. Chen, T. M. Chen, M. C. Chin, J. Chong, B. E. Crook, A. Czaplinska, C. N. Dang, S. Datta, N. R. Dee, A. L. Desaki, T. Desta, E. Diep, T. A. Dolbeare, M. J. Donelan, H. W. Dong, J. G. Dougherty, B. J. Duncan, A. J. Ebbert, G. Eichele, L. K. Estin, C. Faber, B. A. Facer, R. Fields, S. R. Fischer, T. P. Fliss, C. Frensley, S. N. Gates, K. J. Glattfelder, K. R. Halverson, M. R. Hart, J. G. Hohmann, M. P. Howell, D. P. Jeung, R. A. Johnson, P. T. Karr, R. Kawal, J. M. Kidney, R. H. Knapik, C. L. Kuan, J. H. Lake, A. R. Laramee, K. D. Larsen, C. Lau, T. A. Lemon, A. J. Liang, Y. Liu, L. T. Luong, J. Michaels, J. J. Morgan, R. J. Morgan, M. T. Mortrud, N. F. Mosqueda, L. L. Ng, R. Ng, G. J. Orta, C. C. Overly, T. H. Pak, S. E. Parry, S. D. Pathak, O. C. Pearson, R. B. Puchalski, Z. L. Riley, H. R. Rockett, S. A. Rowland, J. J. Royall, M. J. Ruiz, N. R. Sarno, K. Schaffnit, N. V. Shapovalova, T. Sivisay, C. R. Slaughterbeck, S. C. Smith, K. A. Smith, B. I. Smith, A. J. Sodt, N. N. Stewart, K. R. Stumpf, S. M. Sunkin, M. Sutram, A. Tam, C. D. Teemer, C. Thaller, C. L. Thompson, L. R. Varnam, A. Visel, R. M. Whitlock, P. E. Wohnoutka, C. K. Wolkey, V. Y. Wong, M. Wood, *et al.*, "Genome-wide atlas of gene expression in the adult mouse brain," *Nature*, vol. 445, no. 7124, pp. 168–76, 2007. 65

[232] Y. Fujiki, A. L. Hubbard, S. Fowler, and P. B. Lazarow, "Isolation of intracellular membranes by means of sodium carbonate treatment: application to endoplasmic reticulum," *J Cell Biol*, vol. 93, no. 1, pp. 97–102, 1982. 66

[233] B. A. Jordan, B. D. Fernholz, M. Boussac, C. Xu, G. Grigorean, E. B. Ziff, and T. A. Neubert, "Identification and verification of novel rodent postsynaptic density proteins," *Mol Cell Proteomics*, vol. 3, no. 9, pp. 857–71, 2004. 73

[234] Y. Yoshimura, Y. Yamauchi, T. Shinkawa, M. Taoka, H. Donai, N. Takahashi, T. Isobe, and T. Yamauchi, "Molecular constituents of the postsynaptic density fraction revealed by proteomic analysis using multidimensional liquid chromatography-tandem mass spectrometry," *J Neurochem*, vol. 88, no. 3, pp. 759–68, 2004. 73, 75

[235] N. S. Abul-Husn, I. Bushlin, J. A. Moron, S. L. Jenkins, G. Dolios, R. Wang, R. Iyengar, A. Ma'ayan, and L. A. Devi, "Systems approach to explore components and interactions in the presynapse," *Proteomics*, vol. 9, no. 12, pp. 3303–15, 2009. 74, 79

[236] C. Geumann, M. Gronborg, M. Hellwig, H. Martens, and R. Jahn, "A sandwich enzyme-linked immunosorbent assay for the quantification of insoluble membrane and scaffold proteins," *Anal Biochem*, vol. 402, no. 2, pp. 161–9, 2010. 75

[237] O. Berninghausen, M. A. Rahman, J. P. Silva, B. Davletov, C. Hopkins, and Y. A. Ushkaryov, "Neurexin ibeta and neuroligin are localized on opposite membranes in mature central synapses," *J Neurochem*, vol. 103, no. 5, pp. 1855–63, 2007. 75, 81

[238] P. Scheiffele, J. Fan, J. Choih, R. Fetter, and T. Serafini, "Neuroligin expressed in non-neuronal cells triggers presynaptic development in contacting axons," *Cell*, vol. 101, no. 6, pp. 657–69, 2000. 76

[239] E. R. Graf, X. Zhang, S. X. Jin, M. W. Linhoff, and A. M. Craig, "Neurexins induce differentiation of gaba and glutamate postsynaptic specializations via neuroligins," *Cell*, vol. 119, no. 7, pp. 1013–26, 2004. 76

[240] M. B. Dalva, M. A. Takasu, M. Z. Lin, S. M. Shamah, L. Hu, N. W. Gale, and M. E. Greenberg, "Ephb receptors interact with nmda receptors and regulate excitatory synapse formation," *Cell*, vol. 103, no. 6, pp. 945–56, 2000. 76

[241] S. Das, A. D. Bosley, X. Ye, K. C. Chan, I. Chu, J. E. Green, H. J. Issaq, T. D. Veenstra, and T. Andresson, "Comparison of strong cation exchange and sds-page fractionation for analysis of multiprotein complexes," *J Proteome Res*, vol. 9, no. 12, pp. 6696–704, 2010. 76

[242] M. R. Wilkins, E. Gasteiger, J. C. Sanchez, A. Bairoch, and D. F. Hochstrasser, "Two-dimensional gel electrophoresis for proteome projects: the effects of protein hydrophobicity and copy number," *Electrophoresis*, vol. 19, no. 8-9, pp. 1501–5, 1998. 77

[243] K. W. Li, M. P. Hornshaw, R. C. Van Der Schors, R. Watson, S. Tate, B. Casetta, C. R. Jimenez, Y. Gouwenberg, E. D. Gundelfinger, K. H. Smalla, and A. B. Smit, "Proteomics analysis of rat brain postsynaptic density. implications of the diverse protein functional groups for the integration of synaptic physiology," *J Biol Chem*, vol. 279, no. 2, pp. 987–1002, 2004. 77

[244] J. Hartinger, K. Stenius, D. Hogemann, and R. Jahn, "16-bac/sds-page: a two-dimensional gel electrophoresis system suitable for the separation of integral membrane proteins," *Anal Biochem*, vol. 240, no. 1, pp. 126–33, 1996. 77

[245] R. P. Zahedi, C. Meisinger, and A. Sickmann, "Two-dimensional benzyldimethyl-n-hexadecylammonium chloride/sds-page for membrane proteomics," *Proteomics*, vol. 5, no. 14, pp. 3581–8, 2005. 77

[246] J. Stevens, S. M., A. D. Zharikova, and L. Prokai, "Proteomic analysis of the synaptic plasma membrane fraction isolated from rat forebrain," *Brain Res Mol Brain Res*, vol. 117, no. 2, pp. 116–28, 2003. 77

[247] L. J. Foster, C. L. de Hoog, Y. Zhang, X. Xie, V. K. Mootha, and M. Mann, "A mammalian organelle map by protein correlation profiling," *Cell*, vol. 125, no. 1, pp. 187–99, 2006. 78

[248] J. S. Kang, J. H. Tian, P. Y. Pan, P. Zald, C. Li, C. Deng, and Z. H. Sheng, "Docking of axonal mitochondria by syntaphilin controls their mobility and affects short-term facilitation," *Cell*, vol. 132, no. 1, pp. 137–48, 2008. 78

[249] Y. M. Chen, C. Gerwin, and Z. H. Sheng, "Dynein light chain lc8 regulates syntaphilin-mediated mitochondrial docking in axons," *J Neurosci*, vol. 29, no. 30, pp. 9429–38, 2009. 78

[250] G. A. Perkins, J. Tjong, J. M. Brown, P. H. Poquiz, R. T. Scott, D. R. Kolson, M. H. Ellisman, and G. A. Spirou, "The micro-architecture of mitochondria at active zones: electron tomography reveals novel anchoring scaffolds and cristae structured for high-rate metabolism," *J Neurosci*, vol. 30, no. 3, pp. 1015–26, 2010. 78

[251] C. W. Lee and H. B. Peng, "The function of mitochondria in presynaptic development at the neuromuscular junction," *Mol Biol Cell*, vol. 19, no. 1, pp. 150–8, 2008. 78

[252] P. Verstreken, C. V. Ly, K. J. Venken, T. W. Koh, Y. Zhou, and H. J. Bellen, "Synaptic mitochondria are critical for mobilization of reserve pool vesicles at drosophila neuromuscular junctions," *Neuron*, vol. 47, no. 3, pp. 365–78, 2005. 78

[253] R. Chittajallu, S. P. Braithwaite, V. R. Clarke, and J. M. Henley, "Kainate receptors: subunits, synaptic localization and function," *Trends Pharmacol Sci*, vol. 20, no. 1, pp. 26–35, 1999. 80

[254] P. S. Pinheiro, D. Perrais, F. Coussen, J. Barhanin, B. Bettler, J. R. Mann, J. O. Malva, S. F. Heinemann, and C. Mulle, "Glur7 is an essential subunit of presynaptic kainate autoreceptors at hippocampal mossy fiber synapses," *Proc Natl Acad Sci U S A*, vol. 104, no. 29, pp. 12181–6, 2007. 80

[255] M. E. Tremblay, M. Riad, D. Bouvier, K. K. Murai, E. B. Pasquale, L. Descarries, and G. Doucet, "Localization of epha4 in axon terminals and dendritic spines of adult rat hippocampus," *J Comp Neurol*, vol. 501, no. 5, pp. 691–702, 2007. 80

[256] A. Chattopadhyay and E. London, "Fluorimetric determination of critical micelle concentration avoiding interference from detergent charge," *Anal Biochem*, vol. 139, no. 2, pp. 408–12, 1984. 81

[257] J. Almarza, L. Rincon, A. Bahsas, and F. Brito, "Molecular mechanism for the denaturation of proteins by urea," *Biochemistry*, vol. 48, no. 32, pp. 7608–13, 2009. 81

[258] A. G. Leenders, F. H. Lopes da Silva, W. E. Ghijsen, and M. Verhage, "Rab3a is involved in transport of synaptic vesicles to the active zone in mouse brain nerve terminals," *Mol Biol Cell*, vol. 12, no. 10, pp. 3095–102, 2001. 81

[259] S. O. Rizzoli and W. J. Betz, "The structural organization of the readily releasable pool of synaptic vesicles," *Science*, vol. 303, no. 5666, pp. 2037–9, 2004. 82

[260] R. M. Weimer, E. O. Gracheva, O. Meyrignac, K. G. Miller, J. E. Richmond, and J. L. Bessereau, "Unc-13 and unc-10/rim localize synaptic vesicles to specific membrane domains," *J Neurosci*, vol. 26, no. 31, pp. 8040–7, 2006. 82

[261] F. E. Zilly, J. B. Sorensen, R. Jahn, and T. Lang, "Munc18-bound syntaxin readily forms snare complexes with synaptobrevin in native plasma membranes," *PLoS Biol*, vol. 4, no. 10, p. e330, 2006. 82, 83

[262] P. Burkhardt, D. A. Hattendorf, W. I. Weis, and D. Fasshauer, "Munc18a controls snare assembly through its interaction with the syntaxin n-peptide," *EMBO J*, vol. 27, no. 7, pp. 923–33, 2008. 82

[263] C. N. Medine, C. Rickman, L. H. Chamberlain, and R. R. Duncan, “Munc18-1 prevents the formation of ectopic snare complexes in living cells,” *J Cell Sci*, vol. 120, no. Pt 24, pp. 4407–15, 2007. 82

[264] D. Fasshauer, W. Antonin, V. Subramaniam, and R. Jahn, “Snare assembly and disassembly exhibit a pronounced hysteresis,” *Nat Struct Biol*, vol. 9, no. 2, pp. 144–51, 2002. 83

[265] M. Morales, M. A. Colicos, and Y. Goda, “Actin-dependent regulation of neurotransmitter release at central synapses,” *Neuron*, vol. 27, no. 3, pp. 539–50, 2000. 83

[266] S. Sankaranarayanan, P. P. Atluri, and T. A. Ryan, “Actin has a molecular scaffolding, not propulsive, role in presynaptic function,” *Nat Neurosci*, vol. 6, no. 2, pp. 127–35, 2003. 83

[267] T. R. Mahoney, Q. Liu, T. Itoh, S. Luo, G. Hadwiger, R. Vincent, Z. W. Wang, M. Fukuda, and M. L. Nonet, “Regulation of synaptic transmission by rab-3 and rab-27 in caenorhabditis elegans,” *Mol Biol Cell*, vol. 17, no. 6, pp. 2617–25, 2006. 83

[268] A. C. Figueiredo, C. Wasmeier, A. K. Tarafder, J. S. Ramalho, R. A. Baron, and M. C. Seabra, “Rab3gep is the non-redundant guanine nucleotide exchange factor for rab27a in melanocytes,” *J Biol Chem*, vol. 283, no. 34, pp. 23209–16, 2008. 83

[269] L. M. Chavas, S. Torii, H. Kamikubo, M. Kawasaki, K. Ihara, R. Kato, M. Kataoka, T. Izumi, and S. Wakatsuki, “Structure of the small gtpase rab27b shows an unexpected swapped dimer,” *Acta Crystallogr D Biol Crystallogr*, vol. 63, no. Pt 7, pp. 769–79, 2007. 83

[270] L. Deng, P. S. Kaeser, W. Xu, and T. C. Sudhof, “Rim proteins activate vesicle priming by reversing autoinhibitory homodimerization of munc13,” *Neuron*, vol. 69, no. 2, pp. 317–31, 2011. 83

Acknowledgements

I want to thank **Prof. Reinhard Jahn** for giving me the opportunity to work in his group. Reinhard, thank you for your support, the ideas you have shared with me and all the motivation throughout the last years. I really enjoyed working in your lab and I am honored that I could even do experiments with you.

I am deeply grateful to **Dr. John Chua** for his tremendous support throughout my PhD. John, you have been an extraordinary teacher and a great friend to me. Thank you for all the scientific skills you taught me, for all the lively discussions and for guiding me through my PhD. You always knew the right things to say: You motivated me when I was frustrated and you brought me back to earth when I was hyper-active.

I thank **Prof. Ficner** and **Prof. Thumm** for being part of my thesis committee and for their comments and ideas during the committee meetings.

I would like to thank my bench- and office mate **Dr. Hans Dieter Schmitt** for his support during the years, although he had to bear a large number of intensively smelling fruit teas, emotional outbursts and temporary attacks of complete insanity. Dieter, you are a walking scientific wikipedia paired with McGyver skills and equipped with endless sugar supplies. Believe me, this is a compliment! You are amazing.

I want to thank **Maria Druminski** for her technical help and personal commitment. Life is not fair.

I would also like to thank **Dr. Mads Gronborg** for his help with the mass spectrometry part of this thesis. Mads, it was a great pleasure working with you. You are my favorite danish and the only one I know who can wear pullovers with horizontal stripes.

I thank **Prof. Henning Urlaub** for his support and for integrating me into his group. I really enjoyed the summer school last year.

I would also like to thank **Dr. Dietmar Riedel** and **Dr. Dirk Wenzel** for the electron microscopy pictures in this thesis.

Many thanks to the people in the animal facility in tower 6.

Doing a PhD requires endless working hours, therefore I want to thank my present and former colleagues from the department of Neurobiology for the great working atmosphere. I am especially grateful to **Dr. Gottfried Mieskes**, for always having an open door for the needs and problems of the people in the lab and for having the skills to solve almost every one of these problems.

During the time in the lab I met people that have become dear frineds. **Anna, Caro, Julia, Saskia, Ricarda, Constanze, Ulf and Sabrina**, thank you for all the fun times, the uncountable discussions by one or another drink, the tons of sweat shared during running, climbing, swimming or fitness classes and for your friendship over the years.

Finally I want to thank my family for their support and love.

Curriculum Vitae

Personal Data

	Anne Janina Boyken
Address	Lotzestr.2
	Goettingen, Germany
Email	jboyken@gwdg.de
Date of Birth	02. August 1983

Education

2008-2011	**Max-Planck-Institute for Biophysical Chemistry** PhD in the Department of Neurobiology Thesis: Molecular profiling of presynaptic docking sites **Georg-August-University Goettingen** Member of the doctoral program "Biomolecules: Structure-Function-Dynamics" Goettingen Graduate School for Neurosciences and Molecular Biosciences (GGNB).
2006-2007	**Sanofi-Aventis Deutschland GmbH** Diploma in the Department for Metabolic Disorders Thesis: Enzymatic and biophysical investigation of glucose metabolism
2002-2007	**University of Greifswald, Germany** Biochemistry (Diploma)

Teaching

2011	**Tutor of lectures** "Protein Sorting and Processing" in the International MSc/PhD Programs "Molecular Biology" and "Neurosciences"
2008-2010	**Tutor of method courses** "Subcellular Fractionation and Centrifugation" within the International MSc/PhD Program "Molecular Biology" "Co-immunoprecipitation as a technique to study protein-protein interactions" within the Goettingen Graduate School for Neurosciences and Molecular Biosciences (GGNB)
2009	**Supervisor of Labrotations** Momchil Ninov and Jonathan Melin within the the International MSc/PhD Program "Molecular Biology"

Conferences

2011	"Synapses: From Molecules to Circuits and Behavior" Cold Spring Harbor Laboratory Meeting Cold Spring Harbor, USA (poster)
2010	"Horizons in Molecular Biology" Goettingen, Germany (poster)
2010	"Proteomics Basics- High Throughput Data Analysis and Statistics" 4th European Summer School, Brixen, South Italy (poster)

Publications

2010	Chua JJ, Kindler S, Boyken J, Jahn R The architecture of an excitatory synapse J Cell Sci. 2010 Mar 15;123(Pt 6):819-23. Review
2010	Pavlos NJ, Gronborg M, Riedel D, Chua JJ, Boyken J, Kloepper TH, Urlaub H, Rizzoli SO, Jahn R. Quantitative analysis of synaptic vesicle Rabs uncovers distinct yet overlapping roles for Rab3a and Rab27b in Ca2+-triggered exocytosis J Neurosci. 2010 Oct 6;30(40):13441-53

GI number	# identified in biological replicates	protein name	biological replicate #1	biological replicate #2	biological replicate #3	average enrichment	standard deviation	protein localization/function
gi|11693170	3	2-oxoglutarate carrier	SPM	4.5	7.5	6.0	2.1	mitochondria
gi|55742813	3	3-hydroxybutyrate dehydrogenase, type 1	4.3	5.2	9.4	6.3	2.7	mitochondria
gi|83977457	2	3-hydroxyisobutyrate dehydrogenase		SPM	SPM	SPM		mitochondria
gi|20304123	2	3-mercaptopyruvate sulfurtransferase		5.2	7.4	6.3	1.5	mitochondria
gi|189181716	3	3-oxoacid CoA transferase 1	SPM	SPM	8.8	SPM		mitochondria
gi|13591900	3	4-aminobutyrate aminotransferase	4.7	7.4	7.0	6.4	1.5	mitochondria
gi|209969744	3	4-nitrophenylphosphatase domain and non-neuronal SNAP25-like protein homolog 1	5.9	7.3	7.9	7.0	1.1	mitochondria
gi|109478763	3	6.8 kDa mitochondrial proteolipid	SPM	SPM	SPM	SPM		mitochondria
gi|8392836	3	acetyl-Coenzyme A acetyltransferase 1	8.0	6.8	5.8	6.9	1.1	mitochondria
gi|40538860	3	aconitase 2, mitochondrial	5.1	4.7	5.4	5.1	0.4	mitochondria
gi|18543341	3	acyl-CoA synthetase long-chain family member 6	8.3	5.9	2.3	5.5	3.0	mitochondria
gi|62078649	3	acyl-CoA thioesterase 9	SPM	7.8	4.1	5.9	2.6	mitochondria
gi|197313734	2	acyl-Coenzyme A dehydrogenase family, member 9		SPM	SPM	SPM		mitochondria
gi|6978435	2	acyl-Coenzyme A dehydrogenase, very long chain		SPM	SPM	SPM		mitochondria
gi|188595700	2	acylglycerol kinase		9.3	7.8	8.6	1.1	mitochondria
gi|58865518	3	aldehyde dehydrogenase 1B1	SPM	SPM	SPM	SPM		mitochondria
gi|109475727	2	aldehyde dehydrogenase 4 family, member A1		SPM	6.7	6.7		mitochondria
gi|34933197	3	Amine oxidase [flavin-containing] A (Monoamine oxidase type A) (MAO-A)	6.3	6.8	6.4	6.5	0.2	mitochondria
gi|110189667	3	ATP synthase F0 subunit 8	4.1	SPM	SPM	4.1		mitochondria
gi|19705465	3	ATP synthase, H+ transporting, mitochondrial F0 complex, subunit B1	4.5	5.6	2.2	4.1	1.7	mitochondria
gi|9506411	3	ATP synthase, H+ transporting, mitochondrial F0 complex, subunit d	5.7	2.7	3.6	4.0	1.5	mitochondria
gi|17978459	3	ATP synthase, H+ transporting, mitochondrial F0 complex, subunit E	5.7	SPM	4.9	5.3	0.6	mitochondria
gi|109495163	3	ATP synthase, H+ transporting, mitochondrial F0 complex, subunit f, isoform 2	32.7	8.6	SPM	SPM		mitochondria
gi|16758388	3	ATP synthase, H+ transporting, mitochondrial F0 complex, subunit F6	SPM	SPM	SPM	SPM		mitochondria
gi|47058994	3	ATP synthase, H+ transporting, mitochondrial F0 complex, subunit G	SPM	SPM	6.0	6.0		mitochondria
gi|40538742	3	ATP synthase, H+ transporting, mitochondrial F1 complex, alpha subunit 1	6.1	6.1	7.9	6.7	1.0	mitochondria
gi|20806153	3	ATP synthase, H+ transporting, mitochondrial F1 complex, delta subunit	SPM	SPM	SPM	SPM		mitochondria
gi|20806139	3	ATP synthase, H+ transporting, mitochondrial F1 complex, epsilon subunit	SPM	5.8	9.3	7.6	2.5	mitochondria
gi|39930503	3	ATP synthase, H+ transporting, mitochondrial F1 complex, gamma subunit	2.9	3.3	6.7	4.3	2.1	mitochondria
gi|77917538	2	ATPase family, AAA domain containing 3A		SPM	SPM	SPM		mitochondria
gi|77917528	3	ATPase inhibitory factor 1	4.4	5.6	4.6	4.9	0.6	mitochondria
gi|47058990	3	ATP-binding cassette, sub-family B, member 7, mitochondrial precursor	SPM	SPM	SPM	SPM		mitochondria
gi|157822275	3	AU RNA binding protein/enoyl-Coenzyme A hydratase	9.4	6.1	SPM	7.7	2.3	mitochondria
gi|56090628	3	BCS1-like	SPM	SPM	SPM	SPM		mitochondria
gi|81295385	3	biphenyl hydrolase-like (serine hydrolase)	SPM	SPM	SPM	SPM		mitochondria
gi|117647218	3	brain protein 44	8.1	4.3	6.6	6.3	2.0	mitochondria
gi|19424244	3	brain protein 44-like	SPM	7.1	SPM	SPM		mitochondria
gi|62646841	3	Calcium-binding mitochondrial carrier protein Aralar2	SPM	2.6	8.7	5.6	4.3	mitochondria

List of identified proteins in the docked and free vesicle fraction

Appendix I

GI number	# identified in biological replicates	protein name	biological replicate #1	biological replicate #2	biological replicate #3	average enrichment	standard deviation	protein localization/function
gi|157824004	3	CDGSH iron sulfur domain 1	8.4	7.0	5.6	7.0	1.4	mitochondria
gi|18543177	3	citrate synthase	5.6	7.0	5.9	6.2	0.8	mitochondria
gi|157817027	3	coiled-coil-helix-coiled-coil-helix domain containing 3	4.4	8.0	5.1	5.8	1.9	mitochondria
gi|157819769	2	coiled-coil-helix-coiled-coil-helix domain containing 6	SPM	2.0				mitochondria
gi|48675371	3	complement component 1, q subcomponent binding protein	SPM	SPM	SPM	SPM		mitochondria
gi|60678254	3	creatine kinase, mitochondrial 1, ubiquitous	6.9	7.1	6.6	6.9	0.3	mitochondria
gi|110189675	2	cytochrome b		SPM	8.9	8.9		mitochondria
gi|61557037	2	cytochrome b5 reductase 1		SPM	SPM	SPM		mitochondria
gi|20302049	2	cytochrome b5 reductase 3		2.5	7.6	5.1	3.6	mitochondria
gi|110189665	3	cytochrome c oxidase subunit I	SPM	SPM	SPM	SPM		mitochondria
gi|110189718	3	cytochrome c oxidase subunit II	SPM	SPM	SPM	SPM		mitochondria
gi|110189669	3	cytochrome c oxidase subunit III	SPM	SPM	SPM	SPM		mitochondria
gi|8393180	3	cytochrome c oxidase subunit IV isoform 1	3.0	6.4	1.7	3.7	2.4	mitochondria
gi|16758362	3	cytochrome c oxidase subunit Vb	2.2	3.2	10.4	5.3	4.5	mitochondria
gi|157821821	3	cytochrome c oxidase subunit VIIa polypeptide 2 like	2.6	SPM	5.3	4.0	1.9	mitochondria
gi|65301490	3	cytochrome c oxidase subunit VIIb	SPM	7.3	7.4	7.3	0.1	mitochondria
gi|24233541	3	cytochrome c oxidase, subunit Va	1.8	5.1	3.6	3.5	1.7	mitochondria
gi|77736544	3	cytochrome c oxidase, subunit VIa, polypeptide 1	SPM	SPM	SPM	SPM		mitochondria
gi|109465447	3	cytochrome c oxidase, subunit VIb polypeptide 1		6.2	SPM	6.2		mitochondria
gi|160333459	3	cytochrome c oxidase, subunit VIc	SPM	9.6	5.8	7.7	2.7	mitochondria
gi|11968072	3	cytochrome c oxidase, subunit VIIa 2	SPM	SPM	SPM	SPM		mitochondria
gi|197927439	3	cytochrome c oxidase, subunit VIIc	SPM	SPM	SPM	SPM		mitochondria
gi|6978725	3	cytochrome c, somatic	SPM	5.0	SPM	SPM		mitochondria
gi|194473626	3	cytochrome c-1	SPM	4.7	SPM	SPM		mitochondria
gi|109510612	2	Cytochrome c-type heme lyase (CCHL) (Holocytochrome c-type synthase)		10.4	SPM	SPM		mitochondria
gi|19424210	3	dapit protein	SPM	7.1	SPM	SPM		mitochondria
gi|58865478	3	death associated protein 3	SPM	SPM	SPM	SPM		mitochondria
gi|40786469	3	dihydrolipoamide dehydrogenase	9.8	5.3	6.8	7.3	2.3	mitochondria
gi|78365255	3	dihydrolipoamide S-acetyltransferase	7.4	4.5	6.6	6.2	1.5	mitochondria
gi|195927000	3	dihydrolipoamide S-succinyltransferase	SPM	6.9	4.2	5.5	1.9	mitochondria
gi|57527204	3	electron-transfer-flavoprotein, alpha polypeptide	SPM	SPM	SPM	SPM		mitochondria
gi|52138635	2	electron-transferring-flavoprotein dehydrogenase		SPM	SPM	SPM		mitochondria
gi|157821933	3	endo/exonuclease (5~-3~), endonuclease G-like precursor	SPM	SPM	SPM	SPM		mitochondria
gi|17530977	2	enoyl Coenzyme A hydratase, short chain, 1, mitochondrial		5.6	SPM	SPM		mitochondria
gi|51948422	2	es1 protein		5.8	11.0	8.4	3.7	mitochondria
gi|157786896	2	fission 1 (mitochondrial outer membrane) homolog		SPM	5.1	SPM		mitochondria
gi|16758100	2	fractured callus expressed transcript 1		SPM	SPM	SPM		mitochondria
gi|158186722	3	fumarate hydratase 1	7.5	8.5	7.2	7.7	0.7	mitochondria

GI number	# identified in biological replicates	protein name	biological replicate #1	biological replicate #2	biological replicate #3	average enrichment	standard deviation	protein localization/function
gi|68163417	2	fumarylacetoacetate hydrolase domain containing 1		SPM	SPM	SPM		mitochondria
gi|62945328	3	glioblastoma amplified sequence	SPM	3.7	6.7	5.2	2.1	mitochondria
gi|6980956	3	glutamate dehydrogenase 1	5.9	3.5	4.4	4.6	1.2	mitochondria
gi|6980972	3	glutamate oxaloacetate transaminase 2	8.6	7.1	7.0	7.6	0.9	mitochondria
gi|158303294	3	glutaminase isoform a	7.1	4.1	6.3	5.8	1.5	mitochondria
gi|6980978	3	glycerol-3-phosphate dehydrogenase 2	7.5	3.9	6.2	5.9	1.8	mitochondria
gi|13324704	2	GrpE-like 1, mitochondrial		2.5	4.1	3.3	1.1	mitochondria
gi|6981052	3	heat shock 10 kDa protein 1	7.0	SPM	24.4	15.7	12.3	mitochondria
gi|206597443	3	heat shock protein 1 (chaperonin)	4.8	7.4	6.0	6.1	1.3	mitochondria
gi|154816168	3	heat shock protein 9	6.7	5.0	7.6	6.5	1.3	mitochondria
gi|6981022	3	hexokinase 1	5.5	6.9	7.6	6.7	1.1	mitochondria
gi|38454320	3	hormone-regulated proliferation associated protein 20	SPM	9.5	SPM	SPM		mitochondria
gi|109487466	3	hypothetical protein *(NADH:Ubiquinone oxioreductase, 42 kDa (NDUO42))*	8.6	4.9	SPM	6.7	2.7	mitochondria
gi|77917546	3	inner membrane protein, mitochondrial	9.7	5.4	5.8	7.0	2.4	mitochondria
gi|109467571	2	inorganic pyrophosphatase 2		3.5	SPM			mitochondria
gi|62079055	2	isocitrate dehydrogenase 2 (NADP+), mitochondrial	SPM	0.0	8.9	4.5	6.3	mitochondria
gi|16758446	3	isocitrate dehydrogenase 3 (NAD+) alpha	8.0	6.9	4.2	6.3	2.0	mitochondria
gi|55926203	3	isocitrate dehydrogenase 3, beta subunit	6.0	6.8	8.8	7.2	1.4	mitochondria
gi|54020666	3	isocitrate dehydrogenase 3, gamma	8.9	8.6	5.2	7.6	2.1	mitochondria
gi|54400736	3	leucine zipper-EF-hand containing transmembrane protein 1	2.4	0.7	0.9	1.4	0.9	mitochondria
gi|19173766	2	lon peptidase 1, mitochondrial	SPM	0.0	SPM	SPM		mitochondria
gi|42476181	3	malate dehydrogenase, mitochondrial	5.9	8.9	5.9	6.9	1.8	mitochondria
gi|157817153	3	malic enzyme 3, NADP(+)-dependent, mitochondrial	5.4	SPM	9.5	7.5	2.9	mitochondria
gi|56605654	2	metaxin 2		5.1	1.9	3.5	2.3	mitochondria
gi|62660299	3	microsomal glutathione S-transferase 3	SPM	SPM	SPM	SPM		mitochondria
gi|34875107	2	mitchondrial ribosomal protein S7		SPM	SPM	SPM		mitochondria
gi|54792127	3	mitochondrial ATP synthase beta subunit	7.2	5.8	8.2	7.1	1.2	mitochondria
gi|20302061	3	mitochondrial ATP synthase, O subunit	4.8	8.1	4.7	5.9	1.9	mitochondria
gi|197313797	3	mitochondrial carrier homolog 1	SPM	SPM	5.2	SPM		mitochondria
gi|158819029	3	mitochondrial carrier homolog 2	5.2	SPM	7.4	6.3	1.6	mitochondria
gi|27695671	3	mitochondrial carrier triple repeat 1		SPM	SPM	SPM		mitochondria
gi|109472570	2	Mitochondrial glutamate carrier 2	SPM	0.0	4.1	2.0	2.9	mitochondria
gi|55741522	2	mitochondrial protein 18 kDa		SPM	SPM	SPM		mitochondria
gi|57164123	2	mitochondrial ribosomal protein L38		1.3	SPM			mitochondria
gi|157786906	2	mitochondrial ribosomal protein S17		SPM	SPM	SPM		mitochondria
gi|157824010	2	mitochondrial ribosomal protein S31		SPM	SPM	SPM		mitochondria
gi|109464325	3	mitochondrial ribosomal protein S36	SPM	SPM	5.4	SPM		mitochondria
gi|148747393	2	mitochondrial trifunctional protein, alpha subunit		6.5	7.3	6.9	0.5	mitochondria

GI number	# identified in biological replicates	protein name	biological replicate #1	biological replicate #2	biological replicate #3	average enrichment	standard deviation	protein localization/function
gi|148747472	2	mitofusin 2		SPM	SPM	SPM		mitochondria
gi|6981260	3	NADH dehydrogenase (ubiquinone) 1 alpha subcomplex 5	7.4	4.1	3.4	5.0	2.1	mitochondria
gi|47058992	3	NADH dehydrogenase (ubiquinone) 1 alpha subcomplex 11	SPM	SPM	SPM	SPM		mitochondria
gi|157818537	2	NADH dehydrogenase (ubiquinone) 1 alpha subcomplex, 1		8.1	SPM	SPM		mitochondria
gi|164565371	3	NADH dehydrogenase (ubiquinone) 1 alpha subcomplex, 12	3.7	6.5	2.7	4.3	1.9	mitochondria
gi|27718097	3	NADH dehydrogenase (ubiquinone) 1 alpha subcomplex, 13	33.2	2.2	3.7	13.0	17.5	mitochondria
gi|157817861	3	NADH dehydrogenase (ubiquinone) 1 alpha subcomplex, 2	4.1	7.0	7.4	6.2	1.8	mitochondria
gi|189085365	3	NADH dehydrogenase (ubiquinone) 1 alpha subcomplex, 4	5.0	SPM	7.9	6.5	2.0	mitochondria
gi|194473636	3	NADH dehydrogenase (ubiquinone) 1 alpha subcomplex, 6 (B14)	SPM	5.8	SPM	SPM		mitochondria
gi|157824069	2	NADH dehydrogenase (ubiquinone) 1 alpha subcomplex, 7 (B14.5a)		SPM	SPM	SPM		mitochondria
gi|114145517	3	NADH dehydrogenase (ubiquinone) 1 alpha subcomplex, 8	SPM	7.3	SPM	SPM		mitochondria
gi|198278533	3	NADH dehydrogenase (ubiquinone) 1 alpha subcomplex, 9	3.7	2.8	5.6	4.1	1.4	mitochondria
gi|82617686	2	NADH dehydrogenase (ubiquinone) 1 beta subcomplex 4		3.4	SPM			mitochondria
gi|157822261	3	NADH dehydrogenase (ubiquinone) 1 beta subcomplex 8	SPM	SPM	SPM	SPM		mitochondria
gi|157822851	3	NADH dehydrogenase (ubiquinone) 1 beta subcomplex, 11	SPM	SPM	SPM	SPM		mitochondria
gi|157823387	3	NADH dehydrogenase (ubiquinone) 1 beta subcomplex, 5	SPM	7.2	8.8	8.0	1.2	mitochondria
gi|157820465	3	NADH dehydrogenase (ubiquinone) 1 beta subcomplex, 6	SPM	SPM	5.1	SPM		mitochondria
gi|157823197	2	NADH dehydrogenase (ubiquinone) 1 beta subcomplex, 7		SPM	SPM	SPM		mitochondria
gi|187937028	3	NADH dehydrogenase (ubiquinone) 1 beta subcomplex, 9	SPM	SPM	SPM	SPM		mitochondria
gi|157820787	3	NADH dehydrogenase (ubiquinone) 1, alpha/beta subcomplex, 1	SPM	8.2	9.3	8.8	0.8	mitochondria
gi|57164133	3	NADH dehydrogenase (ubiquinone) 1, subcomplex unknown, 2	7.7	2.9	5.0	5.2	2.4	mitochondria
gi|53850628	3	NADH dehydrogenase (ubiquinone) Fe-S protein 1, 75kDa	4.6	6.3	8.4	6.4	1.9	mitochondria
gi|58865384	3	NADH dehydrogenase (ubiquinone) Fe-S protein 2	2.7	5.1	2.6	3.5	1.4	mitochondria
gi|157817227	3	NADH dehydrogenase (ubiquinone) Fe-S protein 3	4.5	8.4	6.7	6.5	2.0	mitochondria
gi|68341995	3	NADH dehydrogenase (ubiquinone) Fe-S protein 4	SPM	5.5	6.9	6.2	1.0	mitochondria
gi|72086149	3	NADH dehydrogenase (ubiquinone) Fe-S protein 5b	2.1	SPM	3.4	2.8	0.9	mitochondria
gi|109460535	3	NADH dehydrogenase (ubiquinone) Fe-S protein 6	SPM	SPM	10.0	SPM		mitochondria
gi|56606108	3	NADH dehydrogenase (ubiquinone) Fe-S protein 7	SPM	SPM	SPM	SPM		mitochondria
gi|157821497	3	NADH dehydrogenase (ubiquinone) Fe-S protein 8	SPM	5.0	6.8	5.9	1.3	mitochondria
gi|55741424	3	NADH dehydrogenase (ubiquinone) flavoprotein 1, 51kDa	8.0	7.5	5.1	6.9	1.5	mitochondria
gi|51092268	3	NADH dehydrogenase (ubiquinone) flavoprotein 2	7.2	SPM	SPM	SPM		mitochondria
gi|162287192	2	NADH dehydrogenase (ubiquinone) flavoprotein 3-like isoform 1		SPM	SPM	SPM		mitochondria
gi|110189663	3	NADH dehydrogenase subunit 1	4.9	7.3	7.1	6.5	1.3	mitochondria
gi|110189672	3	NADH dehydrogenase subunit 4	SPM	5.0	SPM	SPM		mitochondria
gi|110189673	3	NADH dehydrogenase subunit 5	SPM	SPM	SPM	SPM		mitochondria
gi|109467413	3	NADH-ubiquinone oxidoreductase B9 subunit (Complex I-B9) (CI-B9)	SPM	SPM	SPM	SPM		mitochondria
gi|109490343	3	NADH-ubiquinone oxidoreductase PDSW subunit	4.6	5.8	8.3	6.2	1.9	mitochondria
gi|11968102	2	ornithine aminotransferase		SPM	SPM	SPM		mitochondria

GI number	# identified in biological replicates	protein name	biological replicate #1	biological replicate #2	biological replicate #3	average enrichment	standard deviation	protein localization/function
gi|62945278	3	oxoglutarate (alpha-ketoglutarate) dehydrogenase (lipoamide)	6.3	7.5	5.2	6.3	1.1	mitochondria
gi|157819765	2	oxoglutarate dehydrogenase-like		SPM	3.1			mitochondria
gi|157819923	2	patatin-like phospholipase domain containing 8		SPM	7.2	SPM		mitochondria
gi|11968132	3	peroxiredoxin 3	SPM	2.8	SPM	2.8		mitochondria
gi|16758404	3	peroxiredoxin 5 precursor	SPM	6.2	4.3	5.3	1.3	mitochondria
gi|70608189	2	phosphoglycerate mutase family member 5	SPM	SPM	SPM	SPM		mitochondria
gi|13937353	3	prohibitin	SPM	7.7	SPM	SPM		mitochondria
gi|61556754	3	prohibitin 2	9.0	5.0	5.2	6.4	2.3	mitochondria
gi|122427836	2	protein phosphatase 2C, magnesium dependent, catalytic subunit		SPM	SPM	SPM		mitochondria
gi|157823607	3	pyrroline-5-carboxylate synthetase (glutamate gamma-semialdehyde synthetase)	SPM	SPM	SPM	SPM		mitochondria
gi|31543464	3	pyruvate carboxylase	3.3	SPM	5.3	4.3	1.5	mitochondria
gi|124430510	2	pyruvate dehydrogenase (lipoamide) alpha 1		6.5	5.2	5.8	0.9	mitochondria
gi|56090293	3	pyruvate dehydrogenase (lipoamide) beta	9.3	6.5	5.7	7.2	1.9	mitochondria
gi|113205496	3	pyruvate dehydrogenase complex, component X	SPM	4.5	SPM	SPM		mitochondria
gi|32452540	2	ras homolog gene family, member T2		SPM	SPM	SPM		mitochondria
gi|148747459	3	RN protein	9.5	4.9	5.0	6.5	2.7	mitochondria
gi|58865994	3	sideroflexin 1	8.4	9.6	7.0	8.4	1.3	mitochondria
gi|12621120	3	sideroflexin 3	SPM	8.2	2.9	5.6	3.8	mitochondria
gi|23463279	3	sideroflexin 5	SPM	SPM	5.0	SPM		mitochondria
gi|34854800	3	solute carrier family 25 (mitochondrial carrier, Aralar), member 12	SPM	9.3	7.8	8.6	1.1	mitochondria
gi|62078785	3	solute carrier family 25 (mitochondrial carrier, glutamate), member 22	5.0	6.8	10.1	7.3	2.6	mitochondria
gi|109464795	2	solute carrier family 25 , member 31		SPM	SPM	SPM		mitochondria
gi|20806141	3	solute carrier family 25 (mitochondrial carrier; phosphate carrier), member 3	6.5	7.6	10.2	8.1	1.9	mitochondria
gi|8394297	3	solute carrier family 25, member 1 precursor	SPM	9.7	8.8	9.3	0.6	mitochondria
gi|32189355	3	solute carrier family 25, member 4	3.7	6.3	8.0	6.0	2.1	mitochondria
gi|189491614	3	solute carrier family 25, member 46	SPM	SPM	3.4	SPM		mitochondria
gi|32189350	3	solute carrier family 25, member 5	4.4	6.1	8.8	6.4	2.2	mitochondria
gi|51948454	3	sorting and assembly machinery component 50 homolog	SPM	SPM	5.4	SPM		mitochondria
gi|18426858	3	succinate dehydrogenase complex, subunit A, flavoprotein (Fp)	2.1	5.8	6.5	4.8	2.4	mitochondria
gi|209915614	3	succinate dehydrogenase complex, subunit B, iron sulfur (Ip)	6.1	6.6	9.9	7.5	2.1	mitochondria
gi|53850596	3	succinate dehydrogenase complex, subunit C	SPM	5.0	7.4	6.2	1.7	mitochondria
gi|38454310	2	succinate dehydrogenase complex, subunit D, integral membrane protein		SPM	SPM	SPM		mitochondria
gi|109504901	2	Succinate semialdehyde dehydrogenase		SPM	7.0	SPM		mitochondria
gi|139948224	3	succinate-CoA ligase, GDP-forming, alpha subunit	7.2	8.7	7.5	7.8	0.8	mitochondria
gi|158749584	3	succinate-Coenzyme A ligase, ADP-forming, beta subunit	SPM	SPM	SPM	SPM		mitochondria
gi|8394331	3	superoxide dismutase 2	SPM	5.8	4.8	5.3	0.7	mitochondria
gi|62078811	2	threonyl-tRNA synthetase 2, mitochondrial		SPM	SPM	SPM		mitochondria
gi|47058998	2	TOM22 protein		SPM	SPM	SPM		mitochondria

GI number	# identified in biological replicates	protein name	biological replicate #1	biological replicate #2	biological replicate #3	average enrichment	standard deviation	protein localization/function
gi|25742598	3	translocase of inner mitochondrial membrane 10 homolog	SPM	8.2	SPM	SPM		mitochondria
gi|8394449	2	translocase of inner mitochondrial membrane 44 homolog		SPM	9.9	SPM		mitochondria
gi|109461526	3	translocase of inner mitochondrial membrane 50 homolog isoform 2	SPM	SPM	SPM	SPM		mitochondria
gi|23097350	2	translocase of outer mitochondrial membrane 20 homolog		SPM	SPM	SPM		mitochondria
gi|47058988	3	translocase of outer mitochondrial membrane 70 homolog A	2.6	9.1	SPM	5.8	4.6	mitochondria
gi|157821331	2	transmembrane and coiled-coil domain family 3		SPM	SPM	SPM		mitochondria
gi|157820845	3	Tu translation elongation factor, mitochondrial	8.0	5.0	5.3	6.1	1.7	mitochondria
gi|55741544	3	ubiquinol cytochrome c reductase core protein 2	7.7	6.8	5.9	6.8	0.9	mitochondria
gi|109458613	3	ubiquinol-cytochrome c reductase binding protein	4.9	4.5	5.0	4.8	0.2	mitochondria
gi|109500943	3	ubiquinol-cytochrome c reductase complex 7.2kDa protein isoform a	SPM	SPM	SPM	SPM		mitochondria
gi|51948476	3	ubiquinol-cytochrome c reductase core protein I	4.1	4.6	6.7	5.1	1.3	mitochondria
gi|57164091	3	ubiquinol-cytochrome c reductase hinge protein	SPM	6.5	SPM	SPM		mitochondria
gi|109481568	2	ubiquinol-cytochrome c reductase subunit		SPM	SPM	SPM		mitochondria
gi|68341999	3	ubiquinol-cytochrome c reductase, complex III subunit VII	4.1	4.8	8.1	5.7	2.2	mitochondria
gi|57114330	3	ubiquinol-cytochrome c reductase, Rieske iron-sulfur polypeptide 1	3.3	10.3	4.5	6.0	3.7	mitochondria
gi|13786200	3	voltage-dependent anion channel 1	6.3	3.2	6.0	5.2	1.7	mitochondria
gi|13786202	3	voltage-dependent anion channel 2	SPM	2.7	6.1	4.4	2.4	mitochondria
gi|13786204	3	voltage-dependent anion channel 3	SPM	4.2	11.3	7.8	5.1	mitochondria
gi|56605990	3	leucine-rich PPR-motif containing	SPM	SPM	8.2	SPM		mitochondria
gi|157822161	2	catechol-O-methyltransferase domain containing 1		SPM	SPM	SPM		mitochondria
gi|67846070	2	hydroxysteroid dehydrogenase like 1		5.8	SPM	SPM		mitochondria
gi|71043858	2	hydroxysteroid dehydrogenase like 2		SPM	SPM	SPM		mitochondria
gi|197927166	2	1-acylglycerol-3-phosphate O-acyltransferase 5		SPM	SPM	SPM		mitochondria
gi|157821573	3	ganglioside-induced differentiation-associated protein 1-like 1	SPM	3.9	SPM	SPM		mitochondria
gi|157821895	3	ganglioside-induced differentiation-associated-protein 1	SPM	3.1	3.4	3.2	0.2	mitochondria
gi|109474876	2	hypothetical protein		SPM	SPM	SPM		mitochondria
gi|77732522	2	outer membrane protein		SPM	4.2	SPM		mitochondria
gi|158749559	3	bassoon protein	SPM	8.0	6.8	7.4	0.8	Active zone
gi|11559947	2	calcium/calmodulin-dependent serine protein kinase		SPM	SPM	SPM		Active zone
gi|25140983	3	ELKS/RAB6-interacting/CAST family member 2	6.3	SPM	SPM	SPM		Active zone
gi|109497902	3	Liprin-alpha-4	SPM	SPM	9.2	SPM		Active zone
gi|10048483	2	piccolo isoform 1		SPM	SPM	SPM		Active zone
gi|157824053	2	liprin alpha 2		SPM	9.2	SPM		Active zone
gi|16306470	3	regulating synaptic membrane exocytosis 1	SPM	6.6	6.0	6.3	0.4	Active zone
gi|213972596	3	protein tyrosine phosphatase, receptor-type, F interacting protein, binding protein 2	0.5	0.2	0.4	0.4	0.1	Active zone
gi|9507073	3	neuroplastin	SPM	5.6	5.9	5.8	0.2	Adhesion and cell surface molecules
gi|46048609	3	beta-catenin	9.4	4.5	SPM	8.4	3.5	Adhesion and cell surface molecules
gi|157817081	2	catenin (cadherin associated protein), alpha 2		SPM	4.6	SPM		Adhesion and cell surface molecules

GI number	# identified in biological replicates	protein name	biological replicate #1	biological replicate #2	biological replicate #3	average enrichment	standard deviation	protein localization/function
gi|157820047	2	catenin (cadherin associated protein), delta 1	2.3	SPM		SPM		Adhesion and cell surface molecules
gi|109464562	3	Catenin delta-2 (Neurojungin)	SPM	9.3	44.4	SPM	24.9	Adhesion and cell surface molecules
gi|114052921	2	cell adhesion molecule 3	6.9		7.0	7.0	0.1	Adhesion and cell surface molecules
gi|14091742	2	contactin associated protein 1		SPM	7.9	SPM		Adhesion and cell surface molecules
gi|157817598	3	inversin	7.5	SPM	SPM	SPM		Adhesion and cell surface molecules
gi|157817019	2	plakophilin 4		8.9	10.5	9.7	1.1	Adhesion and cell surface molecules
gi|9506469	2	Cd47 molecule	5.3		8.1	6.7	2.0	Adhesion and cell surface molecules
gi|13928706	2	neural cell adhesion molecule 1		7.4	8.4	7.9	0.7	Adhesion and cell surface molecules
gi|61557326	3	receptor accessory protein 6	SPM	5.3	4.4	4.8	0.7	Adhesion and cell surface molecules
gi|30017437	3	glycoprotein m6a	SPM	SPM	4.3	SPM		Adhesion and cell surface molecules
gi|20301986	2	glycoprotein m6b	7.5	SPM		SPM		Adhesion and cell surface molecules
gi|8393415	3	growth associated protein 43	7.8	8.8	10.3	9.0	1.3	Adhesion and cell surface molecules
gi|8850221	2	hippocalcin	SPM		4.6	SPM		Adhesion and cell surface molecules
gi|8393864	3	hippocalcin-like 1	SPM	4.3	4.4	4.3	0.1	Adhesion and cell surface molecules
gi|31543529	2	signal-regulatory protein alpha	5.8		4.9	5.3	0.7	Adhesion and cell surface molecules
gi|6981654	3	Thy-1 cell surface antigen	4.2	3.6	3.9	3.9	0.3	Adhesion and cell surface molecules
gi|109478967	2	cysteine rich transmembrane BMP regulator 1 (chordin like)	SPM		SPM	SPM		Adhesion and cell surface molecules
gi|109481923	2	centrosome protein cep290		SPM	SPM	SPM		centrosome
gi|109499926	2	spindle assembly associated Sfi1 homolog isoform a		SPM	SPM	SPM		centrosome
gi|13242237	2	heat shock protein 8		5.4	7.2	6.3	1.3	Chaperones
gi|28467005	2	heat shock protein 90, alpha (cytosolic), class A member 1		4.6	SPM	SPM		Chaperones
gi|70794764	2	DnaJ (Hsp40) homolog, subfamily A, member 4		2.7	2.9	2.8	0.1	Chaperones
gi|157822779	2	DnaJ (Hsp40) homolog, subfamily C, member 11		SPM	SPM	SPM		Chaperones
gi|6981324	3	prolyl 4-hydroxylase, beta polypeptide	10.8	7.1	8.4	8.8	1.9	Chaperones
gi|84370227	2	DnaJ (Hsp40) homolog, subfamily A, member 3 isoform 1		SPM	SPM	SPM		Chaperones
gi|84781723	3	TNF receptor-associated protein 1	SPM	SPM	5.9	SPM		Chaperones
gi|72255527	3	stomatin (Epb7.2)-like 2	SPM	SPM	SPM	SPM		Cytoskeletal and associated proteins
gi|6981696	2	utrophin	SPM	6.2		SPM		Cytoskeletal and associated proteins
gi|148491097	2	cytoplasmic dynein 1 heavy chain 1			0.9	0.9		Cytoskeletal and associated proteins
gi|9506371	2	actin, alpha 1, skeletal muscle		4.3	3.1	3.7	0.8	Cytoskeletal and associated proteins
gi|13592133	3	actin, beta	7.9	4.4	3.2	5.2	2.4	Cytoskeletal and associated proteins
gi|13591902	2	actinin, alpha 1		SPM	SPM	SPM		Cytoskeletal and associated proteins
gi|57164143	2	ARP2 actin-related protein 2 homolog		5.0	3.0	4.0	1.4	Cytoskeletal and associated proteins
gi|109480041	3	formin 3 CG33556-PA	0.6	0.8	0.8	0.8	0.1	Cytoskeletal and associated proteins
gi|13540714	3	plectin 1	6.2	3.9	SPM	5.0	1.6	Cytoskeletal and associated proteins
gi|11560133	3	tubulin, alpha 1A	6.7	2.1	1.1	3.3	3.0	Cytoskeletal and associated proteins
gi|112984124	3	tubulin, alpha 1B	6.0	2.2	1.2	3.1	2.6	Cytoskeletal and associated proteins
gi|55741524	2	tubulin, alpha 4A		2.3	1.2	1.7	0.8	Cytoskeletal and associated proteins

List of identified proteins in the docked and free vesicle fraction

Appendix I

GI number	# identified in biological replicates	protein name	biological replicate #1	biological replicate #2	biological replicate #3	average enrichment	standard deviation	protein localization/function
gi|145966774	3	tubulin, beta 3	2.9	1.9	0.9	1.9	1.0	Cytoskeletal and associated proteins
gi|158262004	3	tubulin, beta 4	3.0	2.2	1.1	2.1	0.9	Cytoskeletal and associated proteins
gi|27465535	3	tubulin, beta 5	3.0	2.2	1.1	2.1	1.0	Cytoskeletal and associated proteins
gi|109472192	3	Dynein heavy chain at 16F CG7092-PA	SPM	SPM	SPM	SPM		Cytoskeletal and associated proteins
gi|109495859	3	Dynein heavy chain at 89D CG1842-PA	2.2	0.2	1.1	1.2	1.0	Cytoskeletal and associated proteins
gi|109488370	3	dynein heavy chain domain 3	SPM	9.5	SPM	SPM		Cytoskeletal and associated proteins
gi|16758016	3	dynein, cytoplasmic, light peptide	SPM	SPM	9.6	9.9		Cytoskeletal and associated proteins
gi|29789307	2	kinesin family member 1B		SPM	SPM	SPM		Cytoskeletal and associated proteins
gi|109464350	2	Kinesin-like protein KIF2		SPM	3.3	3.3		Cytoskeletal and associated proteins
gi|11559935	2	myosin Va		2.9	2.5	2.7	0.2	Cytoskeletal and associated proteins
gi|13928704	3	myosin, heavy chain 10, non-muscle	SPM	4.4	SPM	SPM		Cytoskeletal and associated proteins
gi|6981236	3	myosin, heavy chain 9, non-muscle	SPM	SPM	SPM	SPM		Cytoskeletal and associated proteins
gi|109508026	2	Beta-2-syntrophin (Syntrophin 3)		0.8	SPM	1.0		Cytoskeletal and associated proteins
gi|109474612	2	Oxygen-regulated protein 1 (Retinitis pigmentosa RP1 protein homolog)		SPM	10.6	SPM		Cytoskeletal and associated proteins
gi|188595680	2	SPHK1 interactor, AKAP domain containing		0.8	0.9	0.9	0.1	Cytoskeletal and associated proteins
gi|31543764	3	alpha-spectrin 2	SPM	7.3	7.2	7.3	0.0	Cytoskeletal and associated proteins
gi|109467596	2	ankyrin 2 isoform 1		SPM	4.6	SPM		Cytoskeletal and associated proteins
gi|9507085	2	septin 3	SPM	SPM		SPM		Cytoskeletal and associated proteins
gi|90577179	3	septin 5	SPM	3.8	5.6	4.7	1.3	Cytoskeletal and associated proteins
gi|166091429	2	septin 7 isoform a	3.9		3.3	3.6	0.4	Cytoskeletal and associated proteins
gi|157819689	3	septin 8	SPM	3.6	5.4	4.5	1.3	Cytoskeletal and associated proteins
gi|164698508	3	septin 9 isoform 2	0.6	1.2	1.2	1.0	0.4	Cytoskeletal and associated proteins
gi|47058982	2	spectrin, beta, erythrocytic		1.0	5.5	3.2	3.2	Cytoskeletal and associated proteins
gi|61557085	2	spectrin, beta, non-erythrocytic 1		SPM	7.3	6.1		Cytoskeletal and associated proteins
gi|158636004	3	flotillin 1	SPM	SPM	SPM	SPM		Endocytosis-related proteins
gi|13929186	3	flotillin 2	SPM	SPM	SPM	SPM		Endocytosis-related proteins
gi|157823677	3	adaptor-related protein complex 2, alpha 1 subunit	0.9	0.7	0.6	0.7	0.1	Endocytosis-related proteins
gi|162138932	3	adaptor-related protein complex 2, alpha 2 subunit	0.8	0.8	0.7	0.7	0.1	Endocytosis-related proteins
gi|18034787	3	adaptor-related protein complex 2, beta 1 subunit	0.9	0.8	0.5	0.8	0.2	Endocytosis-related proteins
gi|16758938	3	adaptor-related protein complex 2, mu 1 subunit	0.5	0.6	0.6	0.6	0.0	Endocytosis-related proteins
gi|56961624	3	adaptor-related protein complex 2, sigma 1 subunit	0.7	0.6	0.6	0.6	0.1	Endocytosis-related proteins
gi|9506497	3	clathrin, heavy chain (Hc)	7.6	4.6	5.2	5.8	1.6	Endocytosis-related proteins
gi|57527421	3	SH3-domain GRB2-like endophilin B2	2.6	1.1	0.7	1.4	1.0	Endocytosis-related proteins
gi|13928818	3	protein tyrosine phosphatase, receptor type, N polypeptide 2	1.8	2.7	1.7	2.0	0.6	Endocytosis-related proteins
gi|16758732	3	reticulon 1	SPM	7.3	5.6	6.4	1.2	ER/Golgi
gi|109492083	2	inositol-requiring 1 alpha		SPM	SPM	SPM		ER/Golgi
gi|13929188	2	reticulon 4		SPM	SPM	SPM		ER/Golgi
gi|209915579	3	thioredoxin domain containing 13	SPM	SPM	6.4	SPM		ER/Golgi

List of identified proteins in the docked and free vesicle fraction

Appendix I

GI number	# identified in biological replicates	protein name	biological replicate #1	biological replicate #2	biological replicate #3	average enrichment	standard deviation	protein localization/function
gi|8392935	3	ATPase, Ca++ transporting, slow twitch 2 isoform a	SPM	7.2	8.0	7.6	0.6	ER/Golgi
gi|25282419	3	calnexin	SPM	4.1	5.2	4.6	0.8	ER/Golgi
gi|109502306	3	kinectin 1		SPM	SPM	SPM		ER/Golgi
gi|21489979	2	ADP-ribosylation factor GTPase activating protein 1		SPM	SPM	SPM		ER/Golgi
gi|77539456	2	complement component 4 binding protein, alpha		SPM	SPM	SPM		Extracellular
gi|109498009	3	hemicentin 1	SPM	SPM	SPM	SPM		Extracellular
gi|13928972	2	ST3 beta-galactoside alpha-2,3-sialyltransferase 3	SPM	SPM		SPM		Extracellular
gi|161783809	2	apolipoprotein B precursor		SPM	SPM	SPM		Extracellular
gi|31542401	2	brain creatine kinase		8.8	9.0	8.9	0.2	Metabolic enzymes
gi|46485440	2	glucose phosphate isomerase	SPM		SPM	SPM		Metabolic enzymes
gi|8393418	3	glyceraldehyde-3-phosphate dehydrogenase	0.3	0.4	0.3	0.3	0.0	Metabolic enzymes
gi|58865398	2	leucine aminopeptidase 3		SPM	SPM	SPM		Metabolic enzymes
gi|13929002	3	phosphofructokinase, muscle	SPM	0.5	0.6	0.6	0.1	Metabolic enzymes
gi|57977273	3	phosphofructokinase, platelet	SPM	1.0	0.7	0.9	0.2	Metabolic enzymes
gi|62664437	2	aldehyde dehydrogenase family 7, member A1		SPM	SPM	SPM		Metabolic enzymes
gi|142349612	2	glutamine synthetase 1		0.8	1.1	0.9	0.1	Metabolic enzymes
gi|201066365	2	3~-phosphoadenosine 5~-phosphosulfate synthase 2	SPM	SPM		SPM		Metabolic enzymes
gi|198386332	3	fumarylacetoacetate hydrolase domain containing 2A	SPM	SPM	SPM	SPM		Metabolic enzymes
gi|62078999	2	TRAF3-interacting JNK-activating modulator		1.3	SPM	1.3		Novel
gi|62079059	3	BM88 antigen	SPM	SPM	9.3	SPM		Novel
gi|62078483	2	OCIA domain containing 1		SPM	SPM	SPM		Novel
gi|109483746	3	F58G4.1	0.6	0.3	0.5	0.5	0.2	Novel
gi|62641302	2	tumor suppressor candidate 5		3.7	3.8	3.8	0.1	Novel
gi|157822793	3	coiled-coil domain containing 109A	SPM	SPM	SPM	SPM		Novel
gi|56090369	2	thioredoxin-related transmembrane protein 2		SPM	SPM	SPM		Novel
gi|109484624	3	transmembrane protease, serine 4	SPM	SPM	SPM	SPM		Novel
gi|51948472	3	transmembrane protein 30A	3.2	2.4	2.1	2.6	0.6	Novel
gi|62660468	2	WD repeat membrane protein PWDMP	SPM		SPM	SPM		Novel
gi|189011652	3	transmembrane protease, serine 13	1.0	1.1	SPM	1.1	0.1	Novel
gi|71361663	3	family with sequence similarity 162, member A	SPM	0.8	8.8	8.4	5.7	Novel
gi|62651891	2	CG13957-PA		SPM	8.9	SPM		Novel
gi|109478621	2	CG32732-PA		SPM	SPM	SPM		Novel
gi|109492012	2	CG7896-PA isoform 1	SPM	SPM		SPM		Novel
gi|109461608	2	hypothetical protein		SPM	SPM	SPM		Novel
gi|62718819	2	hypothetical protein		SPM	SPM	SPM		Novel
gi|109481310	2	hypothetical protein		4.8	SPM	4.8		Novel
gi|157786666	3	hypothetical protein LOC287559	0.7	0.2	0.4	0.5	0.3	Novel
gi|157819311	2	hypothetical protein LOC296968	7.3	SPM		SPM		Novel

GI number	# identified in biological replicates	protein name	biological replicate #1	biological replicate #2	biological replicate #3	average enrichment	standard deviation	protein localization/function
gi|157819829	2	hypothetical protein LOC300783		SPM	2.3	4.8		Novel
gi|157822273	3	hypothetical protein LOC315463	SPM	SPM	8.3	SPM		Novel
gi|62079015	2	hypothetical protein LOC361118		SPM	SPM	SPM		Novel
gi|157821195	2	hypothetical protein LOC362419		SPM	SPM	SPM		Novel
gi|157821401	3	hypothetical protein LOC683512	0.3	SPM	SPM	SPM		Novel
gi|158262028	3	hypothetical protein MGC15854	SPM	6.2	SPM	SPM		Novel
gi|68342019	2	leucine rich repeat containing 17		SPM	SPM	SPM		Novel
gi|109499872	2	Protein C4orf008 homolog	SPM		SPM	SPM		Novel
gi|109510841	3	hypothetical protein Apolipoprotein O	SPM	SPM	SPM	SPM		Novel
gi|56605740	2	WD repeat and FYVE domain containing 1		SPM	SPM	SPM		Novel
gi|56605828	3	trafficking protein particle complex 3	0.7	0.6	0.6	0.6	0.1	Novel
gi|66730294	2	abhydrolase domain containing 12		2.7	6.1	4.4	2.5	Novel
gi|109473862	3	IQ motif and Sec7 domain 1 isoform 2	2.5	SPM	SPM	3.1		Novel
gi|61557143	2	secernin 3	2.2		SPM	2.2		Novel
gi|109464586	3	leucine rich repeat and coiled-coil domain containing 1		0.2	0.4	0.3	0.1	Novel
gi|67846010	2	rogdi homolog		1.5	0.9	1.2	0.5	Novel
gi|109512114	2	testis serine protease 5		SPM	SPM	SPM		Novel
gi|157821409	2	bromodomain and PHD finger containing, 3		SPM	SPM	SPM		Nucleotide metabolism/Protein Synthesis
gi|109499357	2	bromodomain, testis-specific		SPM	SPM	SPM		Nucleotide metabolism/Protein Synthesis
gi|109479775	2	chromosome 14 open reading frame 145 isoform 2		SPM	0.9	1.2		Nucleotide metabolism/Protein Synthesis
gi|109510822	3	DNA polymerase alpha catalytic subunit	0.5	1.3	SPM	0.9	0.6	Nucleotide metabolism/Protein Synthesis
gi|50054162	2	eukaryotic translation elongation factor 1 alpha 2		SPM	1.3	1.4		Nucleotide metabolism/Protein Synthesis
gi|158631185	2	exportin 5	0.7	0.8		0.7	0.1	Nucleotide metabolism/Protein Synthesis
gi|109497472	3	GCN1 general control of amino-acid synthesis 1-like 1	SPM	SPM	SPM	SPM		Nucleotide metabolism/Protein Synthesis
gi|109469681	3	general transcription factor IIIC, polypeptide 4	SPM	SPM	SPM	SPM		Nucleotide metabolism/Protein Synthesis
gi|62990189	2	heterogeneous nuclear ribonucleoprotein R		SPM	SPM	SPM		Nucleotide metabolism/Protein Synthesis
gi|109505578	2	jumonji protein isoform 2		SPM	SPM	SPM		Nucleotide metabolism/Protein Synthesis
gi|71043842	2	myeloid leukemia factor 1 interacting protein		0.4	0.3	0.3	0.0	Nucleotide metabolism/Protein Synthesis
gi|194474010	3	nuclear factor of kappa light polypeptide gene enhancer in B-cells inhibitor-like 2	SPM	SPM	SPM	SPM		Nucleotide metabolism/Protein Synthesis
gi|157822347	2	nuclear receptor binding SET domain protein 1		0.2	0.4	0.3	0.1	Nucleotide metabolism/Protein Synthesis
gi|109512329	3	TAF7-like RNA polymerase II, TATA box binding protein (TBP)-associated factor	SPM	SPM	SPM	SPM		Nucleotide metabolism/Protein Synthesis
gi|38259192	3	topoisomerase (DNA) II alpha	1.6	SPM	1.0	1.2	0.4	Nucleotide metabolism/Protein Synthesis
gi|109459242	2	Transcriptional enhancer factor TEF-1 isoform 5	0.3		4.3	2.3	2.8	Nucleotide metabolism/Protein Synthesis
gi|157818041	2	YEATS domain containing 2	SPM		SPM	SPM		Nucleotide metabolism/Protein Synthesis
gi|157823175	2	zinc finger CCCH type containing 7 A		SPM	SPM	SPM		Nucleotide metabolism/Protein Synthesis
gi|109504984	2	zinc finger protein 192	0.5			0.5		Nucleotide metabolism/Protein Synthesis
gi|169259769	2	zinc finger protein 292	SPM	SPM		SPM		Nucleotide metabolism/Protein Synthesis
gi|109509122	3	ATP-binding cassette sub-family F member 1 (ATP-binding cassette 50)	SPM	9.6	9.6	9.6	0.0	Nucleotide metabolism/Protein Synthesis

List of identified proteins in the docked and free vesicle fraction

Appendix I

GI number	# identified in biological replicates	protein name	biological replicate #1	biological replicate #2	biological replicate #3	average enrichment	standard deviation	protein localization/function
gi|13592077	2	ribosomal protein S27a	4.3		3.8	4.1	0.4	Nucleotide metabolism/Protein Synthesis
gi|34328536	2	single-stranded DNA binding protein 1		SPM	SPM	SPM		Nucleotide metabolism/Protein Synthesis
gi|55926145	3	non-metastatic cells 2, protein (NM23B) expressed in	SPM	9.0	8.5	8.7	0.4	Nucleotide metabolism/Protein Synthesis
gi|9665227	2	post-synaptic density protein 95		SPM	SPM	SPM		Postsynaptic
gi|164663821	3	synaptic Ras GTPase activating protein 1 homolog isoform 1	6.7	SPM	3.9	5.5	1.9	Postsynaptic
gi|14091744	2	kalirin, RhoGEF kinase	SPM		SPM	SPM		Postsynaptic
gi|109483754	2	growth and transformation-dependent protein		SPM	3.4	2.3		record removed
gi|109483500	2	Dmx-like 2		SPM	0.8	0.9		record removed
gi|109503754	2	WD repeat and FYVE domain containing 3		SPM	SPM	SPM		record removed
gi|109481805	3	CG1814-PA, isoform A	SPM	5.6	6.4	6.0	0.6	record removed
gi|109479730	2	CG33714-PB, isoform B		9.0	SPM	SPM		record removed
gi|109470173	3	FLJ44048 protein	SPM	SPM	SPM	SPM		record removed
gi|109497812	3	hypothetical protein	0.6	0.8	1.1	0.8	0.2	record removed
gi|109514756	2	hypothetical protein LOC363337	SPM	SPM		SPM		record removed
gi|8394267	2	sonic hedgehog		SPM	SPM	SPM		Signalling molecules
gi|9507061	3	proprotein convertase subtilisin/kexin type 1 inhibitor	SPM	5.4	SPM	SPM		Signalling molecules
gi|109458044	2	PYRIN-containing APAF1-like protein 7 isoform 2	SPM	SPM		SPM		Signalling molecules
gi|157818451	2	ADP-ribosylation factor-like 8A		SPM	SPM	SPM		Signalling molecules
gi|12408298	2	dipeptidylpeptidase 6		4.4	4.7	4.5	0.2	Signalling molecules
gi|109475021	2	CDK5 regulatory subunit associated protein 2		SPM	SPM	SPM		Signalling molecules
gi|13592021	2	phosphodiesterase 2A, cGMP-stimulated isoform 2		SPM	SPM	SPM		Signalling molecules
gi|6978593	3	calcium/calmodulin-dependent protein kinase II alpha	8.8	5.6	7.4	7.3	1.6	Signalling molecules
gi|108796657	3	calcium/calmodulin-dependent protein kinase II beta isoform2	8.5	6.8	8.4	7.9	1.0	Signalling molecules
gi|6978595	2	calcium/calmodulin-dependent protein kinase II delta		4.5	7.7	6.1	2.3	Signalling molecules
gi|19424316	3	calcium/calmodulin-dependent protein kinase II gamma	9.7	6.4	8.5	8.2	1.7	Signalling molecules
gi|155369271	2	cAMP-dependent protein kinase catalytic subunit alpha	SPM		SPM	SPM		Signalling molecules
gi|109464256	3	cardiomyopathy associated 5	0.8	0.9	1.8	1.2	0.6	Signalling molecules
gi|6981400	2	protein kinase C, gamma		2.6	2.8	2.7	0.1	Signalling molecules
gi|157822659	2	RIO kinase 3		SPM	SPM	SPM		Signalling molecules
gi|132626321	2	serine/threonine kinase 2	SPM		SPM	SPM		Signalling molecules
gi|6981712	2	14-3-3 theta polypeptide	SPM	SPM		SPM		Signalling molecules
gi|62990183	2	14-3-3, zeta polypeptide		SPM	5.1	4.9		Signalling molecules
gi|25742825	2	phosphatidylinositol 4-kinase a		SPM	SPM	SPM		Signalling molecules
gi|9506737	2	GNAS complex locus gnas1-a	9.7		SPM	8.7		Signalling molecules
gi|109487963	3	dedicator of cyto-kinesis 2	0.7	0.8	1.0	0.8	0.2	Signalling molecules
gi|42476092	2	G protein pathway suppressor 1	1.1	1.1		1.1	0.0	Signalling molecules
gi|8394152	3	GTP-binding protein alpha o	8.6	5.0	6.6	6.7	1.8	Signalling molecules
gi|6980962	2	guanine nucleotide binding protein (G protein), alpha inhibiting 1	7.4		6.1	6.7	0.9	Signalling molecules

GI number	# identified in biological replicates	protein name	biological replicate #1	biological replicate #2	biological replicate #3	average enrichment	standard deviation	protein localization/function
gi|13591957	2	guanine nucleotide binding protein, alpha q polypeptide		SPM	3.8	6.2		Signalling molecules
gi|109507443	2	Guanine nucleotide-binding protein G(olf), alpha subunit		8.9	SPM	SPM		Signalling molecules
gi|29789261	2	guanine nucleotide-binding protein, beta 2		6.3	8.7	7.5	1.7	Signalling molecules
gi|148747524	3	guanine nucleotide-binding protein, beta-1 subunit	9.0	6.3	8.7	8.0	1.5	Signalling molecules
gi|19173774	2	RAP2B, member of RAS oncogene family		SPM	5.2	4.7		Signalling molecules
gi|157820415	3	RAS protein activator like 1 (GAP1 like)	10.0	8.4	8.7	9.0	0.8	Signalling molecules
gi|13592039	2	ras related v-ral simian leukemia viral oncogene homolog A		SPM	SPM	SPM		Signalling molecules
gi|157821177	3	triple functional domain (PTPRF interacting)	SPM	SPM	SPM	SPM		Signalling molecules
gi|62079163	3	ATG9 autophagy related 9 homolog A	1.4	0.6	1.5	1.2	0.5	SNARE proteins and trafficking molecules
gi|13027430	2	WD repeat domain 7		SPM	1.8	2.5		SNARE proteins and trafficking molecules
gi|6981602	3	syntaxin binding protein 1	2.5	2.1	2.2	2.3	0.2	SNARE proteins and trafficking molecules
gi|9507127	3	SNAP25-interacting protein	3.9	6.2	7.7	5.9	1.9	SNARE proteins and trafficking molecules
gi|13489067	3	N-ethylmaleimide-sensitive factor	5.1	2.4	2.2	3.3	1.6	SNARE proteins and trafficking molecules
gi|219275534	2	vacuolar protein sorting 13 homolog A		2.7	2.9	2.8	0.1	SNARE proteins and trafficking molecules
gi|25742604	2	vacuolar protein sorting 45 homolog		SPM	SPM	SPM		SNARE proteins and trafficking molecules
gi|12408324	2	complexin 1	7.0	3.7		5.3	2.3	SNARE proteins and trafficking molecules
gi|109471437	2	Syntaxin-16 (Syn16) isoform 1		SPM	SPM	SPM		SNARE proteins and trafficking molecules
gi|13591882	3	synaptosomal-associated protein 25	4.3	4.2	4.1	4.2	0.1	SNARE proteins and trafficking molecules
gi|33667087	3	syntaxin 1A (brain)	3.0	2.9	3.1	3.0	0.1	SNARE proteins and trafficking molecules
gi|6981600	3	syntaxin 1B2	3.5	3.4	3.4	3.4	0.1	SNARE proteins and trafficking molecules
gi|76443677	3	vesicle-associated membrane protein 1	0.9	0.8	0.9	0.9	0.1	SNARE proteins and trafficking molecules
gi|6981614	3	vesicle-associated membrane protein 2	0.7	0.7	0.8	0.7	0.0	SNARE proteins and trafficking molecules
gi|45433570	3	RAB1, member RAS oncogene family	2.1	2.1	2.1	2.1	0.0	Synaptic vesicle
gi|61889071	3	RAB10, member RAS oncogene family	1.8	1.6	1.8	1.7	0.1	Synaptic vesicle
gi|16758368	3	RAB14, member RAS oncogene family	2.8	1.9	1.9	2.2	0.5	Synaptic vesicle
gi|16758202	2	RAB27B, member RAS oncogene family	2.6		SPM	2.5		Synaptic vesicle
gi|13929006	3	RAB2A, member RAS oncogene family	1.9	1.8	2.0	1.9	0.1	Synaptic vesicle
gi|61556789	3	RAB35, member RAS oncogene family	2.2	2.0	1.9	2.1	0.1	Synaptic vesicle
gi|157822741	3	RAB39, member RAS oncogene family	2.8	1.9	1.9	2.2	0.5	Synaptic vesicle
gi|13592037	2	RAB3B, member RAS oncogene family		1.8	1.5	1.7	0.2	Synaptic vesicle
gi|61098195	3	RAB3A, member RAS oncogene family	2.3	1.9	1.9	2.0	0.2	Synaptic vesicle
gi|158749626	3	secretory carrier membrane protein 1	3.2	1.2	1.0	1.8	1.2	Synaptic vesicle
gi|13929020	3	secretory carrier membrane protein 5	0.6	0.6	0.6	0.6	0.0	Synaptic vesicle
gi|109465077	2	Secretory carrier-associated membrane protein 3	1.0	1.1		1.1	0.1	Synaptic vesicle
gi|109499663	3	ATPase, aminophospholipid transporter (APLT), class I, type 8A, member 1	1.6	1.3	1.4	1.4	0.1	Synaptic vesicle
gi|16758754	3	ATPase, H transporting, lysosomal V1 subunit F	1.1	0.9	1.0	1.0	0.1	Synaptic vesicle
gi|18677757	3	ATPase, H+ transporting, lysosomal 16kDa, V0 subunit c	0.6	0.7	0.8	0.7	0.1	Synaptic vesicle
gi|58865424	3	ATPase, H+ transporting, lysosomal 38kDa, V0 subunit d1	1.0	0.9	0.9	0.9	0.0	Synaptic vesicle

List of identified proteins in the docked and free vesicle fraction

Appendix I

GI number	# identified in biological replicates	protein name	biological replicate #1	biological replicate #2	biological replicate #3	average enrichment	standard deviation	protein localization/function
gi|13929110	3	ATPase, H+ transporting, lysosomal accessory protein 1	0.9	0.8	0.9	0.9	0.0	Synaptic vesicle
gi|77627990	3	ATPase, H+ transporting, lysosomal V0 subunit a1	0.9	0.9	0.9	0.9	0.0	Synaptic vesicle
gi|58865560	3	ATPase, H+ transporting, lysosomal V1 subunit C1	1.1	0.9	0.9	1.0	0.2	Synaptic vesicle
gi|40786463	3	ATPase, H+ transporting, lysosomal V1 subunit D	1.1	1.1	1.0	1.1	0.0	Synaptic vesicle
gi|47059104	3	ATPase, H+ transporting, lysosomal V1 subunit G2	0.8	0.9	0.9	0.9	0.1	Synaptic vesicle
gi|62078587	3	ATPase, H+ transporting, lysosomal V1 subunit H	0.9	0.9	0.9	0.9	0.0	Synaptic vesicle
gi|109493234	3	ATPase, H+ transporting, V1 subunit A, isoform 1 isoform 1	0.9	0.9	0.9	0.9	0.0	Synaptic vesicle
gi|13162361	3	cysteine string protein	1.2	1.2	0.9	1.1	0.1	Synaptic vesicle
gi|77157795	3	MAL2 proteolipid protein	0.9	0.8	0.8	0.8	0.0	Synaptic vesicle
gi|160333093	3	mossy-fiber terminal-associated vertebrate-specific presynaptic protein	0.9	0.5	1.0	0.8	0.3	Synaptic vesicle
gi|16758166	3	solute carrier family 17 , member 6	1.0	0.8	0.8	0.9	0.1	Synaptic vesicle
gi|16758726	3	solute carrier family 17 , member 7	1.0	0.8	0.8	0.9	0.1	Synaptic vesicle
gi|74271849	3	solute carrier family 6 (neurotransmitter transporter), member 17	1.7	1.4	1.4	1.5	0.2	Synaptic vesicle
gi|9507159	3	synapsin I isoform a	2.9	1.2	1.6	1.9	0.9	Synaptic vesicle
gi|77404242	3	synapsin II isoform 1	1.7	1.4		1.6	0.2	Synaptic vesicle
gi|8394389	2	synapsin III		1.8	1.9	1.8	0.0	Synaptic vesicle
gi|148747227	3	synaptic vesicle glycoprotein 2a	0.8	0.8	0.8	0.8	0.0	Synaptic vesicle
gi|17105360	3	synaptic vesicle glycoprotein 2b	1.0	0.8	0.9	0.9	0.1	Synaptic vesicle
gi|9507167	3	synaptogyrin 1	0.5	0.6	0.6	0.6	0.0	Synaptic vesicle
gi|157819371	3	synaptogyrin 3	0.5	0.5	0.4	0.5	0.0	Synaptic vesicle
gi|6981622	3	synaptophysin	0.6	0.7	0.7	0.7	0.0	Synaptic vesicle
gi|13027428	2	synaptoporin	0.9		0.7	0.8	0.2	Synaptic vesicle
gi|148356226	3	synaptotagmin 1	1.2	1.1	1.1	1.1	0.1	Synaptic vesicle
gi|6981624	3	synaptotagmin II	1.6	1.2	1.5	1.4	0.2	Synaptic vesicle
gi|9507171	2	synaptotagmin V		1.2	1.5	1.3	0.2	Synaptic vesicle
gi|38454230	3	vacuolar H+ ATPase E1	0.9	1.1	0.9	1.0	0.1	Synaptic vesicle
gi|17105370	3	vacuolar H+ATPase B2	0.9	0.9	0.9	0.9	0.0	Synaptic vesicle
gi|13929106	3	vesicular inhibitory amino acid transporter	0.7	0.8	0.9	0.8	0.1	Synaptic vesicle
gi|61557417	3	zinc transporter ZnT-3	0.8	0.8	0.8	0.8	0.0	Synaptic vesicle
gi|55925610	3	inositol 1,4,5-triphosphate receptor, type 1	6.2	SPM	7.6	6.9	1.0	Transporter/Channel Proteins/Receptors
gi|9507115	2	solute carrier family 1 (glial high affinity glutamate transporter), member 3		10.2	SPM	SPM		Transporter/Channel Proteins/Receptors
gi|157817045	2	chloride channel 6		SPM	SPM	SPM		Transporter/Channel Proteins/Receptors
gi|78126161	2	glial high affinity glutamate transporter isoform b		7.5	10.2	8.9	1.9	Transporter/Channel Proteins/Receptors
gi|155369700	2	toll-like receptor 8		SPM	SPM	SPM		Transporter/Channel Proteins/Receptors
gi|31542335	2	calcium channel, voltage-dependent, alpha2/delta subunit 1 isoform 1	SPM		8.9	SPM		Transporter/Channel Proteins/Receptors
gi|6978583	2	calcium channel, voltage-dependent, beta 3 subunit		SPM	SPM	SPM		Transporter/Channel Proteins/Receptors
gi|16758108	2	hyperpolarization-activated cyclic nucleotide-gated potassium channel 1	SPM		SPM	SPM		Transporter/Channel Proteins/Receptors
gi|6978543	3	Na+/K+ -ATPase alpha 1 subunit	7.8	7.1	8.6	7.8	0.7	Transporter/Channel Proteins/Receptors

GI number	# identified in biological replicates	protein name	biological replicate #1	biological replicate #2	biological replicate #3	average enrichment	standard deviation	protein localization/function
gi|6978547	3	Na+/K+ -ATPase alpha 3 subunit	8.0	7.1	6.8	7.3	0.6	Transporter/Channel Proteins/Receptors
gi|148747253	3	Na+/K+ -ATPase beta 1 subunit	9.0	7.0	9.3	8.4	1.2	Transporter/Channel Proteins/Receptors
gi|16758008	3	plasma membrane calcium ATPase 1	6.5	3.4	8.9	6.3	2.8	Transporter/Channel Proteins/Receptors
gi|6978557	2	plasma membrane calcium ATPase 2		3.4	8.9	6.2	3.9	Transporter/Channel Proteins/Receptors
gi|13929184	2	potassium large conductance calcium-activated channel, subfamily M, alpha member 1		SPM	SPM	SPM		Transporter/Channel Proteins/Receptors
gi|19705463	3	solute carrier family 12 (potassium-chloride transporter), member 5	2.9	4.6	5.2	4.2	1.2	Transporter/Channel Proteins/Receptors
gi|148747140	2	solute carrier family 2 (facilitated glucose transporter), member 3		4.9	4.5	4.7	0.3	Transporter/Channel Proteins/Receptors
gi|62644838	3	solute carrier family 27 (fatty acid transporter), member 4	SPM	SPM	6.6	7.0		Transporter/Channel Proteins/Receptors
gi|17530967	3	solute carrier family 8 (sodium/calcium exchanger), member 2	5.3	3.4	5.2	4.6	1.1	Transporter/Channel Proteins/Receptors
gi|6981558	2	solute carrier family 9 (sodium/hydrogen exchanger), member 1		SPM	5.2	SPM		Transporter/Channel Proteins/Receptors
gi|13242269	2	GABA transporter protein		SPM	SPM	SPM		Transporter/Channel Proteins/Receptors
gi|47576439	2	olfactory receptor Olr1589			3.7	2.1		Transporter/Channel Proteins/Receptors

gene name	protein name
Sept3	septin 3
Sept5	septin 5
Sirpa	signal regulatory protein alpha
Slc17a7	VGlut1
Slc1a2	EAAT1
Slc1a3	EAAT2
Slc30a3	zinc transporter ZnT-3
Slc6a1	GABA transporter protein
Slc6a17	neurotransmitter transporter NTT4
Snap25	SNAP25
Sptan1	spectrin, alpha
Stx1b	syntaxin 1B
Stxbp1	Munc18-1
Syn1	synapsin 1
Syn2	synapsin 2
Syp	synaptophysin
Syt1	synaptotagmin 1
Thy1	Thy-1 cell surface antugen
Tuba1a	tubulin, alpha 1A
Tuba1b	tubulin, alpha 1B
Tubb3	tubulin, beta 3
Tubb5	tubulin, beta 5
Vamp1	synaptobrevin 1
Vamp2	synaptobrevin 2
Ywhaq	14-3-3 theta
Ywhaz	14-3-3 zeta
Acta1	actin, alpha 1
Actb	actin, beta
Ap2b1	AP2 complex, beta 1
Atp1a1	Na/K ATPase alpha 1
Atp1a3	Na/K ATPase alpha 3
Atp1b1	Na/K ATPase beta 1
Atp2b1	PMCA 1
Atp6v0a1	lysosomal ATPase V0 a1
Atp6v0d1	lysosomal ATPase V0 d1
Atp6v1b2	lysosomal ATPase V1 b2
Atp6v1c1	lysosomal ATPase V1 c1
Atp6v1d	lysosomal ATPase V1 d
Atp6v1e1	lysosomal ATPase V1 e1
Cacna2d1	calcium channel a2/d subunit 1
Camk2a	CAMKII alpha
Cd47	CD47 molecule
Cltc	clathrin heavy chain
Cntnap1	Neurexin 4
Dnajc5	cysteine string protein
Gnal	guanine nucleotide-binding protein G(olf) alpha
Gnao1	GTP-binding protein alpha o
Gnaq	guanine nucleotide-binding protein alpha q
Gnb1	guanine nucleotide-binding protein beta 1
Gnb2	guanine nucleotide-binding protein beta 2
Gpm6a	glycoprotein m6a
Hsp90aa1	heat shock protein 90
Hspa8	heat shock protein 8
Ncam1	neuronal cell adhesion molecule 1
Nptn	neuroplastin
Nsf	N-ethylmaleimide-sensitive factor
Plec1	plectin 1
Prkcg	protein kinase C, gamma
Rab14	Rab 15
Rab2a	Rab 2 a
Rab35	Rab 35
Rab3a	Rab 3a

gene name	protein name
Ap2b1	adaptor-related protein complex 2, beta 1 subunit
Ap2a1	adaptor-related protein complex 2, alpha 1 subunit
Ap2a2	adaptor-related protein complex 2, alpha 2 subunit
Ap2m1	adaptor-related protein complex 2, mu 1 subunit
Atp6v0a1	lysosomal ATPase V0 a1
Atp6v1e1	lysosomal ATPase V1 e1
Atp6v1a1	lysosomal ATPase V1 a1
Atp6v1b2	lysosomal ATPase V1 b2
Atp6v1c1	lysosomal ATPase V1 c1
Atp6v0d1	lysosomal ATPase V0 d1
Cltc	clathrin heavy chain
Dync1h1	cytoplasmic dynein 1 heavy chain 1
Nsf	N-ethylmaleimide-sensitive factor
Rab3a	Rab3a
Rims1	Rim 1
Sh3gl2	endophilin B2
Snap25	SNAP25
Stx1a	syntaxin 1A
Stxbp1	Munc18-1
Syn1	synapsin 1
Syn2	synapsin 2
Syt1	synaptotagmin 1
Syt2	synaptotagmin 2
Vamp2	synaptobrevin 2
Camk2a	CAMKII alpha
Gnao1	GTP-binding protein alpha o
Gnb1	guanine nucleotide-binding protein beta 1
Gnb2	guanine nucleotide-binding protein beta 2
Gnai1	guanine nucleotide-binding protein alpha inhibiting 1
Ywhaz	14-3-3 zeta
Atp1a3	Na/K ATPase alpha 3
Ank2	ankyrin 2, neuronal
Ncam1	neuronal cell adhesion molecule 1
Acta1	actin, alpha 1
Actb	actin, beta
Actn1	actinin, alpha 1
Sept3	septin 3
Sept5	septin 5
Sept7	septin 7
Sptan1	spectrin alpha chain, brain
Sptbn1	spectrin beta chain, brain 1
Tubb4	tubulin, beta 4
Tubb3	tubulin, beta 3
Tuba1a	tubulin, alpha 1A
Hsp90aa1	heat shock protein 90
Hspa8	heat shock protein 8
Thy1	Thy-1 cell surface antigen